Quantification of Soil Macropore Characteristics using X-ray Computed Tomography

by

Suman Budhathoki

A thesis submitted to the Graduate Faculty of
Auburn University
in partial fulfillment of the
requirements for the Degree of
Master of Science

Auburn, Alabama
August 7, 2021

Keywords: Preferential flow; Topography, Image analysis, Compaction, Land use

Approved by

Jasmeet Lamba, Chair, Assistant Professor, Department of Biosystems Engineering
Puneet Srivastava, Co-chair, Professor, Department of Biosystems Engineering
Thomas R. Way, Agricultural Engineer, USDA-ARS National Soil Dynamics Lab

Abstract

Soil macropores, such as root channels and earthworm burrows, constitute only a small fraction of the total soil volume but contribute largely to the transport of water and solutes in subsurface flows. One of the challenges in soil hydrology is quantification of soil macropore characteristics. The X-ray computed tomography (CT) is a powerful technique that allows quantification of the 3D soil macropore structure without altering the sample. The goal of this study was to quantify and characterize two-dimensional (2D) and three-dimensional (3D) soil macropore characteristics including, macroporosity, macropore size distribution, macropore length density, and interconnectivity (node density) using CT.

The first part of this study provided quantitative information of different soil macropore characteristics at different topographical locations (upslope, midslope, and downslope) and depths in a 0.40 ha pasture field located in Alabama, USA. The downslope location had significantly less macropore number and macroporosity values in the 0-100 mm soil layer. In addition, macropores at the surface (0-100 mm) of upslope and midslope soils were highly connected as compared to the soils of the downslope location. The results of this study suggest that macropores at the surface (0-100 mm) of the downslope locations are largely affected by trampling induced compaction due to presence of higher soil moisture content at the downslope location, via runoff and seepage losses from the upper slopes. Besides, it was found that macroporosity and ECD measurements could be largely biased because of higher values of coefficient of variation (CV) for a smaller diameter sub-volume cores compared to the larger diameter cores.

In the second part of the study, quantitative evaluation was made on both the spatial and temporal variability in 3D soil macropore structure in a pasture field. The results of this study showed that 3D macropore characteristics may change significantly with time (~0.33 years) and topographical position in the topsoil surface (0-100 mm) layer. Also, pores smaller than 2 mm in diameter were found to be highly sensitive to topographical differences suggesting need of further studies using higher resolution X-ray CT to quantify smaller pores (<0.70 mm).

In the third part of this study, soil macropore characteristics were quantified as a function of land use type and tillage practices in soil cores collected from Wisconsin, USA. The macropores in soil cores collected from fields under conventional tillage were smaller and mostly concentrated near the surface soil layer as compared to the no-till soils, which can be attributed to the disaggregation of the soil structure due to tillage operations. On the other hand, soil cores collected from no-till field and alfalfa had relatively larger and vertical macropores. Overall results of this study will contribute to the enhanced evaluation of soil macropore features with significant implications for flow and contaminant transport modeling in soils.

Acknowledgments

I would like to express my deepest gratitude towards both of my advisors, Dr. Jasmeet Lamba, and Dr. Puneet Srivastava, for providing me an opportunity to pursue Master's degree in their research group. Dr. Lamba's continuous support and encouragement have always helped me take better decisions during my entire study period. I thank him for spending countless hours revising my manuscripts and guiding me both scientifically and personally. I always received his warm welcome and unconditional help even when I knocked on his office door without an appointment. I am equally thankful to my co-advisor, Dr. Puneet Srivastava, for being my mentor and always encouraging me to be an independent researcher. At the same time, I want to express my most profound appreciation to my committee member Dr. Tom Way for his valuable support and feedback during my entire research.

I must acknowledge Dr. Sheela Katuwal for always helping me deal with the research problems. I would also like to express my heartfelt gratitude to Ms. Kritika Malhotra, Mr. Bijoychandra Takhellambam, and Mr. Hemendra Kumar for their valuable help, suggestions, and feedback during my research. I want to thank Ms. Sanjita Wasti, Ms. Pratima Subedi, Mr. Richard Morbidelli, and Dr. Ritesh Karki for always cheering me up and providing constant encouragement for my work. I am grateful to the collaborators from the University of Wisconsin-Madison, Dr. K.G. Karthikeyan, Dr. Francisco Arriaga, and Ms. Colleen Williams, for letting me be part of their research as well. I must acknowledge Marlin R. Siegford, Peyton Heath, Thomas Counts, and staff at the Sand Mountain Research and Extension Center (SMREC) for assistance in this research project. Furthermore, this research would have been incomplete without the support of the funding

agency. Therefore, I would like to acknowledge the USDA-NIFA AFRI grant for supporting this research.

Most importantly, I would like to thank the most important people of my life: my mother, Ms. Lata Budhathoki, my father, Mr. Bishnu Budhathoki, my sister, Ms. Saraswati Budhathoki, and my lovely wife, Ms. Suju Pokhrel, for their unconditional love and support in my life.

Table of Contents

Abstract ii

Acknowledgments iv

Table of Contents vi

List of Tables x

List of Figures xi

List of Abbreviations xiv

Chapter 1 Introduction 1

1.1 Background 1

1.2 Research Objective 3

1.3 Thesis outline 3

1.4 References 4

Chapter 2 Using X-ray Computed Tomography to Quantify Variability in Soil Macropore Characteristics in Pastures 7

2.1 Abstract 7

2.2 Introduction 8

2.3 Materials and methods 12

2.3.1 Study site 12

2.3.2 Soil sampling 13

2.3.3 CT scanning and image analysis 15

2.3.4 Statistical analysis 18

2.4 Results 18

2.4.1 Distribution of macroporosity and number of macropores in different soil layers and slope positions 18
2.4.2 Limiting macroporosity at different slope positions 20
2.4.3 Diameter distribution of macropores in different soil layers and slope positions 20
2.4.4 Macropore connectivity at different slope positions 21
2.4.5 Effect of analyzed soil volume on macropore characteristics 21
2.5 Discussion 22
2.5.1 Spatial distribution of soil macropore characteristics 22
2.5.2 Evaluation of macropore connectivity and limiting macroporosity at different depths and slope locations 25
2.5.3 Diameter distribution of macropores 26
2.5.4 Effect of analyzed soil volume on macropore characteristics 27
2.5.5 Implications of macropore characteristics for flow and contaminant transport 28
2.6 Conclusion 29
2.7 Acknowledgement 30
2.8 References 31
Chapter 3 Characterizing Temporal and Spatial Variability in 3D Soil Macropore Characteristics Using X-ray Computed Tomography 45
3.1 Abstract 45
3.2 Introduction 46
3.3 Materials and methods 49
3.3.1 Study site 49
3.3.2 Soil sampling 50

3.3.3 CT scanning and image processing 51
3.3.4 Quantification of macropore characteristics 52
3.3.5 Statistical analysis 54
3.4 Results and discussion 54
3.4.1 Macropore network characteristics 54
3.4.2 Temporal variation in macropore characteristics 60
3.4.3 Size-dependent variation and implications for flow and contaminant transport 63
3.5 Conclusion 65
3.6 Acknowledgement 66
3.7 References 67
Chapter 4 Impact of Land Use and Tillage Practice on Soil Macropore Characteristics Determined Using X-ray Computed Tomography 79
4.1 Abstract 79
4.2 Introduction 80
4.3 Materials and methods 84
4.3.1 Study sites and soil sampling 84
4.3.2 CT scanning and image processing 85
4.3.3 Quantification of macropore networks 86
4.3.4 Statistical analyses 88
4.4 Results and discussion 88
4.4.1 Macroporosity and macropore number variation with depth 88
4.4.2 Macropore size distribution 91
4.4.3 Quantification of 3D network parameters 93

4.5 Conclusion 97

4.6 Acknowledgement 98

4.7 References 99

Chapter 5 Conclusions 111

Appendix A Photos 113

List of Tables

Table 2.1 Mean (n = 3) soil organic matter (%), sand (%), silt (%), clay (%), and bulk density (g cm^{-3}) at different topographical locations (downslope (DS), midslope (MS) and upslope (US)). Values shown in parentheses are standard deviations. 43

Table 2.2 Average (n = 6) number of macropores, average macropore diameter, and average macroporosity, in the US (upslope), MS (midslope), and DS (downslope) locations. 44

Table 3.1 Mean (Std. Dev.) macropore characteristics at different depths of the US (upslope), MS (midslope), and DS (downslope) locations as determined using computed tomography. 77

Table 3.2 Pearson's correlation matrix of the different CT-derived macropore characteristics of the soil samples. 78

Table 3.3 Pearson's correlation matrix of the different macroporosity classes with 3D macropore characteristics of the soil samples. 78

Table 4.1 Mean (Std. Dev.) macropore characteristics of all soil columns under different land uses and tillage practices 109

Table 4.2 Pearson's correlation matrix of CT-derived 3D macropore characteristics for all the soil samples. 110

List of Figures

Figure 2.1 Schematic diagram (not to scale) of a horizontal plane of a soil column showing cylindrical subsamples of (a) 48.1 mm diameter and (b) 24.05 mm diameter, used for evaluating volume effects on soil macropore characteristics. The height of the samples in all the subsamples were equal to 100 mm. 38

Figure 2.2 Effects of slope position on number of >1 mm soil pores and 0.75-1 mm soil pores in different soil layers. Error bars indicate the standard deviation (n=6). Within each depth, different letters for the slope positions (represented by different colors) indicate significantly different values at the 0.05 probability level. 38

Figure 2.3 Effects of slope position on the >1 mm soil macroporosity and 0.75-1 mm soil macroporosity in different soil layers. Error bars indicate standard deviation (n=6). Within each depth, different letters for the slope positions (represented by different colors) indicate significant difference at the 0.05 probability level. 39

Figure 2.4 Position of the limiting macroporosity in all the samples (n=18) of upslope, midslope and downslope locations. Limited macroporosity is based on each individual slice sampled at 0.625 mm intervals..... 39

Figure 2.5 Distribution of macropores by diameter at US, MS, and DS positions as a function of depth (0-500 mm). 40

Figure 2.6 Interconnectivity (*10^5 no. /m^3) of surface macropores (0-100 mm) as compared to the subsurface interconnectivity (100-500 mm) at different topographical positions in a pasture. Within each slope position, different letters indicate a significant difference in interconnectivity (node density) between the surface and subsurface soil depth ($P<0.05$). 40

Figure 2.7 Coefficient of variation (CV) (n=6) for macroporosity (A), ECD (B), and macropore number (C) obtained using 48.1 mm diameter (V1) and 24.05 mm diameter (V2) sub-sample soil cores at different topographical position..... 42

Figure 3.1 Temporal variation in a) soil macroporosity, b) macropore diameter, c) interconnectivity of macropores, and d) network density at different slope positions (DS, MS, and US). Error bars indicate standard deviation (n=6). For each graph, within each slope position, different letters for the different sampling seasons indicate significant differences at the 0.05 probability level..... 73

Figure 3.2 Effects of slope position on the 0.7-1 mm soil porosity, 1-2 mm soil porosity, and >2 mm soil porosity on the surface (top), transition (middle), and subsurface (bottom) soil layers for the S1 and S2 sampling seasons. Error bars indicate standard deviation (n=6). Within each graph and sampling season, different letters for the different slope positions indicate significant differences at the 0.05 probability level..... 74

Figure 3.3 Three-dimensional visualization of different sized soil macropore networks (<1 mm, 1-2 mm, and >2 mm) for the representative soil columns of (a) upslope (b) midslope (c) downslope samples of Season 1 and Season 2..... 76

Figure 4.1 3D macropore network visualizations of selected soil cores for the four treatments: corn conventional tillage (CT), corn no-tillage (NT), Native grassland (Nat) and Alfalfa (Alf). Macropores are shown in cyan and non-pore in black color in 3D images..... 105

Figure 4.2 Depth distribution of soil macroporosity (%) for all soil cores of corn conventional tillage (CT), corn no-tillage (NT), Native grassland (Nat) and Alfalfa (Alf)..... 105

Figure 4.3 Depth distribution of soil macropore number (-) for all soil cores of corn conventional tillage (CT), corn no-tillage (NT), Native grassland (Nat) and Alfalfa (Alf)..... 106

Figure 4.4 Contribution of different macropore size classes on overall macroporosity (%) in soil cores sampled under corn conventional tillage (CT, 3 replicates), corn no-tillage (NT, 6 replicates), Native grassland (NT, 3 replicates) and Alfalfa (Alf, 3 replicates) fields. Within each diameter class, different letters indicate a significant difference in macroporosity (%) between different treatments ($P<0.05$). Error bars indicate standard deviation..... 106
Figure 4.5 3D macropore characteristics of soil columns submitted to different land use treatments (Alf: Alfalfa; Nat: Native grassland; NT: corn no-tillage) and tillage treatments (CT: corn conventional tillage; NT: corn no-tillage) at different depth layers (surface (0-100 mm), transition (100-250 mm), and subsurface (250-500 mm). Error bars indicate standard deviation. For each graph, within each depth layer, different letters indicate a significant difference in macropore characteristics between different treatments ($P<0.05$). A) Macroporosity, B) Diameter, C) Surface area density, D) Length density, E) Network density, and F) Interconnectivity. 107
Figure 4.6 Mean macropore branch length for soil cores of corn conventional tillage (CT, 3 replicates), corn no-tillage (NT, 6 replicates), Native grassland (Nat, 3 replicates) and Alfalfa (Alf, 3 replicates). Different letters indicate a significant difference in mean macropore branch length between different treatments ($P<0.05$). Error bars indicate the standard deviation..... 108
Figure 4.7 Vertical length distribution of macropores for soil cores of corn conventional tillage (CT), corn no-tillage (NT), Native grassland (NT) and Alfalfa (Alf). The shaded region represents the standard deviation. 108

List of Abbreviations

Alf	Alfalfa
AUCVM	Auburn University College of Veterinary Medicine
CV	Coefficient of variation
CT	Computed tomography or Conventional tillage
DS	Downslope
ECD	Equivalent cylindrical diameter
FOV	Field of view
KV	Kilovolt
MS	Midslope
Nat	Native
NT	No tillage
PTF	Pedotransfer function
PVC	Polyvinyl chloride
ROI	Region of interest
K_{sat}	Saturated hydraulic conductivity
SMREC	Sand Mountain Research and Extension Center
US	Upslope

Chapter 1

Introduction

1.1 Background

In the Sand Mountain region of north Alabama, which is one of the top poultry producing regions in the US, excessive buildup of phosphorus (P) in soils and contamination of nearby water bodies has been a serious threat due to repeated application of poultry litters to the pastures (Sen et al., 2008). Previous studies have shown that loss of P via subsurface flows could be substantial in this region (Lamba et al., 2019). Preferential flow via soil macropores (e.g., root channels, earthworm burrows) can cause rapid transport of surface-applied fertilizers and chemicals into deep soil and even to the groundwater (Jarvis, 2007). Therefore, it is important to understand the macropore characteristics in this region to elucidate the subsurface transport of flow and contaminants.

A relatively new technique of X-ray computed tomography (CT) is a promising approach that can help quantify the soil macropore structure (Katuwal et al., 2015). Although different methods like tension infiltrometer (Cameira et al., 2003), dye tracers (Wahl et al., 2004), and resin impregnation (Singh et al., 1991) have been used widely in the past, these methods are indirect, time-consuming, and less accurate in reflecting the subtle features of the soil pore networks (Amer et al., 2009; Matthews et al., 2010). X-ray CT, on the other hand, is a non-destructive technique that allows quantification of macropores in their true 3D (Helliwell et al., 2013). A major limitation of this method is that it requires a small sample volume to scan soil cores at relatively higher scanning resolutions (Mees et al., 2003). This restricts its usage for quantifying macropores of larger soil columns composed of heterogeneous soil matrices. Nonetheless, X-ray CT techniques have been

successfully used to determine the soil macropore characteristics like connectivity, tortuosity, diameter, and number of macropores (Pires et al., 2019; Luo et al., 2010).

Topographical differences influence the soil properties by controlling the gravity-driven soil movements (Li and McCarty, 2019). Soil properties including moisture content and organic matter content, which largely vary with the topographical location in the field, promote the formation and stabilization of larger pores in the soil (Holden, 2009). However, limited work has been done to quantify the variability in soil macropore characteristics at different topographical locations within a field. The information on the topographical variation of soil macropore characteristics would improve the prediction accuracy of different transport models and understanding of the mechanisms underlying the impact of topography on soil macropores. Besides, macropore characteristics may vary over time depending upon various factors like biological activities, wetting and drying cycles, and management practices (Cameira et al., 2003). Hence, quantification of both temporal and spatial variability of soil macropore characteristics is crucial for the comprehensive understanding of water and contaminant transport in soils.

Similar to the pasture field in north Alabama, repeated application of dairy manure on the row-crop field has become a serious threat to the water bodies in Wisconsin. This necessitates the quantification of soil macropores to elucidate the transport mechanisms in this region. Besides, different factors such as land use and tillage practices can affect the soil macropore characteristics (Cameira et al., 2003; Luo et al., 2010). These differences in the soil macropore system may cause significant changes in soil hydraulic properties and the transport of different contaminants. Therefore, it is essential to investigate the impact of land use and tillage practices on soil macropore characteristics that will help us diagnose changes caused by these practices and design appropriate management guidelines to address the problems concerning water quality.

1.2 Research Objective

The major goal of this study was to quantify soil macropore characteristics under different row crop fields and pasture using X-ray Computed Tomography (CT). The major goal was achieved by accomplishing three specific objectives mentioned below:

1) Quantify the variability in soil macropore characteristics as a function of depth and topographical location in a pasture field.

2) Determine the temporal variability in 3D soil macropore characteristics in different soil depth layers and topographical locations.

3) Quantify effect of different land uses on soil macropore characteristics.

1.3 Thesis outline

Chapter 2 of this thesis presents the use of X-ray Computed Tomography (CT) and image analysis to quantify the soil macropore characteristics under different upslope, midslope, and downslope locations within a pasture field. In Chapter 3, detailed study of both the temporal and spatial variability of different 3D soil macropore characteristics in a pasture field are discussed. Similarly, Chapter 4 pertains to the impact of different land uses and tillage practices on soil macropore characteristics as quantified using CT. Finally, the conclusions of this study and recommendations for the future work are presented in Chapter 5.

1.4 References

Amer, A.M.M., Logsdon, S.D., Davis, D., 2009. Prediction of hydraulic conductivity as related to pore size distribution in unsaturated soils. Soil Sci. 174, 508–515. https://doi.org/10.1097/SS.0b013e3181b76c29

Cameira, M.R., Fernando, R.M., Pereira, L.S., 2003. Soil macropore dynamics affected by tillage and irrigation for a silty loam alluvial soil in southern Portugal. Soil Tillage Res. 70, 131–140. https://doi.org/10.1016/S0167-1987 (02)00154-X

Helliwell, J.R., Sturrock, C.J., Grayling, K.M., Tracy, S.R., Flavel, R.J., Young, I.M., Whalley, W.R., Mooney, S.J., 2013. Applications of X-ray computed tomography for examining biophysical interactions and structural development in soil systems: A review. Eur. J. Soil Sci. 64, 279–297. https://doi.org/10.1111/ejss.12028

Holden, J., 2009. Topographic controls upon soil macropore flow. Earth Surf. Process. Landforms 34, 613–628. https://doi.org/10.1002/esp

Jarvis, N.J., 2007. A review of non-equilibrium water flow and solute transport in soil macropores: principles, controlling factors and consequences for water quality. Eur. J. Soil Sci. 58, 523-546. https://doi.org/10.1111/j.1365-2389.2007.00915.x

Katuwal, S., Norgaard, T., Moldrup, P., Lamandé, M., Wildenschild, D., de Jonge, L.W., 2015. Linking air and water transport in intact soils to macropore characteristics inferred from X-ray computed tomography. Geoderma 237–238, 9–20. https://doi.org/10.1016/j.geoderma.2014.08.006

Lamba, J., Srivastava, P., Way, T.R., Malhotra, K., 2019. Effect of Broiler Litter Application Method on Metal Runoff from Pastures. J. Environ. Qual. 48, 1856–1862. https://doi.org/10.2134/jeq2018.08.0318

Li, X., W. McCarty, G., 2019. Application of Topographic Analyses for Mapping Spatial Patterns of Soil Properties. Earth Obs. Geospatial Anal. [Working Title]. https://doi.org/10.5772/intechopen.86109

Luo, L., Lin, H., Li, S., 2010. Quantification of 3-D soil macropore networks in different soil types and land uses using computed tomography. J. Hydrol. 393, 53–64. https://doi.org/10.1016/j.jhydrol.2010.03.031

Matthews, G.P., Laudone, G.M., Gregory, A.S., Bird, N.R.A., De, A.G., Whalley, W.R., 2010. Measurement and simulation of the effect of compaction on the pore structure and saturated hydraulic conductivity of grassland and arable soil. Water Resour. Res. 46, 1–13. https://doi.org/10.1029/2009WR007720

Mees, F., Swennen, R., Van Geet, M., Jacobs, P., 2003. Applications of X-ray computed tomograpy in the geosciences. Geol. Soc. Spec. Publ. 215, 1–6. https://doi.org/10.1144/GSL.SP.2003.215.01.01

Pires, L.F., Roque, W.L., Rosa, J.A., Mooney, S.J., 2019. 3D analysis of the soil porous architecture under long term contrasting management systems by X-ray computed tomography. Soil Tillage Res. 191, 197–206. https://doi.org/10.1016/j.still.2019.02.018

Sen, S., Srivastava, P., Yoo, K.H., Dane, J.H., Shaw, J.N., Kang M.S., 2008. Runoff generation mechanisms in pastures of the Sand Mountain region of Alabama-a field investigation. Hydrol. Process. 14, 369-385. https://doi.org/10.1002/hyp.7502

Singh, P., Kanwar, R.S., Thompson, M.L., 1991. Macropore Characterization for Two Tillage Systems Using Resin-Impregnation Technique. Soil Sci. Soc. Am. J. 55, 1674–1679. https://doi.org/10.2136/sssaj1991.03615995005500060029x

Wahl, N.A., Bens, O., Buczko, U., Hangen, E., Hüttl, R.F., 2004. Effects of conventional and conservation tillage on soil hydraulic properties of a silty-loamy soil. Phys. Chem. Earth 29, 821–829. https://doi.org/10.1016/j.pce.2004.05.009

Chapter 2

Using X-ray Computed Tomography to Quantify Variability in Soil Macropore Characteristics in Pastures

2.1 Abstract

Soil macropores largely control the transport of water and solutes in subsurface flows. Preferential flow via soil macropores can substantially affect water quality. Hence, it is important to quantify soil macropore characteristics and link this information with the preferential flow behavior in soils. However, whether macropore structure at one slope position within a field is different than that at another is unclear. With differences in the macropore characteristics, each slope position can contribute differently to the runoff and subsurface flows. The objective of this study was to use X-ray computed tomography (CT) and image analysis to characterize soil pore structure (>0.75 mm diameter) at upslope, midslope, and downslope positions within a 0.40 ha pasture field. A total of 18 undisturbed soil columns (150 mm diameter and 500 mm depth) were collected from a pasture field located at the Sand Mountain Research and Extension Center, Alabama, during May 2019. The results indicated that both the macropore number and macroporosity values were lowest at the downslope position in the 0-100 mm soil layer. In contrast, a large number of macropores was observed at the downslope soils for depths below 200 mm. The lowest macroporosity values in the surface layer at the downslope position can be attributed to higher degree of trampling induced compaction due to higher soil moisture content at the downslope location, via runoff and seepage losses from the upper slopes. Likewise, it was found that using smaller diameter soil cores for sampling can cause bias in the soil macropore measurements due to considerably high coefficient of variation compared to the larger diameter soil cores. Macropore interconnectivity at the subsurface layer (100-500 mm) increased from the upslope to the downslope position, whereas at

the soil surface (0-100 mm), the interconnectivity was lowest at the downslope position as compared to the upslope and midslope locations. The results of this study provide quantitative information of different soil macropore characteristics under varying topographical locations and depths in a pasture field. The relevance of topographical variation of different macropore characteristics found in this study should be tested by investigating a wider range of soil types and slopes in pastures.

Keywords: Preferential flow; Compaction; Image analysis; Grazing; Pore size distribution

2.2 Introduction

In recent years, there has been an increasing interest to understand loss of pollutants via subsurface flow pathways, specifically in areas where subsurface flows are significant (McGrath et al., 2010). The hydrologically active macropores (i.e., pore size > 0.3-0.5 mm diameter, Jarvis, 2007) can result in non-equilibrium flow conditions and therefore play an important role in the movement of water and agrochemicals through the soil profile (Luxmoore et al., 1990). Although, macropores represent only a small fraction of the overall soil porosity, they can result in transport of fertilizers and other contaminants to relatively deep depths in soil and even to the groundwater (Jarvis, 2007). Preferential flow via soil macropores in the presence of an impermeable soil layer can result in transport of surface applied fertilizers and other chemicals to relatively long distances within a watershed (Wang et al., 2011). In certain soils, preferential flows can contribute to the transport of more than 90% of water and contaminants (Shaffer et al., 1979). For example, a study in the Walker Branch watershed in eastern Tennessee, USA reported that preferential flow was the predominant mechanism of streamflow generation (Wilson et al., 1990). Therefore, quantification of macropores characteristics can improve our understanding of preferential flows and help develop a reasonable mathematical model (Zhang et al., 2017).

Topographical differences at a field level exert a strong control on soil properties including bulk density, moisture content, and organic matter content, which in turn may contribute to the variation in soil macropores (Hao et al., 2002; Oztas et al., 2003). A small difference in topography can cause major changes in soil development (Rezaei and Gilkers, 2005). Soil properties including moisture content and organic matter content, which are primarily influenced by the topography, promote the formation and stabilization of larger pores in the soil (Grosbellet et al., 2011; Holden, 2009). For example, in a grazed pasture field, macroporosity of the surface soil is influenced by the soil water content, which affects the degree of compaction by trampling. Continuous grazing of pastures can cause reduction in topsoil porosity (Singleton et al., 2000) and vertical pore continuity (Greenwood and McKenzie, 2001) through the disruption of large aggregates and repacking with smaller aggregates to fill existing soil pores (Cattle and Southorn, 2010). Macropore structure damage by such compaction commonly occurs in surface layers and decreases with depth (Drewry et al., 2008). Warren et al. (1986) suggested that the impact of livestock trampling is generally more significant with higher soil moisture content at the time of trampling. However, limited work has been done to investigate how distribution of macropores will change as a result of topographical differences.

X-ray computed tomography (CT) is a relatively new and promising approach to analyze the configuration of soil pores in the soil profile (Rab et al., 2014; Luo et al., 2010). A major advantage of this method is that it is non-destructive and can help quantify macropores in 3-D (Helliwell et al., 2013). An important limitation of this approach is that the ability to detect pores of specific size depends on different interrelated factors including scanner properties and the diameter of the soil samples (Mees et al., 2003). While reducing the diameter of the soil core increases the spatial resolution (i.e., smaller size pores can be detected), smaller cores may fail to capture differences

in the heterogeneous soil matrix. Besides, though CT method itself might be non-destructive, there could be some sampling induced disturbances near the edges of the soil cores, which needs to be addressed before performing any analyses. Other methods, such as dye tracers (e.g., Wahl et al., 2004), resin impregnation (Singh et al., 1991), and tension infiltrometer (e.g., Mohanty et al., 1996; Cameira et al., 2003) have also been widely used for studying macropores in the past. However, measurements of macroporosity using the above-mentioned methods are indirect, time-consuming, and less accurate in reflecting the subtle features of the soil pore networks (Amer et al., 2009; Matthews et al., 2010). Nonetheless, CT techniques have been successfully used to determine the number, size, and distribution of macropores (Warner et al., 1989; Rab et al., 2014; Luo et al., 2010).

Apart from the promising application of the CT technique in the field of soil science, a consistent sampling strategy is needed to allow for comparison of results of different studies. Therefore, it is important to understand the effects of different sampling strategies, specifically effect of size of soil core considered for CT analysis on soil pore characteristics (Rab et al., 2014). Pires et al. (2004) used CT to study soil compaction induced by sampling on soil cores 26 mm in diameter, reported a clear heterogeneity of soil bulk density within the soil sample, with larger values near the edges and the lowest bulk density values along the center of the soil sample. Results of the study conducted by Rab et al. (2014) using a range of core diameters (50 or 65 mm) suggest that macropore characteristics can differ significantly with change in core size. Previous studies have also shown that decreasing the overall size of a soil core results in the reduction of large and continuous pores responsible for preferential flow (Iversen et al., 2001; Picolli et al., 2019). Hence, larger volume soil cores should be sampled to decrease variability in macropore measurements and obtain accurate measurements of the soil macropores (Picolli et al., 2019; Rab et al., 2014).

However, to date, all of the CT studies that specifically focused on effect of sampling volumes on pore characteristics used smaller diameter (<150 mm) soil cores. The smaller diameter cores may fail to reflect the heterogeneity evident in soils. Additionally, the compaction effect of the sampled soil volume is greater for cores with smaller diameter than for the larger ones (Castellini et al., 2020). In this respect, lack of knowledge still exists on the effect of the sampling volume on soil macropore estimates.

Quantification of macropore characteristics in soils, where subsurface flows are substantial, is important to understand pollutant transport processes. In the Sand Mountain region of north Alabama, which is a major poultry-producing region, excessive buildup of phosphorus (P) in soils and contamination of surface water bodies with P has been a serious issue due to the continuous application of poultry litter to the pastures (Sen et al., 2008). Sen et al. (2008) ascertained that both the surface and subsurface runoff generation mechanisms could be responsible for the off-site transport of contaminants in this region. Also, results of a study conducted by Lamba et al. (2012) show that less than 10% of rainfall contributed to surface runoff and more than 90% infiltrated into the soil, suggesting that there might be significant macropore flows in this area. Furthermore, previous studies reported that loss of contaminants (e.g., P, nitrogen, and metals via subsurface flows could be substantial in this region (Lamba et al., 2019, 2013). Therefore, it is very important to understand the macropore characteristics in this region to elucidate subsurface flow mechanisms.

Till date, only one study (Zong-Chao Li et al., 2019) has used CT to quantify the influence of topography on soil macropore characteristics. The results of this study demonstrated a clear distinction in macropore characteristics among three slope positions in an alpine meadow. However, those results were based on relatively small number of replicates (n=3). Besides, their

study area was located in a high-altitude climate zone with mean annual temperature and precipitation of 0.1 °C and 400 mm, respectively, which is completely different than humid subtropical climate at our study site. To our knowledge, no study has reported direct measurements of soil macropore characteristics influenced by the topographical location in pastures. The results of Zong-Chao Li et al. (2019), in conjunction to this study, can provide useful information on the effects of topography on soil macropore characteristics and preferential flow in different land management systems under different climatic conditions. Therefore, the objective of this study was to quantify soil macropore characteristics in different soil layers and slope positions using CT and image analysis. A further objective was to investigate the effect of selecting different image cross-sections on macropore characteristics. We hypothesized that the macropore measurements were linked with the topographical position and depth of the soil sample. The results of this study would provide valuable dataset to understand flow and pollutant transport processes in a region where macropore flows drive the hydrology.

2.3 Materials and methods

2.3.1 Study site

The soil columns investigated in this study were excavated from a hillslope pasture field (34° 17' 02.6" N, 85° 57' 51.8" W) located at the Sand Mountain Research and Extension Center (SMREC) in north Alabama at an elevation of about 350 m above the mean sea level. The site where the study was conducted is an approximately 0.40 ha field with a slope length of 80 m. The site had been grazed by cattle for more than 15 years prior to sampling. Approximately 50 cattle grazed the entire field at a time. To ensure better development and longevity of the tall fescue plant, grazing was discontinued when the height of the grass was 100 mm or less. The slope of the site was 3.4%. The soil at study site are Hartsells fine sandy loam (fine-loamy, siliceous, subactive,

thermic Typic Hapludults) and Wynnville fine sandy loam (fine-loamy, siliceous, subactive, thermic Glossic Fragiudults). The Hartsells soil is well drained with moderate permeability, primarily found on broad smooth plateaus, mountaintops, or hilltops. The parent material of these soils is loamy residuum weathered from sandstone and shale (Soil Survey Staff, 2020). The Wynnville series consists of moderately well drained, slowly permeable soils also formed from sandstone and shale. At the study site, Sen et al. (2008) has reported presence of a restrictive layer near the soil surface that could cause formation of a perched water table during intense rainfall events. Based on an analysis of 30-year normals, mean annual precipitation in this region is 1340 mm, and the mean annual temperature is 14.8 °C. A cool-season grass (Kentucky 31 tall fescue (*Festuca arundinacea* Schreb)) has been growing at the study site for more than 40 years. This grass has an extensive root system which extends to a depth of 900 mm below the soil surface, providing access to water and other resources, and offers better heat and drought tolerance than many other cool-season grasses (Cougnon et al., 2017).

2.3.2 Soil sampling

A total of 18 undisturbed soil columns (150 mm diameter, and 500 mm depth) were collected in May 2019. Six cores were collected from each of three topographical locations (upslope, midslope, and downslope) within the field. The samples were obtained using rigid PVC pipes driven carefully into the soil by utilizing a tractor-mounted soil coring system (Prior et al., 2004). After sampling, the airspace at each end of each soil column in PVC pipe was filled with bubble wrap packing material, and a PVC end cap was fitted over each end of the pipe before transportation. During transportation, a 150 mm thick layer of wood shavings supported the soil columns to serve as cushioning, to minimize disturbance of the soil columns. The samples were then stored at 4 °C until further analysis. In addition to the 18 cores, two extra soil columns were collected from the

field, to allow us to make artificial soil pores of known diameter in the soil. These cores were later used as a reference to allow us to distinguish between the pores and the rest of the soil matrix. Prior to scanning, all the soil columns were saturated with water and left to drain for about 3 days in order to maintain a uniform moisture condition among all cores (Luo et al., 2010). This was done to minimize the variability in the X-ray attenuation value histogram and to make the comparison between different slope positions more consistent. Thus, each soil column was assumed to be at approximately field capacity before scanning. The bottom of each soil core was checked to make sure they are dry enough to avoid any damage while transporting cores for scanning.

Additional 3 soil samples were collected from each topographical location at different depth intervals (0-100 mm, 100-200 mm, 200-300 mm, 300-400 mm, and 400-500 mm) for the analysis of routinely measured soil properties (e.g., bulk density, organic matter content, and texture) (Table 2.1). The sand, silt, and clay percentages of soils were determined using hydrometer method (Bouyoucos, 1962). Organic matter content was determined by the weight loss on ignition method (Huisman et al., 2013). The soil bulk density was calculated as the mass of oven-dried soil divided by its volume. The soil texture and bulk density information was used to estimate saturated hydraulic conductivity (K_{sat}) of top soil surface layer (0-100 mm) using the Rosetta model (Schaap et al., 2001), which is integrated into the HYDRUS software (Šimůnek et al., 2016). Rosetta is a pedotransfer function (PTF) that uses neural network model to predict the soil hydraulic parameters based on easily measured data, such as soil texture and bulk density (Domúnguez-Niño et al., 2020).

2.3.3 CT scanning and image analysis

The soil cores were scanned using a medical GE LightSpeed VCT 64 Slice CT scanner (GE Healthcare, Chicago, IL) installed in the Bailey Small Animal Teaching Hospital at the Auburn University College of Veterinary Medicine (AUCVM). The machine has the ability to take up to 64 slices in one scan, thus, covering 40 mm at 0.625 mm slice thickness in one scan. The scanner was operated with the scanning parameters set to 140 KV, 140 mA, and 1 s exposure time, and this provided detailed projections with relatively little noise. The field of view (FOV) was set to 180 mm producing 16-bit 512x512 images with a voxel size of 0.35x0.35x0.625 mm^3.

These images were analyzed using the ImageJ version 1.52t software (Rueden et al., 2017), which is a digital image processing program developed by the US National Institutes of Health (Bethesda, MD). The software was used to determine the macropore number, macropore diameter (ECD), macroporosity, and inter-connectivity for each stack. To avoid voids near the core walls, the diameter of the core was reduced from 150 mm to 136 mm, and the area beyond this region of interest (ROI) was deleted by using the "clear outside" tool in ImageJ. The slices from the bottom of the core which were void or seemed to be disturbed were excluded from the original stack for analysis. After adjusting the brightness and contrast of the images, a *median filter* with a radius of 1 pixel was used to reduce noise in the images. The "Unsharp mask" command with its default values (radius of 1 pixel and mask weight of 0.6) was used to sharpen and enhance the edges.

The images were segmented using Phansalkar's method of local thresholding which is a modification of Sauvola's thresholding method to deal with low contrast images (Phansalkar et al., 2011). All the images were converted to 8-bit before performing this operation. The threshold value T for the 8-bit images were then calculated as:

$$T = mean * (1 + p * exp(-q * mean) + k * ((stdev / r) - 1)) \quad \ldots\ldots\ldots\ldots\ldots\ldots (1)$$

where mean and stdev are the local mean and standard deviation for a selected window size, respectively. The parameter k is a constant which takes values in the range [0.2, 0.5] whereas, r is the dynamic range of standard deviation which is equal to 0.5 for a normalized image (Phansalkar et al., 2011). These parameters were set to their default values in the ImageJ software (k = 0.25 and r = 0.5) to get the best segmentation results. The values of parameters p and q were 2 and 10, respectively and are fixed in the plugin. The segmentation was carried out using a radius of 5 pixels over which the threshold was computed. All the images were visually inspected for the performance of the segmentation procedure in separating the pores and solids. To determine the parameters of thresholding (i.e., k, r, and the radius), Plexiglas thermoplastic cylinders of two different diameters (3.17 mm and 4.76 mm) were inserted into an undisturbed soil column to create artificial macropores. The Plexiglas rods were pulled out just before CT scanning. The macropore size of the artificial pores with known diameter based on image analysis was compared with the actual pore size for different randomly selected thresholding parameter values. A parameter value was selected if the difference between the actual and the image-analyzed pore size was less than 1.5% for both rod diameters.

The binary images were then analyzed using the "Analyze Particles" tool in ImageJ to determine the number of pores and pore area in a 2-D representation of a slice. Since the pixel resolution was 0.35 mm * 0.35 mm, only those pores with equivalent cylindrical diameter (ECD) greater than twice the resolution i.e., 0.70 mm could be reliably identified using the image processing method. The equivalent cylindrical diameter was calculated based on the surface area using the equation: $ECD = 2(area/\pi)^{0.5}$. We considered pores with ECD >0.75 mm as macropores in this study, similar to Luo et al. (2008) and Luo et al. (2010). This was done to ensure that we were not quantifying

any noise as pores in our analyses. All the pores with ECD smaller than 0.75 mm were considered as noise and removed from the analysis. The number of macropores, diameter, and macroporosity were calculated for each slice and then averaged to quantify the variation with depths. Macropores, especially with diameter (ECD) > 1 mm, promote water movement through the soil profile (Udawatta et al., 2008). Node density, which is the sum of the number of nodes where at least two pore branches connect per unit volume of soil considered, was used to quantify the interconnectivity of the macropores (Luo et al., 2010). A high density of junctions is related to an extensive and well-connected pore network (Munkholm et al., 2012). For this, the BoneJ plug-in (Doube et al., 2010) in the ImageJ software was used. All the macropores were first skeletonized using BoneJ plug-in to determine the number of nodes in each 3D macropore network.

All the pores were divided into two pore-size classes: pores with ECD greater than 0.75 mm and less than 1 mm, and those greater than 1 mm. Thus, both macroporosity and number of pores were determined for these pore classes. The total pore area covered by pores 0.75 - 1 mm, and >1 mm was divided by the total ROI, i.e., 14527 mm^2 to estimate the macroporosity.

In addition, depth to the most restrictive layer was determined for each soil column. For this, macroporosity of each slice perpendicular to the column axis (0.625 mm thickness) along the length of the column was calculated. The slice with least macroporosity was defined as the limiting layer for any particular soil column. Additional analyses were performed to investigate the effect of the sample volume within a core. In the previous studies, soil cores of varying diameter (40 mm – 200 mm) have been collected to determine macropore characteristics. However, depending on the size of the core, soil pore characteristics could vary. To analyze the effects of sample volume on macropore measurements, the thresholded images were sub-sampled twice (Figure 2.1) using the top 0-100 mm depth of each soil sample. Firstly, all the cylindrical cores (136 mm ROI) were

cropped into a concentric rectangular prism to further remove any possible edge effects. The first sub-sampling occurred by cropping the rectangular ROI into 4 cylindrical sub-sample cores (48.1 mm diameter) as depicted in Figure 2.1 (a). A second sub-sampling was done by cropping the rectangular ROI into 16 equal sized cylindrical sub-sample cores (24.05 mm diameter) as shown in Figure 2.1 (b). Variability in soil macropore characteristics for each diameter sub-sample was quantified by calculating the coefficient of variation (CV). Since sample height affects the soil macropore characteristics, the depth of the samples was left unchanged for each sub-sampling. Hence, observed pore characteristics variability may be linked to the difference in soil sample diameter.

2.3.4 Statistical analysis

All statistical analyses were performed using SAS version 9.4 (SAS Institute, USA). The significance test for the effects of slope position on different soil characteristics was done using one-way analysis of variance (ANOVA) within the General Linear Model (GLM) procedure. The Tukey's multiple comparison test was used to compare the soil characteristics as a function of soil depth and topographic location. The normality and homogeneity of variances for all the parameters were tested using Shapiro-wilk test and Levene's test, respectively. A repeated measures analysis with PROC MIXED was used to account for correlation between measurements within the same sample. All statistical tests were conducted at the 95% confidence level.

2.4 Results

2.4.1 Distribution of macroporosity and number of macropores in different soil layers and slope positions

The number of soil macropores followed similar trends for both the macropore size classes at all the topographical locations (Figure 2.2). However, for >1 mm soil pores, the number of

macropores was less in the 100-200 mm depth layer compared to the 0-100 mm layer. The macropore number of 0.75-1 mm pores showed a gradual increase with the depth. Significant differences ($P<0.05$) were found in the number of soil macropores at different topographical locations for a given depth (Figure 2.2). For example, in the shallow soil layer (0-100 mm), the number of macropores for both size classes was significantly less ($P<0.05$) for the downslope location than the midslope and upslope locations. However, at the deeper soil depths (e.g., 200-300 and 300-400 mm), the number of macropores at the downslope location was significantly greater ($P<0.05$) than either the upslope or midslope location.

The distribution of the macroporosity values for the three topographical locations corresponded well with the number of macropores. The soil macroporosity of >1 mm soil pores first declined sharply with increasing depth down to 200 mm and then increased gradually at all the slope positions, whereas a general increase with depth was observed for 0.75-1 mm soil pores (Figure 2.3). Most of the macropores at the downslope location were concentrated in the deep soil layers (250-500 mm). The macropores at the upslope locations were comparatively well distributed throughout the entire depth of the soil column. Significant differences ($P<0.05$) in macroporosity among the three topographical locations were observed only for 0.75-1 mm pores. In the shallow soil layers (0-100 mm and 100-200 mm), macroporosity of 0.75-1 mm soil pores at the downslope location was significantly lower ($P<0.05$) than that of the upslope location. Quantitative data on the soil macropore characteristics are presented in Table 2.2. No significant differences ($P>0.05$) were noted for the overall macropore characteristics (0-500 mm) between any of the slope positions.

2.4.2 Limiting macroporosity at different slope positions

The depth to limiting macroporosity at different topographical positions is presented in Figure 2.4. At the downslope location, the restricting depths were present from 100 to 150 mm, with an average limiting macroporosity value of 0.27%. The restricting depths at the upslope location were also observed within the top 150 mm of soil depth; for two cores the restricting depths were at 60 and 63 mm, while for the other four, the depth ranged from 120 to 150 mm. The limiting macroporosity values for soils at the upslope locations were clearly higher than those at the downslope location. For all the soil columns from the midslope location, the limiting macroporosity values were observed at deeper depths (>150 mm) and the macroporosity values were much higher as compared to the soils at the downslope location.

2.4.3 Diameter distribution of macropores in different soil layers and slope positions

No significant differences were observed in the overall mean macropore size (ECD) among the three slope locations (Table 2.2). The ECD was greater at the downslope location, 1.65 (±0.09) mm, as compared to the midslope, 1.63 (±0.15) mm, and upslope locations, 1.57 (±0.07) mm. At the top 0-100 mm soil layer, the mean macropore diameter at the downslope position was significantly ($P<0.05$) higher, 2.11 (±0.27) mm, compared to 1.80 (±0.15) mm for the upslope position. The ECD distribution of macropores at different slope positions and soil depths was evaluated for six different diameter classes (0.75-1 mm, 1-2 mm, 2-3 mm, 3-4 mm, 4-5 mm, and >5 mm) as shown in Figure 2.5. In all the cores sampled from different topographical locations, the macropore size for the majority of the pores was between 1 and 2 mm (Figure 2.5). Three size classes (0.75-1 mm, 1-2 mm, and 2-3 mm) accounted for more than 80% of all macropores in all the soil layers. At depths below 100 mm, only two size fractions (0.75-1 mm and 1-2 mm) accounted for more than 80% of all the counted macropores. In the 0-100 mm surface layer, the

smallest size fraction (0.75-1 mm) accounted for only about 20% of the counted macropores, whereas at the deeper soil depths (100-200 mm, 200-300 mm, 300-400 mm, and 400-500 mm), size fraction (0.75-1 mm) accounted for more than 30% of the overall detected macropores.

2.4.4 Macropore connectivity at different slope positions

Inter-connectivity, quantified using the node density of macropores, indicated there was a significant effect ($P<0.05$) of depth on the macropore interconnectivity in the soils at the downslope position (Figure 2.6). The inter-connectivity of the surface soil (0-100 mm) at the downslope location was significantly less ($P<0.05$) as compared to the subsurface (100-500 mm) interconnectivity, whereas no significant ($P>0.05$) reduction in interconnectivity was seen in the surface soil layer (0-100 mm) at the upslope and midslope locations. In contrast to the soil at the downslope location, the soil at the midslope and upslope locations had a relatively higher interconnectivity in the surface soil layer (0-100 mm). Overall, subsurface interconnectivity increased from the upslope towards the downslope location.

2.4.5 Effect of analyzed soil volume on macropore characteristics

This analysis was performed with two different sizes of soil cores (48.1 mm and 24.05 mm diameter). The 24.05 mm core showed higher variability in macroporosity and ECD as compared to the 48.1 mm soil core. The coefficient of variation (CV) for macroporosity ranged from 14.8 % to 50.2 % in the 48.1 mm core, whereas for the 24.05 mm core, it ranged from 33.7 % to 88% (Figure 2.7). Specifically, the CV for different macropore characteristics was higher in the downslope location compared to the upslope and midslope locations for both diameter cores. Maximum and minimum CV for ECD was 24.1 % and 3.6 % in the 48.1 mm core, respectively, and 35.2 % and 15.5 % in the 24.05 mm core, respectively. In contrast, macropore number did not show substantial difference in CV between the two sub-volumes.

2.5 Discussion

2.5.1 Spatial distribution of soil macropore characteristics

Results from this study demonstrated that the spatial macropore characteristics were distinctly different for each slope position. In the surface layer (0 to 100 mm), the macropores were relatively larger at all the slope positions (Table 2.2). These macropores were likely formed by root channels and earthworm burrows, whereas smaller and separated macropores just below the surface soil layer were probably the inter-aggregate pores (Luo et al., 2008). In addition, all the soil columns had relatively less macroporosity in the 100-200 mm depth layer. This is consistent with the findings of Sen et al. (2008) who reported presence of a restrictive layer near the surface soil at the study site. The sharp decline in macroporosity values from the first soil layer (0-100 mm) to the second soil layer (100-200 mm) for all the topographical locations can be attributed to both the rooting characteristics of Kentucky-31 tall fescue and long-term grazing. Balkcom et al. (2010), who conducted a study on tillage requirements of different crops at the SMREC also reported a compacted layer below 100 mm of the soil surface. They attributed the presence of this hard pan to winter grazing. In a study of relative rooting depth for different grasses, Brown et al. (2010) reported that more than 65% of the root mass of tall fescue (*F. arundinacea*) was distributed within the top 75 mm of the soil profile, whereas around 75% of the root mass was observed within the top 150 mm depth.

Significantly lower values of the number of macropores, and macroporosity of 0.75-1 mm pores at the surface layer (0-100 mm) at the downslope location were probably due to a combination of two reasons. First, compaction caused by cattle grazing (Luo et al., 2010) and second, greater soil moisture content expected at the surface of the downslope location compared to other topographical locations. Oztas et al. (2003) reported a higher degree of compaction at the

downslope location of a grazed hillslope, due to higher soil moisture contents of downslope locations compared to upslope locations. We speculate that, runoff and seepage from the upper slopes might have caused higher moisture content at the downslope location, and this increased the degree of compaction at the downslope location, caused by animal trampling. Sen et al. (2008) conducted a study at the SMREC and reported that locations within the field that have low K_{sat} values generate the most surface runoff in this area. The estimated saturated hydraulic conductivity (K_{sat}) at different slope positions using Rosetta model in HYDRUS showed that the average K_{sat} values were lower at the downslope location (0-100 mm), 33.8 ± 2.6 mm hr^{-1}, compared to 65.8 ± 16.8 mm hr^{-1} and 49.5 ±11.4 mm hr^{-1} at the midslope and upslope locations, respectively. Significant difference ($P<0.05$) in K_{sat} was observed only between the downslope and midslope locations. Thus, lower values of K_{sat} likely restricted the amount of water infiltrating into the soil profile at the downslope location. In other words, greater clay content, 38.6%, at the downslope location (0-100 mm), compared to 22.6% at the midslope, and 32.8% at the upslope location, might have retained a relatively high-water content at the downslope location, thereby facilitating compaction due to grazing (Table 2.1). This is consistent with the bulk density results (0-100 mm), which showed a relatively higher bulk density value at the downslope, 1.31 g cm^{-3}, compared to 1.17 g cm^{-3} and 1.10 g cm^{-3} at the midslope and upslope locations, respectively (Table 2.1). Similarly, Zong-Chao Li et al. (2019) observed a decrease in average soil macroporosity in the surface layer (0-100 mm) from the upper slopes to the downslope location. However, their study was conducted under an alpine meadow with a relatively steep slope (20 %) as compared to our study (slope = 3.4 %).

The average macroporosity determined for this pasture field ranged from 2.77 ± 0.37 % at the upslope to 3.39 ± 0.32 % at the downslope position (Table 2.2). These values are comparable with

Luo et al. (2010), who reported an average macroporosity of 3.1 % for a fine-loamy soil under pasture (102 mm diameter and 350 mm depth soil cores). Luo et al. (2010) quantified macropores as pores with ECD >0.75 mm, similar to that of our present study, to evaluate the macropore network variation among different land uses and soil types. Muller et al. (2018) observed a decreasing macroporosity with depth under a permanent pasture grazed by cattle and reported an average macroporosity of 6% for two different soils (Andosol and Gleysol), which is higher than the values reported in our study. This is due to the fact that they considered pores greater than or equal to 0.147 mm diameter in their analysis. Moreover, the trend of macroporosity variation with depth found in our study is consistent with the results of Perret et al. (1998) and Hu et al. (2015), who observed a sharp decrease in macroporosity for depths to 200 mm and then macroporosity values increased as the depth increased to 500 mm in grasslands. These fluctuations in the soil macropore characteristics within the 0-500 mm soil depth clearly indicate the importance of using deeper cores to accurately represent the overall macropore structure in an agricultural field. Since different studies use soil cores of various sizes, depth-wise comparison of the soil macropore characteristics should be made rather than comparing characteristics of the entire soil column. Overall, results indicate that soil macropores are prevalent in this region and therefore can be important pathways for subsurface flows potentially resulting in substantial off-site transport of pollutants. Besides, soil compaction due to grazing livestock increases the amount of tension-free water near the surface, so presence of macropores may facilitate the transport of water and contaminants to the subsoil and surface waters (Vuaille et al., 2020). Sen et al. (2008) reported that out of 26 rainfall events monitored at this study site from January 2006 to January 2007, only 8 storm events generated surface runoff. Furthermore, Lamba et al. (2012) reported that more than 90% of the rainfall infiltrates in this region and subsurface flows could be important pathway for

pollutant transport. Hence, results of our study in conjunction with Sen et al (2008) and Lamba et al. (2012) indicate that soil macropores play an important role in generation of subsurface flows in this region.

2.5.2 Evaluation of macropore connectivity and limiting macroporosity at different depths and slope locations

In addition to macroporosity, macropore diameter, macropore number and connectivity are key variables that affect the transport phenomenon in soil (Hu et al., 2018; Katuwal et al., 2015). High node density (interconnectivity) in soil is related to highly connected root networks and movement of earthworms and other organisms in the soil profile. Higher degrees of interconnectivity among the macropores in the downslope (Figure 2.6) could be because of favorable conditions for biota activities in the soil at the downslope location. However, significantly less interconnectivity at the surface (0-100 mm) of the downslope as compared to its subsurface interconnectivity (Figure 2.6) can be attributed to trampling effects of the cattle along with the high soil moisture content. The presence of compacted surface layer (0-100 mm) with less interconnected macropores could limit the transport capacity of macropores (Gerke et al., 2015) at the downslope location. However, it is worth noting that interconnectivity is likely associated with bridging connections formed by smaller pores (Vogel et al., 2010). The highly connected macropores at the surface (0-100 mm) of upslope and midslope soils might assist in lateral mixing of the flow with the soil matrix resulting in more homogenous flow through the soil profile (Katuwal et al., 2015). Therefore, in addition to the macroporosity and interconnectivity of the macropores, an important requirement for the functionality of the pores for transport processes is that the pores are continuous and vertically connected to improve air and water permeability throughout the soil profile (Pagenkemper et al., 2014), which needs further investigation.

Further analysis was conducted to investigate the limiting macroporosity values and its position in the soil profile. Flow and contaminant transport are strongly restricted at the "bottlenecks" in soil profile; thus, quantifying the position and macroporosity of limiting layer is important in understanding the soil hydraulic properties (Katuwal et al., 2015, Zhang et al., 2019). The restricting macroporosity layer was relatively closer to the soil surface at the downslope location as compared to the other topographical locations. Also, downslope location had the least values of limiting macroporosity compared to the US and MS locations. Based on these results, it is expected that flow at the downslope location could be largely restricted within the top 100 to 150 mm of the soil profile. On the other hand, this restrictive layer was observed deeper into the soil profile (>200 mm) at the MS location. The relative differences in the interconnectivity and limiting macroporosity results indicate that subsurface flow and transport mechanism could vary substantially with the topographical locations in the field.

2.5.3 Diameter distribution of macropores

As stated earlier the ECD of the macropores, in general, was larger at the downslope location as compared to the other topographical locations (Table 2.2). However, significant difference was observed only at the surface 0-100 mm soil layer. The larger ECD in the 0-100 mm downslope soil layer could be attributed to the higher organic matter content (6%), and higher clay content (38.6%), as compared to the midslope and upslope locations (Table 2.1). The finer texture and high organic matter content are favorable for earthworms and plant root growth (Luo et al., 2010). During soil sampling, we observed earthworms and some termites in the surface layer of the downslope soils but not at the other two slope positions. The results of ECD distribution shown in Figure 2.5 indicated that majority of the pores (>80%) in the soil cores have ECD less than 3 mm. This is consistent with previous findings by Hu et al. (2015), which reported that three size

fractions (< 1 mm, 1-2 mm, and 2-3 mm) accounted for more than 50% of the detected macropores in a shrub-encroached grassland. Besides, the fraction of smaller diameter pores (0.75-1 mm) was relatively less at the surface (0-100 mm) as compared to the deeper soil layers. In summary, the distribution of ECD with depth corresponded well with the distribution of roots of Kentucky-31 tall fescue (Brown et al., 2010). The most common macropore diameters observed in this study (0.75-1 mm and 1-2 mm) were consistent with the average root diameter of the plant as reported in a study by Głąb (2007). Therefore, our results show that the variation in macropore size in the soil profile was greatly influenced by the root characteristics of Kentucky 31 tall fescue.

2.5.4 Effect of analyzed soil volume on macropore characteristics

The large values of CV obtained in this study could be due to heterogeneity of the soil moisture within the soil profile (Gubiani et al., 2011), which likely affected the macropore characteristics. Higher variability in soil macroporosity and ECD for a 24.05 mm diameter core compared to a 48.1 mm diameter emphasize the bias of selecting a small core volume on the macropore characteristics measurements. Rab et al. (2014) reported that decreasing the volume of a 50 mm diameter soil core from 100% to 20% of the original volume had a significant effect ($P<0.05$) on mean pore diameter. However, their results were mostly based on the sampling induced compaction that affected the soil macropores near the edges as compared to the smaller sub-volumes taken at the center. Besides, they used a 50 mm diameter soil core, which is much smaller than the core used in this study. Since we analyzed only 96.2 mm portion of our 150 mm diameter core, we expect our results to be negligibly affected by the sampling induced compaction and the spatial variability of the soil properties played a major role. Picolli et al. (2019), who sub-sampled a 100 mm diameter core twice into progressively reducing sub-volumes, found that total porosity reduced significantly with decreasing volumes. However, since they changed the depth of soil core

during each sub-sampling, this discrepancy could be largely due to variation with depth, which is common. Nonetheless, these differences in measurements highlight the importance of sampling cores which are larger in diameter and will better represent variability in soil pore characteristics. Many authors have used smaller cores of diameter less than 150 mm to obtain a higher scan resolution, however it is important to considerate the effect of sampling smaller cores (<150 mm) on macropore characteristics. Overall, using larger diameter cores can help provide representative measurements of the soil macropore characteristics.

2.5.5 Implications of macropore characteristics for flow and contaminant transport

All the pores in the soil profile that are larger than 1 mm in equivalent diameter and are drained at field capacity are termed as macropores (Luxmoore et al., 1990, Perret et al., 1998). However, macropores are usually defined by considering both the data availability and the scale at which problem is to be addressed (Luo et al., 2008). In this study, we defined macropores as pores with ECD >0.75 mm. In a study conducted by Muller et al. (2018), near-saturated hydraulic conductivity was best predicted using the macroporosity consisting of macropores with diameters between 0.75 mm and 3 mm. Numerous studies in the past have demonstrated that the presence of soil macropores results in rapid downward movement of contaminants which may lead to groundwater and surface water pollution. Quantification of macropore characteristics help provide a better understanding of fate and transport processes of contaminants within the soil profile (Mooney and Morris, 2008; Jarvis et al., 1991). Borah and Kalita (1999) reported an improvement in the predictive capability of a solute leaching model (LEACHM) with the addition of a macropore flow component.

The differences in macropore characteristics among the different slope positions and depths imply that the soil hydraulic properties vary as a function of topographical location. Because of the

presence of macropores, contaminants may quickly bypass the soil profile and reach groundwater or nearby surface water through subsurface flows. Based on results of this study, it is expected that macropores would play a more prominent role in contaminant transport at the upslope and midslope locations, as compared to the downslope area. However, such an interpretation would be misleading in areas where there is a frequent ponding of water over a compacted soil surface. The presence of compacted and highly restrictive soil layer (<150 mm) could allow ponding of tension-free water near the surface of the downslope making macropores the "hotspots" for water and contaminant leaching, compared to the soils at the other slope positions. Overall, flow through the macropores are not controlled by one particular macropore characteristics; the susceptibility to preferential flow has to be inferred from multiple factors including pore continuity (Pagenkemper et al., 2014) and soil hydrologic conditions (Koestel and Jorda, 2014). The macropore characteristics quantified in this study need to be linked to soil hydraulic properties to better understand the flow and contaminant transport processes and develop appropriate management practices.

2.6 Conclusion

The study quantified variation in soil macropore characteristics at different depths at upslope, midslope, and downslope locations within a pasture field. The results show a clear and consistent evidence that macropore characteristic variation within the field was not random but indeed linked to the topographical position in the field. However, evidence of differences was observed only in the surface layer (0-100 mm). Similarly, topographical position influenced macropores of different sizes. For pores <1 mm diameter, both mean macropore number and macroporosity were significantly lower at the downslope location, at the surface layer (0-100 mm), compared to the soils at the upslope and midslope locations at the same depth. However, no significant differences

were seen between the three topographical positions for pores >1 mm at any depths. Lower surface interconnectivity and limiting macroporosity values were observed at downslope positions as compared to the other slope positions. This likely resulted from higher degree of compaction due to trampling at the downslope location, which is expected to have a high soil moisture content compared to upslope and midslope locations. In addition, architecture of the plant roots appears to have played an important role in variation of macropore characteristics. In comparing the variability associated with using different diameters soil cores for characterizing macroporosity, we found that macroporosity and ECD measurements could be largely biased because of higher values of CV for a smaller diameter sub-volume cores compared to the larger diameter cores. This result gives confidence in using cores with larger diameters (≥150 mm) to better estimate parameters such as ECD and macroporosity. Because of relatively high variation in different soil macropore characteristics, more replicates for each topographical positions might be needed to draw firmer conclusions on the dependence between slope positions and macropore characteristics. It also needs to be confirmed that the topographical variation of soil macropore characteristics found in this study are relevant for other pasture fields with different soil type – slope combinations.

2.7 Acknowledgement

This work was supported by the USDA-NIFA AFRI award # 2018-67019-27806, USDA-NIFA Hatch Project (ALA014-1-19052), and the Alabama Agricultural Experiment Station. We thank Marlin R. Siegford, Peyton Heath, Thomas Counts, Takhellambam Bijoychandra Singh, and staff at the Sand Mountain Research and Extension Center for assistance in this research project.

2.8 References

Amer, A.M.M., Logsdon, S.D., Davis, D., 2009. Prediction of hydraulic conductivity as related to pore size distribution in unsaturated soils. Soil Sci. 174, 508–515. https://doi.org/10.1097/SS.0b013e3181b76c29

Balkcom, K.S., Reeves, D.W., Kemble, J.M., Dawkins, R.A., Raper, R.L., 2010. Tillage requirements of sweet corn, field pea, and watermelon following stocker cattle grazing. J. Sustain. Agric. 34, 169–182. https://doi.org/10.1080/10440040903482571

Borah, M. J., and Kalita P. K. 1999. Development and evaluation of a macropore flow component for LEACHM. Trans. ASABE 42, 65–78.

Bouyoucos, G.J., 1962. Hydrometer Method Improved for Making Particle Size Analyses of Soils 1 . Agron. J. 54, 464–465. https://doi.org/10.2134/agronj1962.00021962005400050028x

Brown, R.N., Percivalle, C., Narkiewicz, S., DeCuollo, S., 2010. Relative rooting depths of native grasses and amenity grasses with potential for use on roadsides in New England. HortScience 45, 393–400. https://doi.org/10.21273/hortsci.45.3.393

Cameira, M.R., Fernando, R.M., Pereira, L.S., 2003. Soil macropore dynamics affected by tillage and irrigation for a silty loam alluvial soil in southern Portugal. Soil Tillage Res. 70, 131–140. https://doi.org/10.1016/S0167-1987(02)00154-X

Castellini, M., Giglio, L., Modugno, F., 2020. Sampled soil volume effect on soil physical quality determination: A case study on conventional tillage and no-tillage of the soil under winter wheat. Soil Syst. 4, 1–13. https://doi.org/10.3390/soilsystems4040072

Cattle, S.R., Southorn, N.J., 2010. Macroporosity of pasture topsoils after three years of set-stocked and rotational grazing by sheep. Aust. J. Soil Res. 48, 43–57. https://doi.org/10.1071/SR09004

Cougnon, M., De Swaef, T., Lootens, P., Baert, J., De Frenne, P., Shahidi, R., Roldán-Ruiz, I., Reheul, D., 2017. In situ quantification of forage grass root biomass, distribution and diameter classes under two N fertilisation rates. Plant Soil 411, 409–422. https://doi.org/10.1007/s11104-016-3034-7

Domúnguez-Niño, J.M., Arbat, G., Raij-Hoffman, I., Kisekka, I., Girona, J., Casadesús, J., 2020. Parameterization of soil hydraulic parameters for HYDRUS-3D simulation of soil water dynamics in a drip-irrigated orchard. Water (Switzerland) 12. https://doi.org/10.3390/W12071858

Doube, M., Klosowski, M.M., Arganda-Carreras, I., Cordelières, F.P., Dougherty, R.P., Jackson, J.S., Schmid, B., Hutchinson, J.R., Shefelbine, S.J., 2010. BoneJ: Free and extensible bone image analysis in ImageJ. Bone 47, 1076–1079. https://doi.org/10.1016/j.bone.2010.08.023

Drewry, J.J., Cameron, K.C., Buchan, G.D., 2008. Pasture yield and soil physical property responses to soil compaction from treading and grazing - A review. Aust. J. Soil Res. 46, 237–256. https://doi.org/10.1071/SR07125

Gerke, K.M., Sidle, R.C., Mallants, D., 2015. Preferential flow mechanisms identified from staining experiments in forested hillslopes. Hydrol. Process. 29, 4562–4578. https://doi.org/10.1002/hyp.10468

Głąb, T. 2007. Effect of soil compaction on root system morphology and yields of tall fescue. Int. Agrophysics. 21, 233–239.

Greenwood, K.L., McKenzie, B.M., 2001. Grazing effects on soil physical properties and the consequences for pastures: A review. Aust. J. Exp. Agric. 41, 1231-1250.https://doi.org/10.1071/EA00102

Grosbellet, C., Vidal-Beaudet, L., Caubel, V., Charpentier, S., 2011. Improvement of soil structure formation by degradation of coarse organic matter. Geoderma 162, 27–38. https://doi.org/10.1016/j.geoderma.2011.01.003

Gubiani, P.I., Reichert, J.M., Reinert, D.J., Gelain, N.S., 2011. Implications of the variability in soil penetration resistance for statistical analysis. Rev. Bras. Cienc. do Solo 35, 1491–1498. https://doi.org/10.1590/s0100-06832011000500003

Hao, Y., Lal, R., Owens, L.B., Izaurralde, R.C., Post, W.M., Hothem, D.L., 2002. Effect of cropland management and slope position on soil organic carbon pool at the North Appalachian Experimental Watersheds. Soil Tillage Res. 68, 133–142. https://doi.org/10.1016/S0167-1987(02)00113-7

Helliwell, J.R., Sturrock, C.J., Grayling, K.M., Tracy, S.R., Flavel, R.J., Young, I.M., Whalley, W.R., Mooney, S.J., 2013. Applications of X-ray computed tomography for examining biophysical interactions and structural development in soil systems: A review. Eur. J. Soil Sci. 64, 279–297. https://doi.org/10.1111/ejss.12028

Holden, J., 2009. Topographic controls upon soil macropore flow. Earth Surf. Process. Landforms 34, 613–628. https://doi.org/10.1002/esp

Huisman, N.L.H., Karthikeyan, K.G., Lamba, J., Thompson, A.M., Peaslee, G., 2013. Quantification of seasonal sediment and phosphorus transport dynamics in an agricultural

watershed using radiometric fingerprinting techniques. J. Soils Sediments 13, 1724–1734. https://doi.org/10.1007/s11368-013-0769-0

Hu, X., Li, Z., Li, X., Wang, P., Zhao, Y., Liu, L., Lu, Y., 2018. Soil Macropore Structure Characterized by X-Ray Computed Tomography Under Different Land Uses in the Qinghai Lake Watershed, Qinghai-Tibet Plateau. Pedosphere 28, 478–487. https://doi.org/10.1016/S1002-0160(17)60334-5

Hu, X., Li, Z.C., Li, X.Y., Liu, Y., 2015. Influence of shrub encroachment on CT-measured soil macropore characteristics in the Inner Mongolia grassland of northern China. Soil Tillage Res. 150, 1–9. https://doi.org/10.1016/j.still.2014.12.019

Iversen, B. V., Schjønning, P., Poulsen, T.G., Moldrup, P., 2001. In situ, on-site and laboratory measurements of soil air permeability: Boundary conditions and measurement scale. Soil Sci. 166, 97–106. https://doi.org/10.1097/00010694-200102000-00003

Jarvis, N.J., Jansson, P. -E, Dik, P.E., Messing, I., 1991. Modelling water and solute transport in macroporous soil. I. Model description and sensitivity analysis. Eur. J. Soil Sci. 42, 59–70. https://doi.org/10.1111/j.1365-2389.1991.tb00091.x

Jarvis, N.J., 2007. A review of non-equilibrium water flow and solute transport in soil macropores: principles, controlling factors and consequences for water quality. Eur. J. Soil Sci. 58, 523-546. https://doi.org/10.1111/j.1365-2389.2007.00915.x

Katuwal, S., Norgaard, T., Moldrup, P., Lamandé, M., Wildenschild, D., de Jonge, L.W., 2015. Linking air and water transport in intact soils to macropore characteristics inferred from X-ray computed tomography. Geoderma 237–238, 9–20. https://doi.org/10.1016/j.geoderma.2014.08.006

Koestel, J., Jorda, H., 2014. What determines the strength of preferential transport in undisturbed soil under steady-state flow? Geoderma 217–218, 144–160. https://doi.org/10.1016/j.geoderma.2013.11.009

Lamba, J., Way, T.R., Srivastava, P., Sen, S., Wood, C.W., Yoo, K.H., 2012. Surface transport of nutrients from surface-broadcast and subsurface-banded broiler litter. Trans. ASABE 55, 979–985. http://dx.doi.org/10.13031/2013.41530.

Lamba, J., Srivastava, P., Way, T.R., Malhotra, K., 2019. Effect of Broiler Litter Application Method on Metal Runoff from Pastures. J. Environ. Qual. 48, 1856–1862. https://doi.org/10.2134/jeq2018.08.0318

Lamba, J., Srivastava, P., Way, T.R., Sen, S., Wood, C.W., Yoo, K.H., 2013. Nutrient Loss in Leachate and Surface Runoff from Surface-Broadcast and Subsurface-Banded Broiler Litter. J. Environ. Qual. 42, 1574–1582. https://doi.org/10.2134/jeq2013.02.0064

Luo, L., Lin, H., Halleck, P., 2008. Quantifying Soil Structure and Preferential Flow in Intact Soil Using X-ray Computed Tomography. Soil Sci. Soc. Am. J. 72, 1058–1069. https://doi.org/10.2136/sssaj2007.0179

Luo, L., Lin, H., Li, S., 2010. Quantification of 3-D soil macropore networks in different soil types and land uses using computed tomography. J. Hydrol. 393, 53–64. https://doi.org/10.1016/j.jhydrol.2010.03.031

Luxmoore, R.J., Jardine, P.M., Wilson, G. V., Jones, J.R., Zelazny, L.W., 1990. Physical and chemical controls of preferred path flow through a forested hillslope. Geoderma 46, 139–154. https://doi.org/10.1016/0016-7061(90)90012-X

Matthews, G.P., Laudone, G.M., Gregory, A.S., Bird, N.R.A., De, A.G., Whalley, W.R., 2010. Measurement and simulation of the effect of compaction on the pore structure and saturated hydraulic conductivity of grassland and arable soil. Water Resour. Res. 46, 1–13. https://doi.org/10.1029/2009WR007720

McGrath, G.S., Hinz, C., Sivapalan, M., Dressel, J., Pütz, T., Vereecken, H., 2010. Identifying a rainfall event threshold triggering herbicide leaching by preferential flow. Water Resour. Res. 46, 1–12. https://doi.org/10.1029/2008WR007506

Mees, F., Swennen, R., Van Geet, M., Jacobs, P., 2003. Applications of X-ray computed tomograpy in the geosciences. Geol. Soc. Spec. Publ. 215, 1–6. https://doi.org/10.1144/GSL.SP.2003.215.01.01

Mohanty, B.P., Horton, R., Ankeny, M.D., 1996. Infiltration and macroporosity under a row crop agricultural field in a glacial till soil. Soil Sci. 161, 205–213. https://doi.org/10.1097/00010694-199604000-00001

Mooney, S.J., Morris, C., 2008. A morphological approach to understanding preferential flow using image analysis with dye tracers and X-ray Computed Tomography. Catena 73, 204–211. https://doi.org/10.1016/j.catena.2007.09.003

Müller, K., Katuwal, S., Young, I., McLeod, M., Moldrup, P., de Jonge, L.W., Clothier, B., 2018. Characterising and linking X-ray CT derived macroporosity parameters to infiltration in soils with contrasting structures. Geoderma 313, 82–91. https://doi.org/10.1016/j.geoderma.2017.10.020

Munkholm, L.J., Heck, R.J., Deen, B., 2012. Soil pore characteristics assessed from X-ray micro-CT derived images and correlations to soil friability. Geoderma 181–182, 22–29. https://doi.org/10.1016/j.geoderma.2012.02.024

Oztas, T., Koc, A., Comakli, B., 2003. Changes in vegetation and soil properties along a slope on overgrazed and eroded rangelands. J. Arid Environ. 55, 93–100. https://doi.org/10.1016/S0140-1963(02)00267-7

Pagenkemper, S.K., Puschmann, D.U., Peth, S., Horn, R., 2014. Investigation of Time Dependent Development of Soil Structure and Formation of Macropore Networks as Affected by Various Precrop Species. Int. Soil Water Conserv. Res. 2, 51–66. https://doi.org/10.1016/S2095-6339(15)30006-X

Perret, J., Prasher, S.O., Kanlzas, A., Langford, C., 1998. Characterization of macropore morphology in a sandy loam soil using X-ray computer assisted tomography and geostatistical analysis. Can. Water Resour. J. 23, 143–165. https://doi.org/10.4296/cwrj2302143

Phansalkar, N., More, S., Sabale, A., Joshi, M., 2011. Adaptive Local Thresholding for Detection of nuclei in diversity stained cytology images. Int. Conf. Commun. Signal Process. 218–220. https://doi.org/10.1109/ICCSP.2011.5739305

Piccoli, I., Schjønning, P., Lamandé, M., Zanini, F., Morari, F., 2019. Coupling gas transport measurements and X-ray tomography scans for multiscale analysis in silty soils. Geoderma 338, 576–584. https://doi.org/10.1016/j.geoderma.2018.09.029

Pires, L.F., Arthur, R.C.J., Correchel, V., Bacchi, O.O.S., Reichardt, K., Camponez Do Brasil, R.P., 2004. The use of gamma ray computed tomography to investigate soil compaction due to core sampling devices. Brazilian J. Phys. 34, 728–731. https://doi.org/10.1590/S0103-97332004000500006

Prior, S.A., Runion, G.B., Torbert, H.A., Erbach, D.C., 2004. A hydraulic coring system for soil–root studies. Agron. J. 96:1202–1205. https://doi.org/10.2134/agronj2004.1202

Rab, M.A., Haling, R.E., Aarons, S.R., Hannah, M., Young, I.M., Gibson, D., 2014. Evaluation of X-ray computed tomography for quantifying macroporosity of loamy pasture soils. Geoderma 213, 460–470. https://doi.org/10.1016/j.geoderma.2013.08.037

Rezaei, S.A., Gilkes, R.J., 2005. The effects of landscape attributes and plant community on soil physical properties in rangelands. Geoderma 125, 145–154. https://doi.org/10.1016/j.geoderma.2004.07.011

Rueden, C.T., Schindelin, J., Hiner, M.C., DeZonia, B.E., Walter, A.E., Arena, E.T., Eliceiri, K.W., 2017. ImageJ2: ImageJ for the next generation of scientific image data. BMC Bioinformatics 18, 1–26. https://doi.org/10.1186/s12859-017-1934-z

Schaap, M.G., Leij, F.J., Th. Van Genuchten, M., 2001. ROSETTA: A computer program for estimating soil hydraulic parameters with hierarchical pedotransfer functions. J. Hydrol. 251, 163–176.

Sen, S., Srivastava, P., Yoo, K.H., Dane, J.H., Shaw, J.N., Kang M.S., 2008. Runoff generation mechanisms in pastures of the Sand Mountain region of Alabama-a field investigation. Hydrol. Process. 14, 369-385. https://doi.org/10.1002/hyp.7025

Sen, S., Srivastava, P., Dane, J.H., Yoo, K.H., Shaw, J.N., 2010. Spatial-temporal variability and hydrologic connectivity of runoff generation areas in a North Alabama pasture-implications for phosphorus transport. Hydrol. Process. 24, 342–356. https://doi.org/10.1002/hyp.7502

Shaffer, K.A., Fritton, D.D., Baker, D.E., 1979. Drainage Water Sampling in a Wet, Dual-Pore Soil System. J. Environ. Qual. 8, 241–246. https://doi.org/10.2134/jeq1979.00472425000800020022x

Šimůnek, J., Th. Van Genuchten, M., Šejna, M., 2016. Recent Developments and Applications of the HYDRUS Computer Software Packages. Vadose Zo. J. 15, 1–25. https://doi.org/10.2136/vzj2016.04.0033

Singh, P., Kanwar, R.S., Thompson, M.L., 1991. Macropore Characterization for Two Tillage Systems Using Resin-Impregnation Technique. Soil Sci. Soc. Am. J. 55, 1674–1679. https://doi.org/10.2136/sssaj1991.03615995005500060029x

Singleton, P.L., Boyes, M., Addison, B., 2000. Effect of treading by dairy cattle on topsoil physical conditions for six contrasting soil types in Waikato and Northland, New Zealand, with implications for monitoring. New Zeal. J. Agric. Res. 43, 559–567. https://doi.org/10.1080/00288233.2000.9513453

Soil Survey Staff, Natural Resources Conservation Service, United States Department of Agriculture. Web Soil Survey. Available online at the following link: http://websoilsurvey.sc.egov.usda.gov/. Accessed 20 November 2020.

Udawatta, R.P., Anderson, S.H., Gantzer, C.J., Garrett, H.E., 2008. Influence of Prairie Restoration on CT-Measured Soil Pore Characteristics. J. Environ. Qual. 37, 219–228. https://doi.org/10.2134/jeq2007.0227

Vogel, H.J., Weller, U., Schlüter, S., 2010. Quantification of soil structure based on Minkowski functions. Comput. Geosci. 36, 1236–1245. https://doi.org/10.1016/j.cageo.2010.03.007

Vuaille, J., Daraghmeh, O., Abrahamsen, P., Jensen, S.M., Nielsen, S.K., Munkholm, L.J., Green, O., Petersen, C.T., 2020. Wheel track loosening can reduce the risk of pesticide leaching to surface waters. Soil Use Manag. 1–15. https://doi.org/10.1111/sum.12641

Wahl, N.A., Bens, O., Buczko, U., Hangen, E., Hüttl, R.F., 2004. Effects of conventional and conservation tillage on soil hydraulic properties of a silty-loamy soil. Phys. Chem. Earth 29, 821–829. https://doi.org/10.1016/j.pce.2004.05.009

Wang, Y., Zhang, B., Lin, L., Zepp, H., 2011. Agroforestry system reduces subsurface lateral flow and nitrate loss in Jiangxi Province, China. Agric. Ecosyst. Environ. 140, 441–453. https://doi.org/10.1016/j.agee.2011.01.007

Warner, G.S., Nieber, J.L., Moore, I.D., Geise, R.A., 1989. Characterizing Macropores in Soil by Computed Tomography. Soil Sci. Soc. Am. J. 53, 653–660. https://doi.org/10.2136/sssaj1989.03615995005300030001x

Warren, S.D., Nevill, M.B., Blackburn, W.H., Garza, N.E., 1986. Soil Response to Trampling Under Intensive Rotation Grazing. Soil Sci. Soc. Am. J. 50, 1336–1341. https://doi.org/10.2136/sssaj1986.03615995005000050050x

Wilson, G.V., Jardine, P.M., Luxmoore, R.J., Jones, J.R., 1990. Hydrology of a Forested Hillslope during Storm Events. Geoderma 46, 119–138. https://doi.org/10.1016/0016-7061(90)90011-W

Zhang, X., Zhu, J., Wendroth, O., Matocha, C., Edwards, D., 2019. Effect of Macroporosity on Pedotransfer Function Estimates at the Field Scale. Vadose Zo. J. 18, 1–15. https://doi.org/10.2136/vzj2018.08.0151

Zhang, Y., Zhang, X., Zhang, Z., Niu, J., Zhang, M., 2017. Water flow and preferential flow: A State-of-the-Art throughout the literature. Hydrol. Earth Syst. Sci. Discuss. 1–68. https://doi.org/10.5194/hess-2017-210

Zong-Chao Li, Hu, X., Li, X.Y., Huang, Y.M., Wu, X.C., Wang, P., Liu, L.Y., 2019. Quantification of Soil Macropores at Different Slope Positions under Alpine Meadow Using Computed Tomography in the Qinghai Lake Watershed, NE Qinghai–Tibet. Eurasian Soil Sci. 52, 1391–1401. https://doi.org/10.1134/S1064229319110152

Figures:

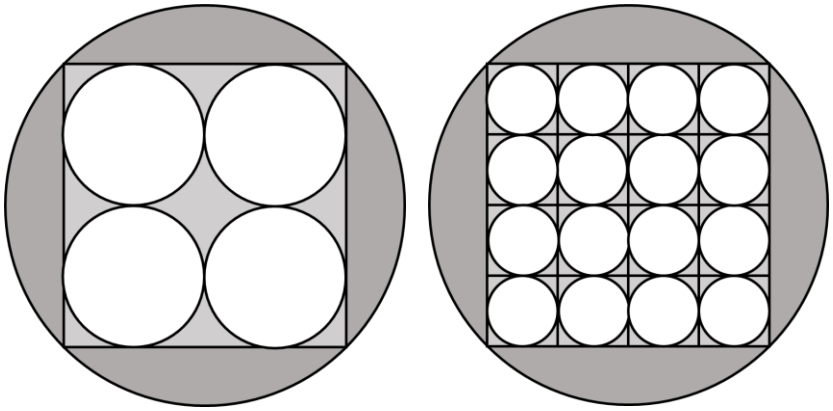

(a) (b)

Figure 2.1 Schematic diagram (not to scale) of a horizontal plane of a soil column showing cylindrical subsamples of (a) 48.1 mm diameter and (b) 24.05 mm diameter, used for evaluating volume effects on soil macropore characteristics. The height of the samples in all the subsamples were equal to 100 mm.

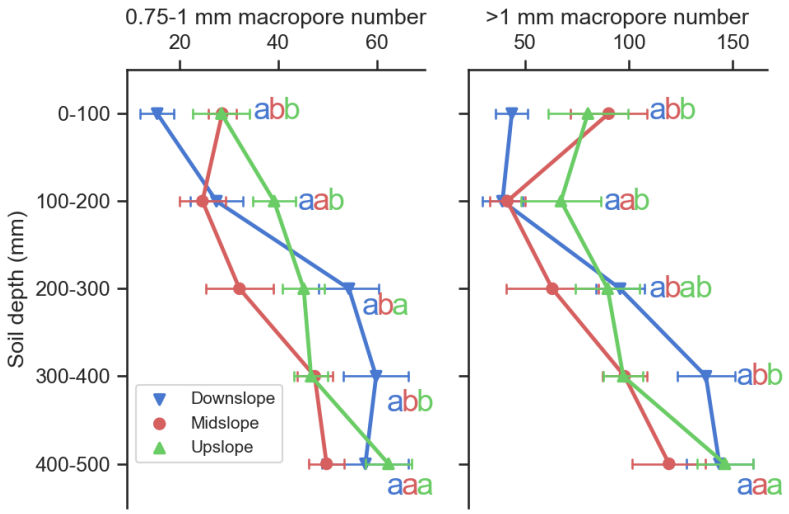

Figure 2.2 Effects of slope position on number of >1 mm soil pores and 0.75-1 mm soil pores in different soil layers. Error bars indicate the standard deviation (n=6). Within each depth, different letters for the slope positions (represented by different colors) indicate significantly different values at the 0.05 probability level.

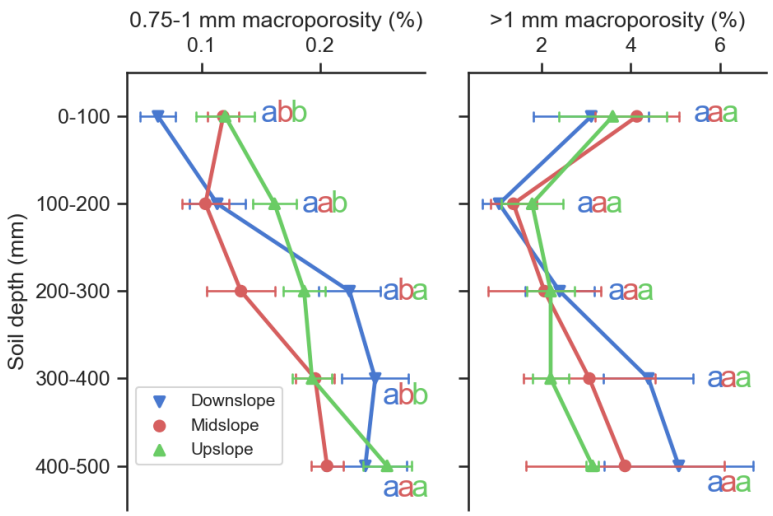

Figure 2.3 Effects of slope position on the >1 mm soil macroporosity and 0.75-1 mm soil macroporosity in different soil layers. Error bars indicate standard deviation (n=6). Within each depth, different letters for the slope positions (represented by different colors) indicate significant difference at the 0.05 probability level.

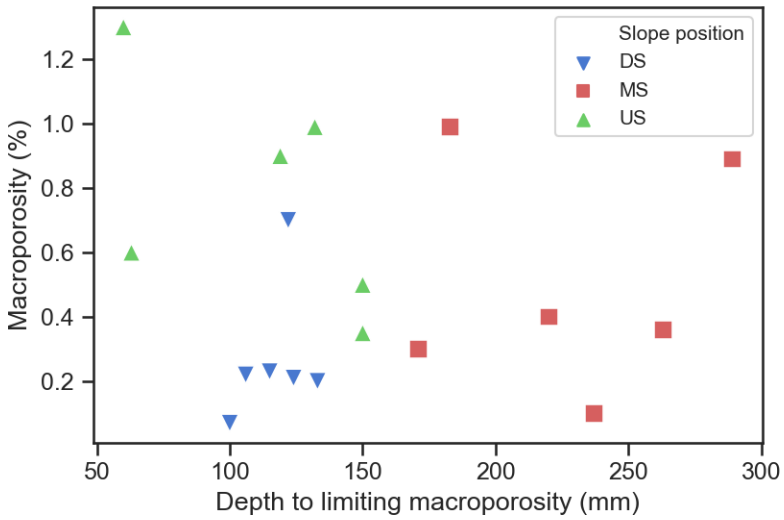

Figure 2.4 Position of the limiting macroporosity in all the samples (n=18) of upslope, midslope and downslope locations. Limited macroporosity is based on each individual slice sampled at 0.625 mm intervals.

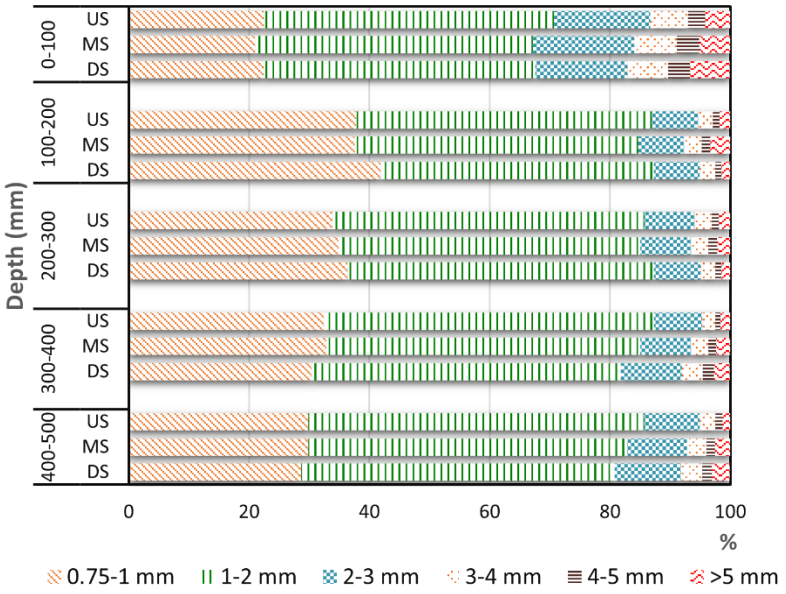

Figure 2.5 Distribution of macropores by diameter at US, MS, and DS positions as a function of depth (0-500 mm).

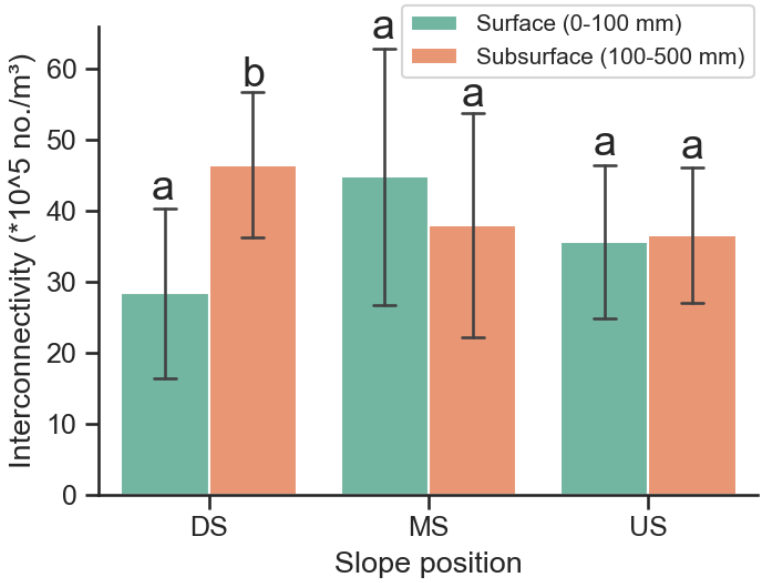

Figure 2.6 Interconnectivity (*10^5 no. /m^3) of surface macropores (0-100 mm) as compared to the subsurface interconnectivity (100-500 mm) at different topographical positions in a pasture. Within each slope position, different letters indicate a significant difference in interconnectivity (node density) between the surface and subsurface soil depth ($P<0.05$).

A

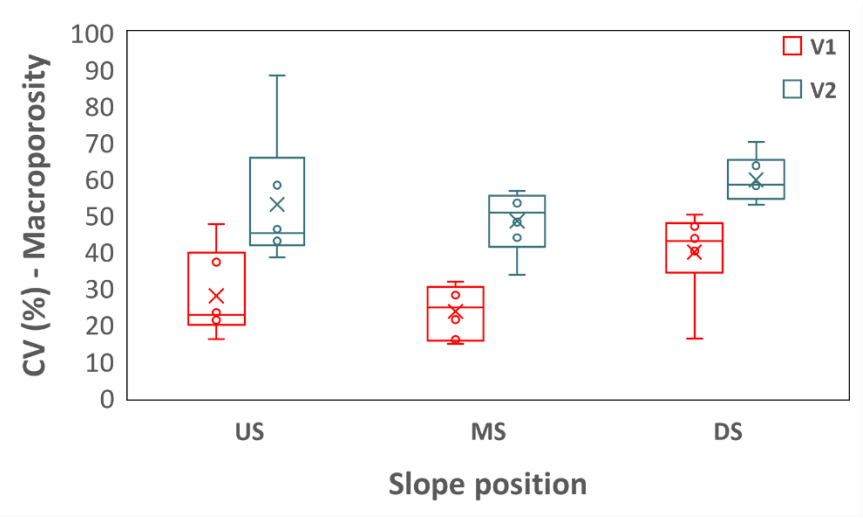
CV (%) - Macroporosity
100
90
80
70
60
50
40
30
20
10
0
V1
V2
US
MS
DS
Slope position

B

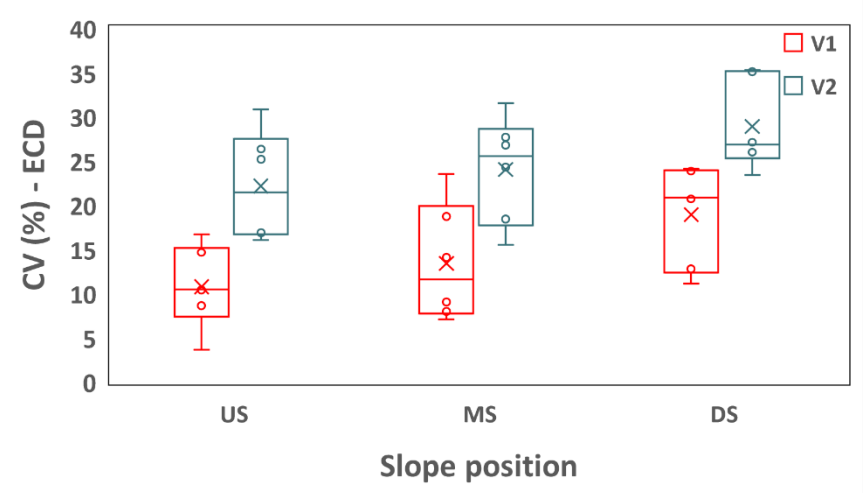
CV (%) - ECD
40
35
30
25
20
15
10
5
0
V1
V2
US
MS
DS
Slope position

C

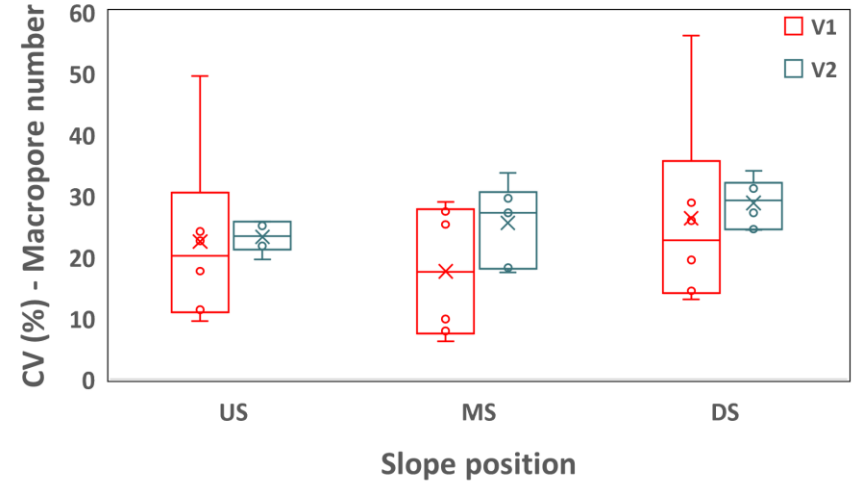

Figure 2.7 Coefficient of variation (CV) (n=6) for macroporosity (A), ECD (B), and macropore number (C) obtained using 48.1 mm diameter (V1) and 24.05 mm diameter (V2) sub-sample soil cores at different topographical position.

Tables:

Table 2.1 Mean (n = 3) soil organic matter (%), sand (%), silt (%), clay (%), and bulk density (g cm^{-3}) at different topographical locations (downslope (DS), midslope (MS) and upslope (US)). Values shown in parentheses are standard deviations.

Depth (mm)	Slope position	Organic matter (%)	Sand (%)	Silt (%)	Clay (%)	Dry bulk density (g cm^{-3})
0-100	**DS**	6.00 (±0.05) a	53.90 (±1.53) a	7.50 (±1.30) a	38.60 (±2.03) a	1.31 (±0.14) a
	MS	3.93 (±0.19) b	68.80 (±2.63) b	8.70 (±3.99) a	22.60 (±1.50) b	1.17 (±0.11) a
	US	4.75 (±0.28) c	58.00 (±0.12) a	9.20 (±1.23) a	32.80 (±1.33) a	1.10 (±0.07) a
100-200	**DS**	3.28 (±0.10) a	60.40 (±1.46) a	8.60 (±2.24) a	31.00 (±1.96) a	1.18 (±0.17) a
	MS	3.23 (±0.26) a	69.00 (±2.66) b	6.90 (±1.55) a	24.10 (±1.50) b	1.17 (±0.18) a
	US	3.28 (±0.12) a	59.5 0(±1.53) a	6.9 0(±0.04) a	33.60 (±1.49) a	1.22 (±0.11) a
200-300	**DS**	2.31 (±0.23) a	61.60 (±2.47) a	8.50 (±1.40) a	29.90 (±1.46) a	1.19 (±0.21) a
	MS	2.83 (±0.19) a	73.40 (±3.87) b	6.90 (±2.93) a	19.70 (±1.47) b	1.44 (±0.06) a
	US	2.65 (±0.33) a	61.90 (±3.11) a	8.10 (±2.57) a	30.00 (±0.72) a	1.39 (±0.04) a
300-400	**DS**	2.54 (±0.21) a	66.70 (±4.39) a	9.80 (±4.08) a	23.50 (±0.72) a	1.30 (±0.15) a
	MS	2.61 (±0.33) a	73.50 (±4.01) a	5.60 (±3.29) a	21.00 (±2.67) a	1.44 (±0.10) a
	US	2.98 (±0.26) a	66.10 (±2.72) a	6.90 (±1.30) a	27.10 (±1.49) a	1.35 (±0.05) a
400-500	**DS**	2.42 (±0.45) a	68.80 (±3.96) a	9.40 (±3.28) a	21.80 (±0.69) a	1.24 (±0.13) a
	MS	2.37 (±0.17) a	74.00 (±0.69) a	6.80 (±1.27) b	19.20 (±1.47) a	1.29 (±0.02) a
	US	2.52 (±0.15) a	68.40 (±1.52) a	7.70 (±1.51) a	23.90 (±0.01) a	1.35 (±0.12) a

Within each depth, mean values of different soil properties followed by the same letter at different topographical positions are not significantly different at the 0.05 probability level. Textural classification was according to the USDA soil taxonomy; Measured by hydrometer method; Clay fraction < 0.002 mm, Silt fraction 0.05-0.002 mm, and Sand fraction 0.05-2 mm (Bouyoucos, 1962)

Table 2.2 Average (n = 6) number of macropores, average macropore diameter, and average macroporosity, in the US (upslope), MS (midslope), and DS (downslope) locations.

Slope position	Number of macropores (no.) (mean ± SD) **	Macropore size (mm) (mean ± SD) **	Macroporosity (%) (mean ± SD) **	Mean macropore diameter (mm) (mean ± SD) at different depths *				
				0-100 mm	100-200 mm	200-300 mm	300-400 mm	400-500 mm
DS	135 (±14) a	1.65 (±0.09) a	3.39 (±0.32) a	2.11 (±0.27) a	1.39 (±0.09) a	1.41 (±0.07) a	1.62 (±0.13) a	1.68 (±0.18) a
MS	115 (±14) a	1.63 (±0.15) a	3.00 (±1.04) a	1.92 (±0.10) ab	1.55 (±0.15) a	1.50 (±0.17) a	1.55 (±0.23) a	1.60 (±0.29) a
US	130 (±18) a	1.57 (±0.07) a	2.77 (±0.37) a	1.80 (±0.15) b	1.45 (±0.12) a	1.47 (±0.07) a	1.45 (±0.08) a	1.48 (±0.05) a

* Within each depth, values followed by the same letter are not significantly different at the 0.05 probability level.
**Mean values of different properties followed by the same letter at different topographical positions are not significantly different at the 0.05 probability level. Data in the parentheses are standard deviations (n = 6).

Chapter 3

Characterizing Temporal and Spatial Variability in 3D Soil Macropore Characteristics Using X-ray Computed Tomography

3.1 Abstract

The influence of soil macropores on the transport of water and solutes in subsurface flows has long been known. Preferential flow via soil macropores can have a large effect on water quality. Hence, it is important to quantify soil macropore characteristics to better understand preferential flow behavior in soils. Currently, little information exists on the changes in soil macroporosity in response to topographical position within a field and how macropore characteristics change temporally within a field. Therefore, the objective of this study was to use X-ray computed tomography (CT) and image analysis to quantify temporal and spatial variability in 3D soil macropore structure in a 0.40 ha pasture field. A total of 36 undisturbed soil columns, 150 mm in diameter and 500 mm in length, were collected during May and September of 2019. The macropore characteristics differed significantly between different topographical positions and sampling seasons, especially at the surface layer (0-100 mm) depth. The soil macropores at the downslope position were sparsely distributed in the surface soil layer. This was attributed to a relatively higher degree of grazing-induced compaction due to higher soil moisture at the downslope position, as compared to the upper slope locations. In contrast, dense macropore networks were observed at the downslope positions for depths greater than 250 mm. The results of this study provide quantitative information on 3D soil macropore characteristics under varying topographical locations and time in a pasture field.

Keywords: Image analysis; Macropores; Preferential flow; Soil Structure; X-ray Computed Tomography

3.2 Introduction

Soil macropores, such as root channels, earthworm burrows, inter-aggregate voids play a central role in fluid flow and contaminant transport in soil through preferential flows (Jarvis, 2007). Water flux through these macropores can be as high as 70% of the total flux, even though they constitute only a small fraction of the total soil volume (Watson and Luxmoore, 1986). Wilson et al. (1990) reported that preferential flow through macropores was the predominant mechanism of streamflow generation in one of the watersheds in eastern Tennessee. Different macropore characteristics (e.g., macropore number, diameter, connectivity, and pore size distribution) affect the rate, flow, and retention of water and contaminants through macropores (Luo et al., 2010a; Udawatta et al., 2008; Katuwal et al., 2015). Based on the past literature (Luo et al., 2010b; Smet et al., 2018), it is clear that water flow and contaminant transport processes in the soil can be linked to different macropore characteristics. Therefore, it is important to understand macropore characteristics in agricultural landscapes to further improve our understanding of the fate and transport processes of various contaminants (e.g., phosphorus (P), nitrogen (N), metals).

Soil properties can influence various macropore characteristics. For example, soil moisture and organic matter content promote the formation and stabilization of macropores in soils (Grosbellet et al., 2011; Holden, 2009). The differences in soil properties affect the degree of compaction by trampling in grazed fields (Grosbellet et al., 2011), which in turn may contribute to the variation in soil macropores. For example, in a continuously grazed pasture, the topsoil porosity (Singleton et al., 2000) and vertical pore continuity (Greenwood and McKenzie, 2001) are usually affected by the disruption of large soil aggregates and repacking with smaller ones to fill the existing soil

pores (Cattle and Southorn, 2010). In addition to the trampling-induced compaction, even a slight difference in the topography can cause major changes in soil development (Rezaei and Gilkers, 2005). Topography affects soil properties at local scales by controlling gravity-driven soil movements (Li and McCarty, 2019). Consequently, information on the topographical variation of soil macropore characteristics would improve the prediction accuracy of different transport models and understanding of the mechanisms underlying the topographic impacts on soil macropores. Similarly, the soil macropores may change over time depending upon various factors, such as, wetting and drying cycles, biological activities, and management practices (Cameira et al., 2003). Zhang et al. (2016) conducted a study to quantify temporal changes in soil macropores under different slope positions and land uses and found that there was a significant interaction effect of slope position and time on soil macropores. They attributed this discrepancy in soil macroporosity, in part, to the variation in water content in space and time within the field. Nonetheless, macropores still constitute a major challenge for modeling transport processes because of their high spatiotemporal variability (Jury et al., 2011). This makes quantification of both temporal and spatial variability of soil macropores crucial for understanding transport of water and contaminants in soils.

X-ray computed tomography (CT) has emerged as a non-destructive and non-invasive technique to visualize and quantify soil structure (Rab et al., 2014; Katuwal et al., 2015). Although characterization of two-dimensional (2D) soil porosity using methods, such as, dye tracers (Wahl et al., 2004), resin impregnation (Singh et al., 1991), and tension infiltrometer (Cameira et al., 2003) have long been studied, the use of X-ray CT enables quantification of macropore geometry in three dimensions (3D) (Pires et al., 2019; Singh et al., 2021). The 3D image analysis of soil macropores is the only way to quantify macropore connectivity and tortuosity, which are important

macropore parameters governing flow and contaminant transport through soils (Jassogne et al., 2007; Luo et al., 2010a). The CT approach, however, requires a small sample volume to scan soil cores at relatively higher scanning resolutions (Mees et al., 2003). This limits its usage for characterizing macropores of larger soil columns composed of heterogeneous soil matrices. Nonetheless, X-ray CT image analysis has been successfully used to determine parameters like connectivity, tortuosity, diameter, and density of macropores (Pulido-Moncada et al., 2020, Pires et al., 2019).

In the Sand Mountain region of north Alabama, excessive buildup of P in soils is a serious issue due to intensive application of poultry litter to pastures (Sen et al., 2008). Lamba et al. (2012) conducted a study on the transport of nutrients in this area and reported that more than 90% of rainfall infiltrated into the soil, while less than 10% of rainfall contributed to surface runoff. This suggests a possibility of substantial subsurface flows responsible for the off-site transport of contaminants in this area. Besides, Sen et al. (2008) suggested from their study that both the surface and subsurface runoff generation mechanisms could contribute to the off-site transport of contaminants in this region. Therefore, to investigate contaminant transport processes in this region, it is important to quantify the spatial and temporal changes in macropore characteristics to elucidate the subsurface flow mechanisms.

Limited work has been done to understand spatial and temporal variation in macropore characteristics (Zhang et al., 2016). Most of the previous studies (e.g., Zong-Chao Li et al., 2019; Holden, 2008) assessing topographical effects on soil macropores have been limited to analysis of samples collected during a one-time sampling. However, it is important to understand how macropore characteristics change as a function of time. Zhang et al. (2016) investigated temporal changes in soil macropores of surface soil indirectly using tension infiltrometers at different slope

positions, however, losing sight of subsoil and true 3D macropore networks including connectivity, length, and tortuosity. It is important to quantify macropore characteristics in their true 3D representation to understand the macropore impacts on the soil hydraulic functions (Luo et al., 2010a; Katuwal et al., 2015). Furthermore, the subsoil macropores created by deep roots might be more important in influencing the effect of topography on overall soil macropore characteristics. To fully capture the heterogeneity evident in soils, it is therefore important to analyze macropores in relatively deeper soil profiles. To our knowledge, no study has been conducted that focused on both the temporal and topographical variation in 3D soil macropore networks in pastures. Hence, the specific objectives of this study were to (1) quantify the 3D soil macropore characteristics in different soil layers and slope positions and (2) investigate the temporal variation in soil macropore characteristics using computed tomography. Overall, this study aimed to provide a comprehensive understanding of the interaction between the landscape position and macropore characteristics in a pasture field. It was hypothesized that topographical dependence of macropore characteristics may change over time and such changes will depend on the depth within the soil profile.

3.3 Materials and methods

3.3.1 Study site

Soil columns were collected from a hillslope pasture field located at the Sand Mountain Research and Extension Center (SMREC) (34° 17' 02.6" N, 85° 57' 51.8" W) in north Alabama. The site where the study was conducted had an average slope of 3.4%, at an elevation of about 350 m above mean sea level, and a slope length of 80 m. The site had been grazed by cattle for more than 15 years. The soil types at the study site were Wynnville fine sandy loam (fine-loamy, siliceous, subactive, thermic Glossic Fragiudults) and Hartsells fine sandy loam (fine-loamy, siliceous, subactive, thermic Typic Hapludults). The Wynnville soil is moderately well drained with slow

permeability, primarily found on nearly level to sloping mountain plateaus. The Hartsells soil is well-drained, moderately permeable, and primarily found on broad smooth plateaus, mountaintops, or hilltops. The parent material of these soils is sandstone and shale (Soil Survey Staff, 2020). The long-term average annual precipitation in this region is 1340 mm and the average annual temperature is 14.8 °C. A significant portion of annual precipitation falls during winter (average 370 mm) and early spring (average 260 mm) in the form of rainfall (Sen et al., 2010). A cool-season grass (Kentucky 31 Tall Fescue (*Festuca arundinacea* Schreb.)) was grown at the study site. This grass has an extensive root system that extends to a depth of 90 cm below the soil surface, providing access to water and other resources, and offers better heat and drought tolerance than many other cool-season grasses (Cougnon et al., 2017).

3.3.2 Soil sampling

A total of 36 undisturbed soil columns (150 mm diameter and 500 mm depth) were collected from the pasture field to evaluate the effects of topographical variation on soil macropore structure. Soil samples were collected in two consecutive sampling seasons [Season 1 (S1), May 2019, and Season 2 (S2), September 2019] to quantify temporal variation in macropore characteristics. During each sampling event, six cores were collected from each of three topographical locations (upslope (US), midslope (MS), and downslope (DS)) within the field. No cattle were allowed to graze on the field between the sampling seasons S1 and S2. This was done to avoid any recent trampling on the soil. For extracting the soil cores, PVC pipes were driven carefully into the soil utilizing a tractor-mounted soil coring system (Prior et al., 2004). After sampling, the airspace at both ends of the core was filled with bubble wrap packing material and secured firmly with plastic end caps before transportation. A 150 mm thick layer of wood shavings supported the soil columns to serve as cushioning and minimize disturbance of the soil columns during transportation. The

samples were then stored at 4 °C until further analysis. In addition to the 36 cores, two extra soil columns were collected, to make artificial soil pores of known diameter in the soil. These cores were used as a reference, as described in later section, to separate the pores from the rest of the soil matrix.

3.3.3 CT scanning and image processing

A medical GE LightSpeed VCT 64 Slice CT scanner (GE Healthcare, Chicago, IL) was used to acquire CT scan images of the soil samples. This scanner was installed in the Bailey Small Animal Teaching Hospital at the Auburn University College of Veterinary Medicine (AUCVM). The machine can take up to 64 slices in one scan, thus, covering 40 mm at 0.625 mm slice thickness in one scan. X-ray projections were taken at 140 KV, 140 mA, and 1 s exposure time, and this provided 16-bit 512×512 images with a voxel size of 0.35×0.35×0.625 mm^3.

The images were analyzed using the public domain software program ImageJ version 1.52t (Rueden et al., 2017), which is a digital image processing program developed by the US National Institutes of Health (Bethesda, MD). To avoid voids near the core walls, the diameter of the core portion which was analyzed, was reduced from 150 mm to 136 mm, and the area beyond this region of interest (ROI) was deleted by using the "clear outside" tool in ImageJ. The ROI was then rescaled to a new voxel size of 0.35×0.35×x0.35 mm^3 to facilitate further image processing and analysis (Zhang et al., 2019). The slices from the bottom of the core which seemed to be disturbed were excluded as well from the original stack for analysis. A median filter with a radius of 1 pixel was used to reduce noise in the images. To enhance the edges of the pores and improve the contrast, the "Unsharp mask" command with its default values (radius of 1 pixel and mask weight of 0.6) was used before any further analysis.

The images were segmented using Phansalkar's algorithm of auto-local thresholding which is a modification of Sauvola's thresholding method to deal with low contrast images (Phansalkar et al., 2011). In this method, the threshold value of each pixel was calculated using a radius of 5 pixels and default values for other parameters set in ImageJ software (i.e. k = 0.25 and r = 0.5). To determine the parameters of thresholding (i.e., k, r, and the radius), we inserted Plexiglas thermoplastic cylindrical rods of two different diameters (3.17 mm and 4.76 mm) into the soil core to create artificial macropores, which were pulled out just before CT scanning. The macropore diameter of the artificial pores was based on randomly selected thresholding parameter values. The diameter of each artificial pore was then compared with the actual pore diameter. A parameter value [0.2, 0.5] was randomly selected until the difference between the actual and the image-analyzed pore diameter was less than 1.5% for both rod diameters. All the images were visually inspected for the performance of the segmentation procedure in separating the pores and solids.

3.3.4 Quantification of macropore characteristics

For the 3D structure analysis, the binary images were analyzed using only the pores with volumes > 8 voxels to avoid misclassification of noise from the porous fraction of the images (Pires et al., 2020; Jefferies et al., 2014). The macropore characteristics that were quantified include macroporosity, macropore diameter, surface area density, macropore length density, network density, node density, and tortuosity. Macroporosity was calculated as the percentage of the total volume of CT-derived macropores to the volume of the ROI. The macropore diameter was determined using a local thickness algorithm proposed by Dougherty and Kunzelmann (2007) within the BoneJ plugin in ImageJ (Doube et al., 2010). The mean diameter of macropores (MD) was then calculated as:

$$MD = \frac{\sum_{i=1}^{n} D_i V_i}{\sum_{i=1}^{n} V_i} \quad \text{.....(1)}$$

where D_i and V_i are the diameter and volume of each macropore, respectively. After all the image processing and analyses, macropores ≥ 0.70 mm in diameter were quantified in this study. The surface area density was calculated as the total wall area of the macropores in a unit volume. All the macropores were skeletonized with "Skeletonize 3D" and the "Analyze Skeleton" modules within the BoneJ plugin in ImageJ to determine the macropore length. To reduce the effect of noisy skeletons, only the macropore branches larger than 4 voxels in length were used to compute the length density (Zhang et al., 2019). The length density was then calculated as the length of the macropores per unit volume. Macropore network density, i.e., number of macropore networks per unit volume, and tortuosity, i.e., the ratio of actual macropore length to the straight-line distance, were both derived from the output of the "Skeletonize 3D" image analysis. To quantify the interconnectivity of macropores, the node density (the number of nodes where at least two macropore branches connect per unit volume) was determined for each macropore network. A high density of junctions is related to an extensive and well-connected pore network (Munkholm et al., 2012).

After preliminary analyses of the images, it was found that macropore network characteristics were not constant with depth. Hence, we decided to divide the entire soil column into 3 subvolumes: a surface layer (0-100 mm), the transition layer (100-250 mm), and the subsurface layer (250-500 mm). All the macropore characteristics were calculated for the entire column section, and individually for the 3 subvolumes. In addition, to investigate the effects of slope position and sampling season on different sizes of macropores, all the pores were divided into three pore-size classes: a) 0.70-1 mm, b) 1-2 mm, and c) >2 mm in diameter.

3.3.5 Statistical analysis

We used SAS version 9.4 (SAS Institute, USA) to perform all the statistical analyses. The Kruskal-Wallis test was used to test the effect of slope position on different soil macropore characteristics. Also, we examined the effect of sampling season and pore size class on soil macropore characteristics for different soil layers. The correlation between different macropore characteristics was tested using Pearson's correlation coefficient (r). All statistical tests were conducted at the 95% confidence level.

3.4 Results and discussion

3.4.1 Macropore network characteristics

Table 3.1 shows the CT-derived macropore characteristics for different sampling seasons and slope positions at three soil depth intervals. The macropore characteristics differed significantly under multiple cases, but we did not observe a clear trend between macropore characteristics and slope position. Significant differences in macroporosity between different slope positions were seen only at the surface (0-100 mm) and the subsurface layer (250-500 mm). The variation of macropore characteristics with depth presented in Table 3.1 supports the partitioning of the soil cores into three depth layers, i.e., surface (0-100 mm), transition (100-250 mm), and subsurface (250-500 mm) layer. Generally, values of different macropore characteristics (e.g., macroporosity, surface area density, length density) were lower at the surface (0-100 mm) of DS compared to the MS and US position in both the sampling seasons, S1 and S2, which may be an indication of the high degree of compaction at the DS. For example, at the surface (0-100 mm), the macroporosity values were lowest at the DS for both S1 and S2; however, at the subsurface (250-500 mm), relatively larger macroporosity values were observed at the DS compared to the MS and US positions. The surface runoff from the US and MS might have caused higher moisture content at the DS position,

which likely enhanced compaction at the DS position compared to US and MS positions. The saturated hydraulic conductivity (Ksat) values were estimated at different slope positions using the Rosetta model (ver. 1.2) (Schaap et al., 2001) in HYDRUS (Šimůnek et al., 2016). The Rosetta model is a pedotransfer function that uses basic soil data such as soil texture and bulk density to predict the hydraulic parameters of soil based on a neural network model (Domúnguez-Niño et al., 2020). The lowest Ksat values were reported at the downslope location (0-100 mm), 33.8 (±2.6) mm hr^{-1}, compared to 65.8 (±16.8) mm hr^{-1} and 49.5 (±11.4) mm hr^{-1} at the midslope and upslope locations, respectively. The lower values of Ksat likely restricted the amount of water infiltrating into the soil profile at the downslope location (Sen et al., 2008), thereby, facilitating a higher degree of compaction compared to the upper slope, due to higher moisture content at the downslope location. Oztas et al. (2003) observed high bulk density values at the footslope position along a grazed hillslope in Turkey, and reported that typically DS locations on a hillslope are wetter than US and MS positions. Our field was not grazed in between S1 and S2 and thus the macropore networks have not been impacted by the animal trampling within this period. We expect the soil samples collected in S1 to be relatively more influenced by the animal traffic compared to the soil samples collected in S2 because grazing was stopped one month before the S1 sampling.

Macropore connectivity and tortuosity are important properties that can influence water flow and contaminant transport more than the macropore volume alone (Luo et al., 2010a). The tortuosity ranged from 1.27 to 1.33 at different depths and slope positions. Katuwal et al. (2015) also reported a similar range of tortuosity values on the surface soil (0-200 mm depth) of an agricultural field under red fescue (Festuca rubra L.) and attributed this to the presence of a significant proportion of large and vertical biopores. The soils at the US were significantly less ($P<0.05$) tortuous under multiple cases compared to the DS and MS soils. Smaller tortuosity values could be due to low

biological activity (Muller et al., 2018) in the US position compared to the MS and DS positions. Furthermore, more tortuous macropores in the DS compared to the US may be due to the greater competition for food among earthworms in the soil (Luo et al., 2010a). Although earthworm abundance quantification was beyond the scope of our study, we noticed few earthworms and few insects on the surface of the DS during soil sampling. At DS, both the organic matter content (6%) and clay content (38.6%) were higher than the soils at the MS and US position, in the surface (0-100 mm) depth. The organic matter content at MS and US were 3.93% and 4.75%, respectively, and the clay content were 22.60% and 32.80%, respectively in the surface (0-100 mm) depth. The variation of mean macropore diameter with slope position was distinctly different for the two seasons at the surface layer (0-100 mm). In the 0-100 mm soil depth, the mean macropore diameter in S1 was higher at the DS than at the MS and US, however, the difference was not significant. Conversely, lower mean macropore diameter was observed at the DS in S2 (0-100 mm) compared to the MS ($P<0.05$) and the US ($P>0.05$). This reduction in mean macropore diameter at the DS can be attributed to the increase in the proportion of smaller diameter macropores (0.7-1 mm) from S1 to S2 (Figure 3.2). Results from Bottinelli et al. (2014) showed that only smaller macropores (0.24-0.5 mm and 0.5-1 mm in diameter) fully regenerated following heavy traffic in a forest ecosystem. However, their study was based on a 2-3 year period which provided sufficient time for the macropores to regenerate compared to that in our study (0.33 years). Physical processes like wetting-drying cycles are mostly responsible for macroporosity changes, acting much more in the upper soil layer than in deeper layers (Bottinelli et al., 2014). As illustrated by Pulido-Moncada et al. (2020), a decrease in the mean macropore diameter, i.e., an increase in the density of small pores could also be related to the development of fine roots in the tall fescue plant during the sampling season S1 and S2.

The surface area density, length density, and network density were significantly ($P<0.05$) lower in the DS than the US position in the 0-100 mm soil depth in both S1 and S2. Moreover, surface interconnectivity (0-100 mm) was lower in the DS than the US position in both S1 and S2, however, a significant difference ($P<0.05$) was observed only in S2. The lower interconnectivity in the 0-100 mm depth and higher interconnectivity in the 250-500 mm depth at the DS position corroborates the findings of Muller et al. (2018), who reported higher macropore connectivity in pasture soils with larger macroporosities. Although their study was based on pores greater than or equal to 0.147 mm in diameter, this indicates that there could be a strong correlation between macroporosity and interconnectivity for smaller pores (0.147 – 0.70 mm) that were not considered in this study. There was a strong positive correlation of macroporosity with surface area density ($r = 0.88$), length density ($r = 0.84$), and interconnectivity ($r = 0.83$) (Table 3.2). Previous studies have also reported similar correlations between the different macropore characteristics (Katuwal et al., 2015; Luo et al., 2010a). Similar to Katuwal et al. (2015), a relatively high correlation coefficient was observed between surface area density and length density ($r = 0.97$) compared to the other characteristics, while tortuosity was only weakly correlated with macroporosity and other macropore characteristics. The results from this study along with the previous investigations imply that macroporosity values alone could be used as an indicator of the pore interconnectivity. Only macropore diameter was negatively correlated with the connectivity of macropore networks. This is because macropore connectivity is pore-size dependent and increases with the inclusion of small pores that form connecting bridges between different pore networks (Vogel et al., 2010). Macropore characteristics in the transition layer (100-250 mm) showed relatively smaller differences between slope positions compared to the other depths. This is likely because the transition layer at all the slope positions may have already been compacted to the same extent due

to long-term grazing (>15 years) at the study site. For example, in a study on tillage requirements of different crops at the SMREC, Balkcom et al. (2010) reported the presence of a hard pan whose upper surface was 100 mm below the soil surface, which they attributed to winter grazing. In the subsurface (250-500 mm) layer, the trend of macropore variation with slope position was similar for both S1 and S2. However, contrary to the surface layer (0-100 mm), relatively higher values of macropore characteristics were observed at the DS compared to the MS and US positions in the subsurface (250-500 mm) layer. Despite a highly compacted surface soil (0-100 mm) at the DS, higher values of interconnectivity and other macropore characteristics in the subsurface layer (250-500 mm) were likely because of favorable conditions for biota activities in the soil at the DS as compared to the other slope positions.

The mean macroporosity determined for this pasture field (2.70% in the US and 2.95% in the DS) is comparable with Luo et al. (2010a), who reported an average macroporosity of 3.1% for a fine-loamy soil under pasture. Perret et al. (1998) reported similar values of macroporosity between 2.1% and 3.8% using soil samples from sandy loam soil under a grassland field. However, values in this study are substantially lower compared to the macroporosity of forest soils (7.6%) as reported by Zhang et al. (2017). This is because forest soils tend to have deeper and well-developed macropore networks which are related to stable and high vegetation cover, thicker and well-distributed root networks, high organic matter content, and less anthropogenic disturbance (less soil compaction) compared to other land uses (Zhang et al., 2017). In another study, Katuwal et al. (2015) computed the macroporosity range between 0.38% and 1.66%, with an average of 0.9% for sandy loam and loam soil cores under red fescue. The comparison with the previous studies in different land uses was based on the fact that the lowest boundary of macropore diameter quantified was comparable in all of these studies (e.g., 0.75 mm for Luo et al., 2010a; 1.2 mm for

Katuwal et al., 2015; 1 mm for Perret et al. (1998); 0.75 mm for Zhang et al., 2017). The relatively smaller macroporosity values reported by Katuwal et al. (2015) compared to our study could be, in part, because Katuwal et al. (2015) did not account for macropores 0.70-1.2 mm in diameter which could have largely influenced the overall macroporosity results in their study. Overall, these results show that the macroporosity values reported in this study are comparable with those of other agricultural soils and grasslands, however, forest soils tend to have relatively higher macroporosity due to more complex and deeper root networks as compared to the other fields. Nonetheless, all of the previous studies were based on samples collected during a single season and a single landscape position, without considering the temporal and topographical variation in soil macropores that could exist within the field, which were considered in our study.

The above findings indicate that topographical location can have a significant impact on macropore characteristics, especially on the surface (0-100 mm) depth of a pasture field. This results from grazing-induced compaction on the surface and variation in soil properties (e.g., moisture content) due to topography, which can have a substantial impact on macropore development. We did not observe significant differences ($P>0.05$) while comparing the overall macroporosity among different slope positions. This indicates the importance of quantifying macropores for different depths, which can have significant differences among the different slope positions. Although previous studies reported a significant influence of topographical position on soil macroporosity (Zong-Chao Li et al., 2019; Zhang et al., 2016), no efforts were made to quantify the 3D macropore characteristics at different depths of the soil profile. Smaller values of macroporosity and interconnectivity at the DS indicate highly compacted surface (0-100 mm) soil compared to the upper slope position. This could limit the water flow rate in macropores, so fewer contaminants may bypass the soil matrix and reach groundwater and nearby surface water at the DS compared

to the MS and US soils. In contrast, strong preferential transport will be triggered in soil macropores under saturated and near-saturated conditions in highly compacted soils (Jarvis, 2007). We observed that the transition layer (100-250 mm) was relatively more compacted in all the slope positions as compared to the other depth layers. This could result in the transport of water and contaminants laterally above the compacted layer which can have a substantial effect on the nearby surface water quality. Overall, the results indicate that soil macropores are prevalent in this area and therefore can be important pathways for substantial off-site transport of pollutants.

3.4.2 Temporal variation in macropore characteristics

The macroporosity, interconnectivity, and network density values were generally higher for S2 compared to S1, however, the differences were significant ($P<0.05$) for only the interconnectivity and macroporosity at the US position (Figure 3.1). The macropore diameter, however, showed a declining trend from S1 to S2 at the downslope (DS) and upslope (US) positions. Soils at the upslope were probably less affected by compaction due to grazing compared to the downslope soils, as a significant ($P<0.05$) increase in macroporosity and interconnectivity was seen in the S2, compared to S1. Based on the topography, typically the downslope locations are better supplied with water and nutrients compared to upper slope positions. This causes greater forage production at the downslope locations, thereby attracting grazing cattle and inducing a higher degree of compaction due to livestock trampling (Warren et al., 1986).

Changes in the macropore characteristics with sampling season were significant ($P<0.05$) for only the surface layer (0-100 mm) (except for surface area density at the transition 100-250 mm layer, which increased significantly ($P<0.05$) from 0.052 mm^2 mm^{-3} to 0.074 mm^2 mm^{-3} at the DS) (Table. 1). In the surface layer (0-100 mm), macroporosity, surface area density, length density, and interconnectivity increased significantly ($P<0.05$) from S1 to S2 at the US position. In contrast,

significant changes at the DS position were observed for only the length density and network density, which increased from S1 to S2 in the surface layer (0-100 mm). The mean macropore diameter, however, declined significantly ($P<0.05$) from 3.54 (±1.20) mm in S1 to 1.81 (±0.19) mm in S2 at the DS surface layer (0-100 mm). The macropore characteristics in the subsurface layer (250-500 mm) did not change significantly ($P>0.05$) between sampling seasons S1 and S2, however, an increasing trend was seen at all the slope locations. The changes in macropore characteristics were observed mostly in the upper soil layers relative to deeper soil layers. This was likely due to physical processes like wetting and drying cycles that promote macropore regeneration, which act much more in the upper soil layer than in deeper layers (Bottinelli et al., 2014). Additionally, the significant interaction between slope position and time of sampling might have resulted from the variations of water content in space and time (Heddadj and Gascuel-Odoux, 1999).

Further, the above findings indicate that macropore characteristics can increase significantly in the surface layer (0-100 mm) in a short period of time (0.33 years). Such an increase can be attributed to the regeneration of smaller macropores (<1 mm in diameter) due to frequent wetting and drying cycles (Bottinelli et al., 2014) and the development of fine roots (Pulido-Moncada et al., 2020). Although soil deformation due to grazing normally reduces pore functions (e.g., air capacity and permeability), the soil can recover its functional integrity after wetting and drying cycles (Dec et al., 2011). Bodner et al. (2013) demonstrated that within-season variability of the pore size distribution was strongly related to the wetting-drying cycles as compared to the other factors, such as soil mechanical disturbance during the season. Similarly, Dorner et al. (2010) reported a 5% change in the soil porosity between summer and winter simply as a result of wetting-drying cycles in volcanic ash soil. Also, Zhang et al. (2016), who showed a significant interaction of slope

position and measuring date affecting effective porosity (>0.25 mm) of surface soil, attributed regeneration of soil macropores to wetting and drying cycles that occurred within a period of 2 months. With the increase in the proportion of smaller diameter pores (<1 mm) due to wetting and drying cycles, we expected a substantial reduction in mean macropore diameter in S2 compared to S1. Although the macroporosity (0.7-1 mm) of the entire field increased from 0.26% in S1 to 0.31% in S2, we observed a remarkable increase only at the surface (0-100 mm) of the DS position (Figure 3.2). At the DS (0-100 mm), macroporosity due to smaller diameter pores (0.7-1 mm) in S2 was twice the macroporosity value observed in S1 (0.18% in S1 and 0.36% in S2). Thus, a significant reduction in macropore diameter (0-100 mm) from S1 to S2 at the DS can be attributed to the increase in the 0.7-1 mm pores. Contrastingly, the development of fine roots that contributed to macropore formation between S1 and S2 was expected more at the DS compared to the upper slope positions because of biologically more active soils at the downslope position. Higher organic matter content (6%), and higher clay content (38.6%) were observed at the DS soils (0-100 mm), as compared to the MS and US locations. The finer texture and high organic matter content are favorable for root growth and earthworms (Luo et al., 2010a). Despite regeneration of macropores, no significant change in overall macroporosity was observed in the soils at the DS position between S1 and S2. This is likely because of substantial grazing compaction at the DS topsoil compared to the US position. Although the overall macropore characteristics did not vary substantially between the different slope positions and sampling seasons (Figure 3.1), significant differences in surface (0-100 mm) macropore characteristics among the different slope positions and sampling seasons imply that slope-wise variation may change significantly with time, especially at the surface (0-100 mm) depth. Therefore, it is important to quantify the macropore characteristics at different

depths multiple times for a better understanding of the temporal macropore variation at different slope locations.

3.4.3 Size-dependent variation and implications for flow and contaminant transport

The CT-derived macropores in all the slope positions and sampling seasons were visualized for pore size intervals 0.7-1 mm, 1-2 mm, and >2 mm, and 3D images are shown in Figure 3.2. Macropores >2 mm were scantly distributed over the entire column section compared to the <1 mm and 1-2 mm diameter macropores (Figure 3.3). However, contribution by >2 mm macropores to the overall macroporosity was relatively higher compared to the smaller macropores (Figure 3.2). Well-distributed 0.7-1 mm and 1-2 mm diameter macropores are consistent with the average root diameter of the Kentucky 31 tall fescue as reported in a study by Głąb (2007). Macropores at the MS position were relatively larger and continuous than those at other slope positions. The smaller and randomly distributed macropores (0.7-1 mm and 1-2 mm) were likely created by fine root channels or the inter-aggregate macropores, such as those formed as a result of wetting and drying cycles (Luo et al., 2010a). Larger macropores (>2 mm) could be associated with well-developed roots or formed by earthworms (Luo et al., 2010a).

The significant differences in macroporosity ($P<0.05$) between different slope positions were observed only for pores smaller than 2 mm in diameter, except for the subsurface (250-500 mm) layer in S2 where DS soils had significantly higher macroporosity (>2 mm) than the US soils. For the surface layer (0-100 mm), macroporosity of 0.7-1 mm pores was significantly less at the DS compared to the MS and US position in S1. However, this trend was inconsistent with the macroporosity results of S2. Similar slope-wise macroporosity trends were observed in both S1 and S2 samples for pores 0.7-1 mm and 1-2 mm diameter in all the depth layers. Generally, macroporosity of 0.7-1 mm pores at different slope positions and sampling seasons, exhibited less

variability at deeper depths compared to the larger diameter pores (>1 mm) which had highly fluctuating macroporosity values throughout the entire column section. The significantly less macroporosity at the surface layer (0-100 mm) of DS is probably associated with compaction due to trampling, favored by the presence of relatively wetter soil at DS compared to the upper slopes.

The correlation analyses for different macropore size classes and 3D characteristics showed that interconnectivity, length density, surface density, and tortuosity were highly correlated for the larger macropore fractions (>2 mm) in the soil column (Table 3). This indicates that larger macroporosities were associated with a well-connected macropore network. Muller et al. (2018), who quantified macropores > 0.147 mm in diameter under a grazed pasture, reported a highly connected macropore network consisting of only larger macropore sizes (0.75-3 mm in diameter). They were able to best predict the near-saturated hydraulic conductivity using this macropore class. Based on the results of this study and Muller et al. (2018), we expect relatively larger pores (>2 mm in diameter) to be more influential in major water and contaminant transport because of their highly interconnected network. In our study, the much higher contribution by pores >2 mm to the overall macroporosity (Figure 3.2) indicates that soil macropores play an important role in the generation of subsurface flows in this region, as suggested by Lamba et al. (2012) and Sen et al. (2008).

Zong-Chao Li et al. (2019) investigated soil macroporosity (>1 mm in diameter) at different slope positions under alpine meadow and found that US soils induced greater macroporosity and more macropores than the MS and DS soils. However, the findings of the present study suggest that slope-wise variation may be different for different soil depths and different pore size classes. Because of the differences in macropore characteristics, especially at the surface (0-100 mm) depth, the soil hydraulic properties would differ among the different slope positions. A highly

compacted 0-100 mm layer could allow ponding of tension-free water near the surface of the DS making macropores the “hotspots” for water and contaminant leaching compared to the MS and US soils (Vuaille et al., 2020). Also, the presence of a dense macropore network at the surface layer (0-100 mm) of US and MS soils might assist lateral mixing of the flow with the soil matrix resulting in more homogenous flow through the soil profile (Katuwal et al., 2015). Hence, the effect of higher interconnectivity can be contradictory to preferential flow at the MS and US positions. Overall, the flow properties are not exclusively controlled by one particular macropore characteristic. The susceptibility to preferential flow has to be inferred from multiple factors, such as pore continuity (Pagenkemper et al., 2014; Zhang et al., 2019) and hydrologic conditions (Koestel and Jorda, 2014), which needs further investigation. Also, found that the trend of slope-wise macropore variation might change significantly with time because of their dynamic nature, especially at the surface layer (0-100 mm). Although, this study suggested some variation in slope-wise macroporosity trends for the two sampling seasons, more samples collected over repeated time intervals might be needed to draw a finer conclusion about the macropore variability between different slope positions.

3.5 Conclusion

The purpose of this study was to quantify the 3D soil macropore network at upslope, midslope, and downslope locations in two different sampling seasons within a pasture field. The results show clear and consistent evidence that topographical position largely influenced the 3D soil macropore characteristics in the field. Likewise, macropore characteristics changed significantly with time. However, evidence of temporal and topographical differences was observed only in the surface layer (0-100 mm) layer. Soil at the downslope location had significantly smaller surface area density, length density, and network density at the surface layer (0-100 mm) for both the sampling

seasons, compared to the soil at the upslope locations at the same depth. This was likely due to a higher degree of compaction due to grazing at the downslope location, favored by the presence of relatively wetter soil compared to the upslope location. In analyzing the pore size-dependent variation in macroporosity, pores smaller than 2 mm in diameter were found to be highly sensitive to topographical differences. Further efforts should focus on using a higher resolution X-ray CT for the investigation of pores <0.70 mm to draw firmer conclusions on the effect of slope location on macropore characteristics.

3.6 Acknowledgement

This work was supported by a USDA-NIFA AFRI grant (award # 2018-67019-27806), USDA-NIFA Hatch Project (ALA014-1-19052), and the Alabama Agricultural Experiment Station. We thank Marlin R. Siegford, Peyton Heath, Thomas Counts, and staff at the Sand Mountain Research and Extension Center for assistance with this research.

3.7 References

Balkcom, K.S., Reeves, D.W., Kemble, J.M., Dawkins, R.A., Raper, R.L., 2010. Tillage requirements of sweet corn, field pea, and watermelon following stocker cattle grazing. J. Sustain. Agric. 34, 169–182. https://doi.org/10.1080/10440040903482571

Bodner, G., Scholl, P., Loiskandl, W., Kaul, H.P., 2013. Environmental and management influences on temporal variability of near saturated soil hydraulic properties. Geoderma 204–205, 120–129. https://doi.org/10.1016/j.geoderma.2013.04.015

Bottinelli, N., Hallaire, V., Goutal, N., Bonnaud, P., Ranger, J., 2014. Impact of heavy traffic on soil macroporosity of two silty forest soils: Initial effect and short-term recovery. Geoderma 217–218, 10–17. https://doi.org/10.1016/j.geoderma.2013.10.025

Cameira, M.R., Fernando, R.M., Pereira, L.S., 2003. Soil macropore dynamics affected by tillage and irrigation for a silty loam alluvial soil in southern Portugal. Soil Tillage Res. 70, 131–140. https://doi.org/10.1016/S0167-1987 (02)00154-X

Cattle, S.R., Southorn, N.J., 2010. Macroporosity of pasture topsoils after three years of set-stocked and rotational grazing by sheep. Aust. J. Soil Res. 48, 43–57. https://doi.org/10.1071/SR09004

Cougnon, M., De Swaef, T., Lootens, P., Baert, J., De Frenne, P., Shahidi, R., Roldán-Ruiz, I., Reheul, D., 2017. In situ quantification of forage grass root biomass, distribution and diameter classes under two N fertilisation rates. Plant Soil 411, 409–422. https://doi.org/10.1007/s11104-016-3034-7

Dec, D., Dörner, J., Balocchi, O., 2011. Temporal and spatial variability of structure dependent properties of a volcanic ash soil under pasture in southern Chile. Chil. J. Agric. Res. 71, 293–303. https://doi.org/10.4067/s0718-58392011000200015

Monaco, M.A., Dexter, M., Tamburro, J., 2017. Introduction to SAS Studio. Biostat. Comput. Anal. Heal. Data using SAS 143–145. https://doi.org/10.1016/b978-1-78548-111-6.50010-1

Domúnguez-Niño, J.M., Arbat, G., Raij-Hoffman, I., Kisekka, I., Girona, J., Casadesús, J., 2020. Parameterization of soil hydraulic parameters for HYDRUS-3D simulation of soil water dynamics in a drip-irrigated orchard. Water (Switzerland) 12. https://doi.org/10.3390/W12071858

Dörner, J., Dec, D., Peng, X., Horn, R., 2010. Effect of land use change on the dynamic behaviour of structural properties of an Andisol in southern Chile under saturated and unsaturated hydraulic conditions. Geoderma 159, 189–197. https://doi.org/10.1016/j.geoderma.2010.07.011

Doube, M., Klosowski, M.M., Arganda-Carreras, I., Cordelières, F.P., Dougherty, R.P., Jackson, J.S., Schmid, B., Hutchinson, J.R., Shefelbine, S.J., 2010. BoneJ: Free and extensible bone image analysis in ImageJ. Bone 47, 1076–1079. https://doi.org/10.1016/j.bone.2010.08.023

Dougherty, R., Kunzelmann, K.-H., 2007. Computing Local Thickness of 3D Structures with ImageJ. Microsc. Microanal. 13, 1678–1679. https://doi.org/10.1017/s1431927607074430

Głąb, T. 2007. Effect of soil compaction on root system morphology and yields of tall fescue. Int. Agrophysics. 21, 233–239.

Greenwood, K.L., McKenzie, B.M., 2001. Grazing effects on soil physical properties and the consequences for pastures: A review. Aust. J. Exp. Agric. 41, 1231-1250.https://doi.org/10.1071/EA00102

Grosbellet, C., Vidal-Beaudet, L., Caubel, V., Charpentier, S., 2011. Improvement of soil structure formation by degradation of coarse organic matter. Geoderma 162, 27–38. https://doi.org/10.1016/j.geoderma.2011.01.003

Heddadj, D., Gascuel-Odoux, C., 1999. Topographic and seasonal variations of unsaturated hydraulic conductivity as measured by tension disc infiltrometers at the field scale. Eur. J. Soil Sci. 50, 275–283. https://doi.org/10.1046/j.1365-2389.1999.00232.x

Holden, J., 2009. Topographic controls upon soil macropore flow. Earth Surf. Process. Landforms 34, 613–628. https://doi.org/10.1002/esp

Jarvis, N.J., 2007. A review of non-equilibrium water flow and solute transport in soil macropores: Principles, controlling factors and consequences for water quality. Eur. J. Soil Sci. 58, 523–546. https://doi.org/10.1111/j.1365-2389.2007.00915.x

Jassogne, L., McNeill, A., Chittleborough, D., 2007. 3D-visualization and analysis of macro- and meso-porosity of the upper horizons of a sodic, texture-contrast soil. Eur. J. Soil Sci. 58, 589–598. https://doi.org/10.1111/j.1365-2389.2006.00849.x

Jefferies, D.A., Heck, R.J., Thevathasan, N. V., Gordon, A.M., 2014. Characterizing soil surface structure in a temperate tree-based intercropping system using X-ray computed tomography. Agrofor. Syst. 88, 645–656. https://doi.org/10.1007/s10457-014-9699-0

Jury, W.A., Or, D., Pachepsky, Y., Vereecken, H., Hopmans, J.W., Ahuja, L.R., Clothier, B.E., Bristow, K.L., Kluitenberg, G.J., Moldrup, P., Šimůnek, J., Th. van Genuchten, M., Horton, R., 2011. Kirkham's Legacy and Contemporary Challenges in Soil Physics Research. Soil Sci. Soc. Am. J. 75, 1589–1601. https://doi.org/10.2136/sssaj2011.0115

Katuwal, S., Norgaard, T., Moldrup, P., Lamandé, M., Wildenschild, D., de Jonge, L.W., 2015. Linking air and water transport in intact soils to macropore characteristics inferred from X-ray computed tomography. Geoderma 237–238, 9–20. https://doi.org/10.1016/j.geoderma.2014.08.006

Koestel, J., Jorda, H., 2014. What determines the strength of preferential transport in undisturbed soil under steady-state flow? Geoderma 217–218, 144–160. https://doi.org/10.1016/j.geoderma.2013.11.009

Lamba, J., Way, T.R., Srivastava, P., Sen, S., Wood, C.W., Yoo, K.H., 2012. Surface transport of nutrients from surface-broadcast and subsurface-banded broiler litter. Trans. ASABE 55, 979–985.

Li, X., W. McCarty, G., 2019. Application of Topographic Analyses for Mapping Spatial Patterns of Soil Properties. Earth Obs. Geospatial Anal. Earth Obs. https://doi.org/10.5772/intechopen.86109

Luo, L., Lin, H., Li, S., 2010a. Quantification of 3-D soil macropore networks in different soil types and land uses using computed tomography. J. Hydrol. 393, 53–64. https://doi.org/10.1016/j.jhydrol.2010.03.031

Luo, L., Lin, H., Schmidt, J., 2010b. Quantitative Relationships between Soil Macropore Characteristics and Preferential Flow and Transport. Soil Sci. Soc. Am. J. 74, 1929–1937. https://doi.org/10.2136/sssaj2010.0062

Mees, F., Swennen, R., Van Geet, M., Jacobs, P., 2003. Applications of X-ray computed tomograpy in the geosciences. Geol. Soc. Spec. Publ. 215, 1–6. https://doi.org/10.1144/GSL.SP.2003.215.01.01

Müller, K., Katuwal, S., Young, I., McLeod, M., Moldrup, P., de Jonge, L.W., Clothier, B., 2018. Characterising and linking X-ray CT derived macroporosity parameters to infiltration in soils with contrasting structures. Geoderma 313, 82–91. https://doi.org/10.1016/j.geoderma.2017.10.020

Munkholm, L.J., Heck, R.J., Deen, B., 2012. Soil pore characteristics assessed from X-ray micro-CT derived images and correlations to soil friability. Geoderma 181–182, 22–29. https://doi.org/10.1016/j.geoderma.2012.02.024

Oztas, T., Koc, A., Comakli, B., 2003. Changes in vegetation and soil properties along a slope on overgrazed and eroded rangelands. J. Arid Environ. 55, 93–100. https://doi.org/10.1016/S0140-1963 (02)00267-7

Pagenkemper, S.K., Puschmann, D.U., Peth, S., Horn, R., 2014. Investigation of Time Dependent Development of Soil Structure and Formation of Macropore Networks as Affected by Various

Precrop Species. Int. Soil Water Conserv. Res. 2, 51–66. https://doi.org/10.1016/S2095-6339(15)30006-X

Perret, J., Prasher, S.O., Kanlzas, A., Langford, C., 1998. Characterization of macropore morphology in a sandy loam soil using X-ray computer assisted tomography and geostatistical analysis. Can. Water Resour. J. 23, 143–165. https://doi.org/10.4296/cwrj2302143

Phansalkar, N., More, S., Sabale, A., Joshi, M., 2011. Adaptive Local Thresholding for Detection of Nuclei in Diversity Stained Cytology Images. 2011 Int. Conf. Commun. Signal Process. 218–220.

Pires, L.F., Auler, A.C., Roque, W.L., Mooney, S.J., 2020. X-ray microtomography analysis of soil pore structure dynamics under wetting and drying cycles. Geoderma 362, 114103. https://doi.org/10.1016/j.geoderma.2019.114103

Pires, L.F., Roque, W.L., Rosa, J.A., Mooney, S.J., 2019. 3D analysis of the soil porous architecture under long term contrasting management systems by X-ray computed tomography. Soil Tillage Res. 191, 197–206. https://doi.org/10.1016/j.still.2019.02.018

Prior, S.A., Runion, G.B., Torbert, H.A., Erbach, D.C., 2004. A hydraulic coring system for soil–root studies. Agron. J. 96:1202–1205. https://doi.org/10.2134/agronj2004.1202

Pulido-Moncada, M., Katuwal, S., Ren, L., Cornelis, W., Munkholm, L., 2020. Impact of potential bio-subsoilers on pore network of a severely compacted subsoil. Geoderma 363, 114154. https://doi.org/10.1016/j.geoderma.2019.114154

Rab, M.A., Haling, R.E., Aarons, S.R., Hannah, M., Young, I.M., Gibson, D., 2014. Evaluation of X-ray computed tomography for quantifying macroporosity of loamy pasture soils. Geoderma 213, 460–470. https://doi.org/10.1016/j.geoderma.2013.08.037

Rezaei, S.A., Gilkes, R.J., 2005. The effects of landscape attributes and plant community on soil physical properties in rangelands. Geoderma 125, 145–154. https://doi.org/10.1016/j.geoderma.2004.07.011

Rueden, C.T., Schindelin, J., Hiner, M.C., DeZonia, B.E., Walter, A.E., Arena, E.T., Eliceiri, K.W., 2017. ImageJ2: ImageJ for the next generation of scientific image data. BMC Bioinformatics 18, 1–26. https://doi.org/10.1186/s12859-017-1934-z

Schaap, M.G., Leij, F.J., Th. van Genuchten, M., 2001. Rosetta: A computer program for estimating soil hydraulic parameters with hierarchical pedotransfer functions 251, 163–176.

Sen, S., Srivastava, P., Yoo, K.H., Dane, J.H., Shaw, J.N., Kang M.S., 2008. Runoff generation mechanisms in pastures of the Sand Mountain region of Alabama-a field investigation. Hydrol. Process. 14, 369-385. https://doi.org/10.1002/hyp.7025

Sen, S., Srivastava, P., Dane, J.H., Yoo, K.H., Shaw, J.N., 2010. Spatial-temporal variability and hydrologic connectivity of runoff generation areas in a North Alabama pasture-implications for phosphorus transport. Hydrol. Process. 24, 342–356. https://doi.org/10.1002/hyp.7502

Šimůnek, J., Th. van Genuchten, M., Šejna, M., 2016. Recent Developments and Applications of the HYDRUS Computer Software Packages. Vadose Zo. J. 15, 1–25. https://doi.org/10.2136/vzj2016.04.0033

Singh, N., Kumar, S., Udawatta, R.P., Anderson, S.H., de Jonge, L.W., Katuwal, S., 2021. X-ray micro-computed tomography characterized soil pore network as influenced by long-term application of manure and fertilizer. Geoderma 385, 114872. https://doi.org/10.1016/j.geoderma.2020.114872

Singh, P., Kanwar, R.S., Thompson, M.L., 1991. Macropore Characterization for Two Tillage Systems Using Resin-Impregnation Technique. Soil Sci. Soc. Am. J. 55, 1674–1679. https://doi.org/10.2136/sssaj1991.03615995005500060029x

Singleton, P.L., Boyes, M., Addison, B., 2000. Effect of treading by dairy cattle on topsoil physical conditions for six contrasting soil types in Waikato and Northland, New Zealand, with implications for monitoring. New Zeal. J. Agric. Res. 43, 559–567. https://doi.org/10.1080/00288233.2000.9513453

Smet, S., Beckers, E., Plougonven, E., Léonard, A., Degré, A., 2018. Can the pore scale geometry explain soil sample scale hydrodynamic properties? Front. Environ. Sci. 6. https://doi.org/10.3389/fenvs.2018.00020

Soil Survey Staff, Natural Resources Conservation Service, United States Department of Agriculture. Web Soil Survey. Available online at the following link: http://websoilsurvey.sc.egov.usda.gov/. Accessed 20 November 2020.

Udawatta, R.P., Anderson, S.H., Gantzer, C.J., Garrett, H.E., 2008. Influence of Prairie Restoration on CT-Measured Soil Pore Characteristics. J. Environ. Qual. 37, 219–228. https://doi.org/10.2134/jeq2007.0227

Vogel, H.J., Weller, U., Schlüter, S., 2010. Quantification of soil structure based on Minkowski functions. Comput. Geosci. 36, 1236–1245. https://doi.org/10.1016/j.cageo.2010.03.007

Vuaille, J., Daraghmeh, O., Abrahamsen, P., Jensen, S.M., Nielsen, S.K., Munkholm, L.J., Green, O., Petersen, C.T., 2020. Wheel track loosening can reduce the risk of pesticide leaching to surface waters. Soil Use Manag. 1–15. https://doi.org/10.1111/sum.12641

Wahl, N.A., Bens, O., Buczko, U., Hangen, E., Hüttl, R.F., 2004. Effects of conventional and conservation tillage on soil hydraulic properties of a silty-loamy soil. Phys. Chem. Earth 29, 821–829. https://doi.org/10.1016/j.pce.2004.05.009

Wang, Y., Zhang, B., Lin, L., Zepp, H., 2011. Agroforestry system reduces subsurface lateral flow and nitrate loss in Jiangxi Province, China. Agric. Ecosyst. Environ. 140, 441–453. https://doi.org/10.1016/j.agee.2011.01.007

Warren, S.D., Nevill, M.B., Blackburn, W.H., Garza, N.E., 1986. Soil Response to Trampling Under Intensive Rotation Grazing. Soil Sci. Soc. Am. J. 50, 1336–1341. https://doi.org/10.2136/sssaj1986.03615995005000050050x

Watson, K.W., Luxmoore, R.J., 1986. Estimating Macroporosity in a Forest Watershed by use of a Tension Infiltrometer. Soil Sci. Soc. Am. J. 50, 578–582. https://doi.org/10.2136/sssaj1986.03615995005000030007x

Wilson, G.V., Jardine, P.M., Luxmoore, R.J., Jones, J.R., 1990. Hydrology of a Forested Hillslope during Storm Events. Geoderma 46, 119–138. https://doi.org/10.1016/0016-7061 (90)90011-W

Zhang, J., Xu, Z., Li, F., Hou, R., Ren, Z., 2017. Quantification of 3D macropore networks in forest soils in Touzhai valley (Yunnan, China) using X-ray computed tomography and image analysis. J. Mt. Sci. 14, 474–491. https://doi.org/10.1007/s11629-016-4150-9

Zhang, Z., Lin, L., Wang, Y., Peng, X., 2016. Temporal change in soil macropores measured using tension infiltrometer under different land uses and slope positions in subtropical China. J. Soils Sediments 16, 854–863. https://doi.org/10.1007/s11368-015-1295-z

Zhang, Z., Liu, K., Zhou, H., Lin, H., Li, D., Peng, X., 2019. Linking saturated hydraulic conductivity and air permeability to the characteristics of biopores derived from X-ray computed tomography. J. Hydrol. 571, 1–10. https://doi.org/10.1016/j.jhydrol.2019.01.041

Zong-Chao Li, Hu, X., Li, X.Y., Huang, Y.M., Wu, X.C., Wang, P., Liu, L.Y., 2019. Quantification of Soil Macropores at Different Slope Positions under Alpine Meadow Using Computed Tomography in the Qinghai Lake Watershed, NE Qinghai–Tibet. Eurasian Soil Sci. 52, 1391–1401. https://doi.org/10.1134/S1064229319110152

Figures:

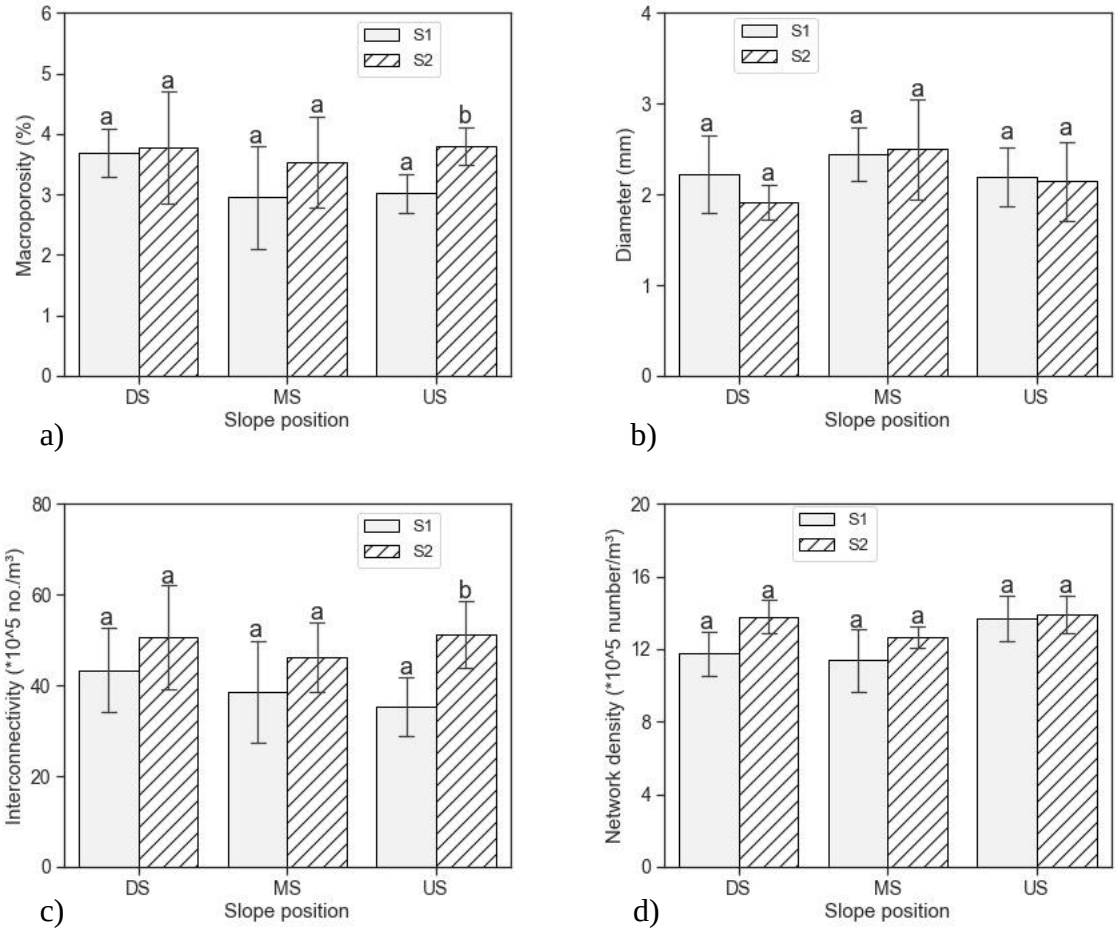

Figure 3.1 Temporal variation in a) soil macroporosity, b) macropore diameter, c) interconnectivity of macropores, and d) network density at different slope positions (DS, MS, and US). Error bars indicate standard deviation (n=6). For each graph, within each slope position, different letters for the different sampling seasons indicate significant differences at the 0.05 probability level.

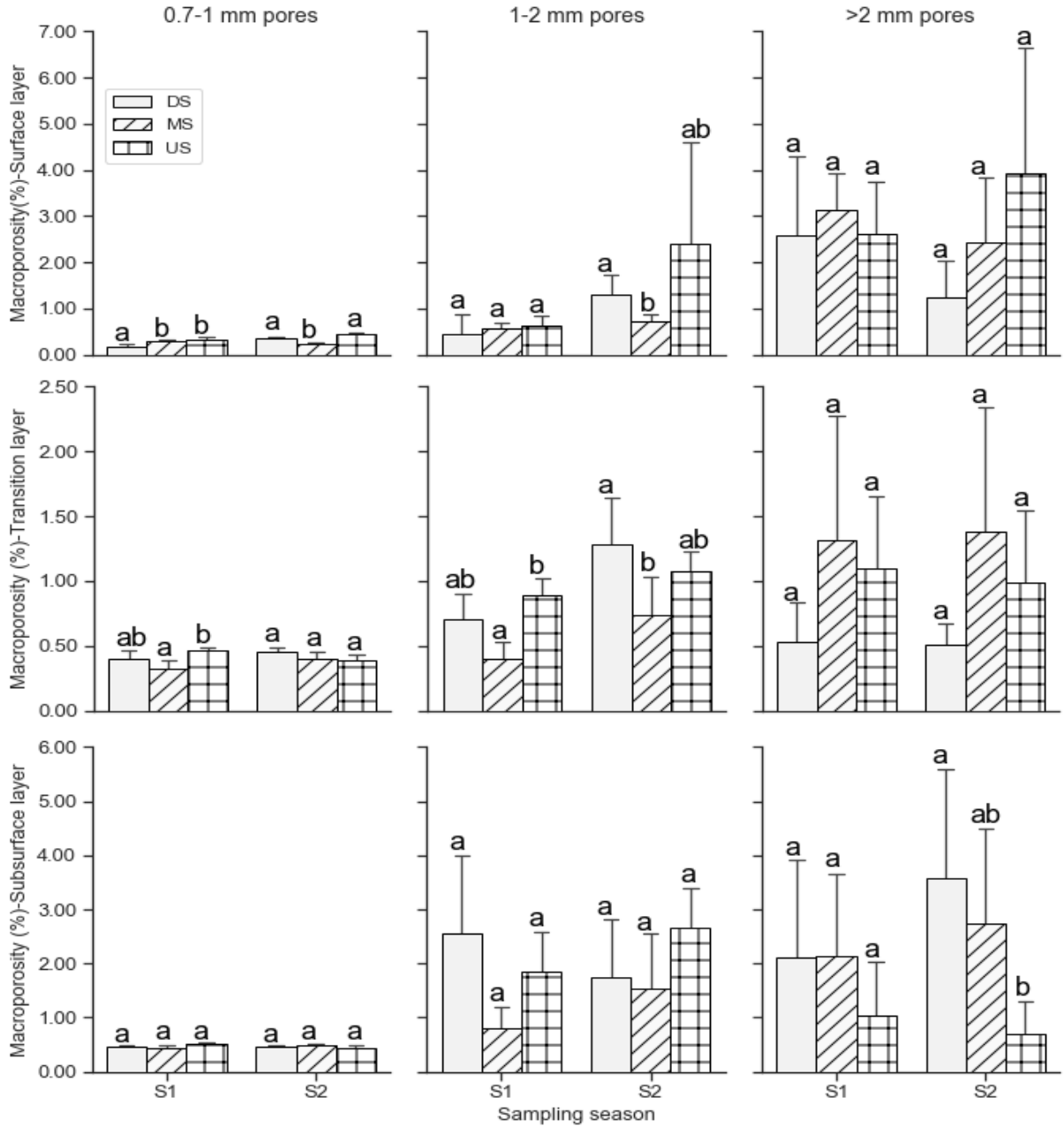

Figure 3.2 Effects of slope position on the 0.7-1 mm soil porosity, 1-2 mm soil porosity, and >2 mm soil porosity on the surface (top), transition (middle), and subsurface (bottom) soil layers for the S1 and S2 sampling seasons. Error bars indicate standard deviation (n=6). Within each graph and sampling season, different letters for the different slope positions indicate significant differences at the 0.05 probability level.

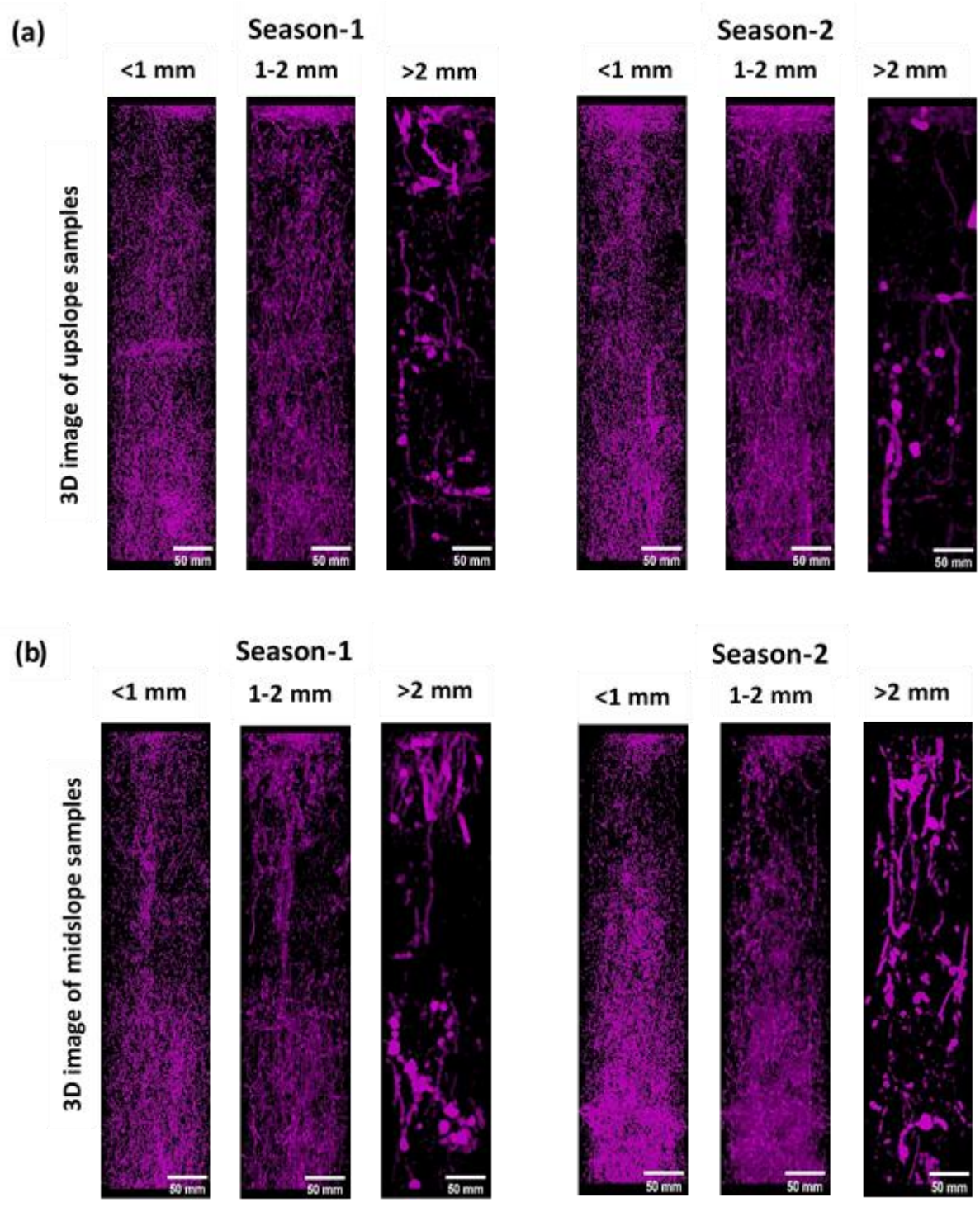
(a)
Season-1
Season-2
<1 mm
1-2 mm
>2 mm
<1 mm
1-2 mm
>2 mm
3D image of upslope samples
50 mm
(b)
Season-1
Season-2
<1 mm
1-2 mm
>2 mm
<1 mm
1-2 mm
>2 mm
3D image of midslope samples
50 mm

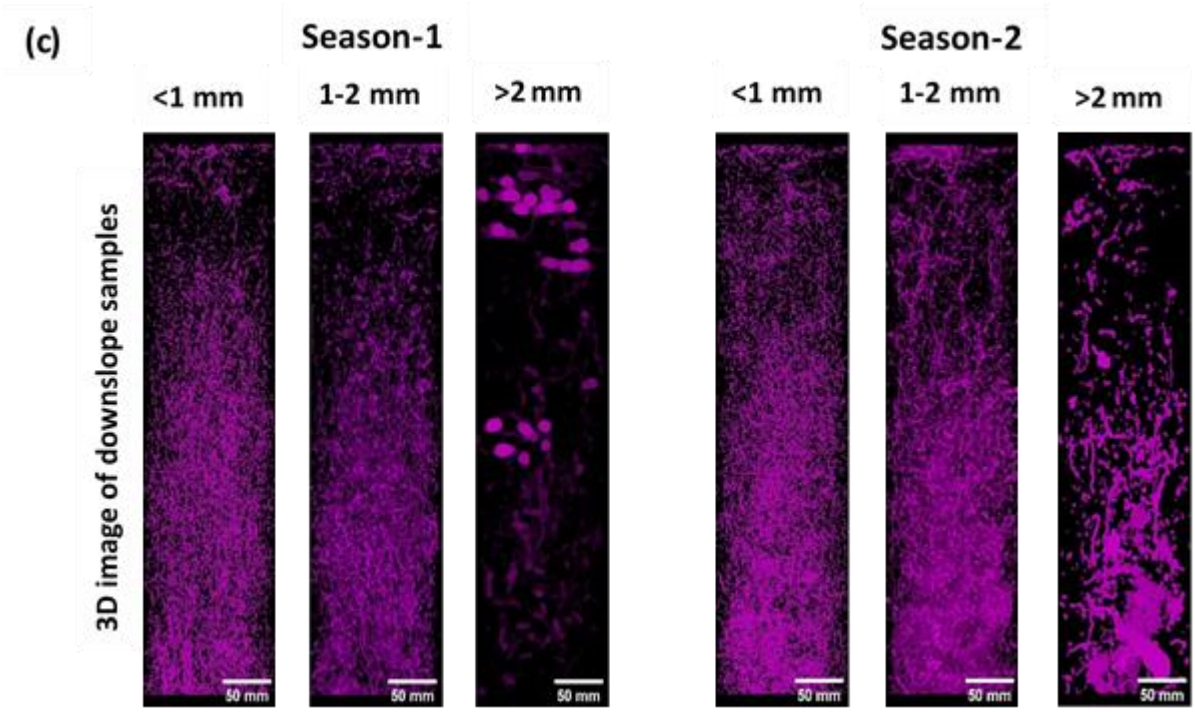

Figure 3.3 Three-dimensional visualization of different sized soil macropore networks (<1 mm, 1-2 mm, and >2 mm) for the representative soil columns of (a) upslope (b) midslope (c) downslope samples of Season 1 and Season 2.

Tables:

Table 3.1 Mean (Std. Dev.) macropore characteristics at different depths of the US (upslope), MS (midslope), and DS (downslope) locations as determined using computed tomography.

Soil layer	Season	Slope position	Macroporosity (%)	Surface area density (mm^2 mm^{-3})	Macropore diameter (mm)	Length density (mm mm^{-3}))	Interconnectivity of macropores (*10^5 number m^{-3})	Network density (*10^5 number m^{-3}))	Tortuosity
Surface (0-100 mm)	S1	DS	3.21 (1.65)	0.058 (0.017)a	3.54 (1.20)A	0.012 (0.003)Aa	28.26 (13.12)	5.50 (1.35)Aa	1.31 (0.015)ab
		MS	4.00 (0.85)	0.090 (0.019)^{ab}	2.89 (0.46)	0.019 (0.005)ab	44.65 (19.78)	10.17 (0.90)b	1.32 (0.007)a
		US	3.78 (0.99)A	0.089 (0.015)A^{b}	2.75 (0.86)	0.020 (0.004)Ab	35.49 (11.85)A	12.18 (3.02)b	1.29 (0.017)b
	S2	DS	2.92 (0.78)a	0.088 (0.019)a	1.81 (0.19)Ba	0.020 (0.004)Ba	52.43 (16.11)a	12.32 (1.32)Bb	1.33 (0.011)a
		MS	3.39 (1.56)a	0.079 (0.031)a	2.82 (0.77)b	0.017 (0.007)a	39.37 (21.26)a	8.73 (1.38)a	1.31 (0.009)ab
		US	6.77 (1.18)Bb	0.171 (0.011)Bb	2.60 (0.95)ab	0.042 (0.008)Bb	109.86 (17.19)Bb	15.76 (1.64)c	1.31 (0.007)b
Transition (100-250 mm)	S1	DS	1.63 (0.40)	0.052 (0.010)Aa	1.99 (0.62)	0.011 (0.002)a	15.73 (6.14)	10.94 (1.81)a	1.30 (0.012)
		MS	2.05 (1.04)	0.054 (0.021)ab	2.43 (0.44)	0.012 (0.004)ab	28.58 (14.41)	9.27 (1.88)a	1.29 (0.008)
		US	2.45 (0.54)	0.074 (0.017)b	2.03 (0.29)	0.016 (0.004)b	28.37 (14.10)	13.96 (0.64)b	1.29 (0.005)
	S2	DS	2.25 (0.41)	0.074 (0.012)B	1.62 (0.08)a	0.015 (0.002)	26.11 (7.55)	13.97 (1.54)	1.30 (0.008)ab
		MS	2.53 (0.93)	0.068 (0.017)	2.60 (0.74)b	0.013 (0.004)	35.58 (15.79)	12.00 (1.93)	1.31 (0.009)a
		US	2.44 (0.54)	0.070 (0.007)	2.29 (0.74)ab	0.016 (0.002)	25.80 (6.84)	12.56 (0.87)	1.29 (0.007)b
Subsurface (250-500 mm)	S1	DS	5.13 (0.86)a	0.138 (0.013)a	1.94 (0.21)	0.031 (0.003)a	65.26 (16.59)	14.50 (1.61)	1.28 (0.008)a
		MS	3.40 (1.30)a	0.094 (0.021)b	2.13 (0.55)	0.022 (0.005)b	47.48 (22.36)	14.07 (2.92)	1.28 (0.005)a
		US	3.41 (0.53)b	0.108 (0.012)ab	1.70 (0.11)	0.025 (0.003)ab	44.77 (8.97)	16.87 (0.69)	1.27 (0.000)b
	S2	DS	5.78 (1.32)a	0.150 (0.023)a	2.07 (0.23)a	0.031 (0.005)a	74.34 (18.26)a	15.88 (1.44)	1.28 (0.005)a
		MS	4.76 (0.92)ab	0.128 (0.013)ab	2.33 (0.64)a	0.029 (0.004)a	64.85 (8.43)ab	15.85 (0.72)	1.28 (0.010)a
		US	3.80 (0.38)b	0.114 (0.011)b	1.74 (0.20)b	0.025 (0.002)a	50.70 (11.21)b	14.81 (2.25)	1.27 (0.006)b

Within each soil layer, within each column, means followed by the same letter (lower case for slope position and upper case for sampling season) are not significantly different at the 0.05 probability level. The absence of letters indicates no significant differences for that property.

Table 3.2 Pearson's correlation matrix of the different CT-derived macropore characteristics of the soil samples.

	A1	A2	A3	A4	A5	A6	A7
Macroporosity (A1)	1.00	0.88***	0.29*	0.84***	0.83***	0.05	-0.13
Surface area density (A2)		1.00	-0.09	0.97***	0.87***	0.36**	-0.16
Mean diameter (A3)			1.00	-0.10	-0.09	-0.26	0.10
Length density (A4)				1.00	0.86***	0.37**	-0.26
Interconnectivity (A5)					1.00	0.05	-0.11
Network density (A6)						1.00	0.05
Tortuosity (A7)							1.00

Significance levels: *0.1, **0.05, ***0.001.

Table 3.3 Pearson's correlation matrix of the different macroporosity classes with 3D macropore characteristics of the soil samples.

	A1	A2	A3	A4	A5	A6	A7
0.7-1 mm porosity (A1)	1.00	0.60***	-0.39**	-0.01	0.26	0.28*	0.027
1-2 mm porosity (A2)		1.00	-0.69***	0.02	0.12	0.16	0.08
>2 mm porosity (A3)			1.00	0.59***	0.56***	0.52**	-0.14
Interconnectivity (A4)				1.00	0.87***	0.86***	-0.11
Surface area density (A5)					1.00	0.97***	-0.26
Length density (A6)						1.00	-0.26
Tortuosity (A7)							1.00

Significance levels: *0.1, **0.05, ***0.001.

Chapter 4

Impact of Land Use and Tillage Practice on Soil Macropore Characteristics Determined Using X-ray Computed Tomography

4.1 Abstract

Quantification of soil macropores is important to enhance our understanding of preferential flow behavior in soils. However, knowledge of 3D soil architecture of different land uses in a continental climate region is limited. The X-ray computed tomography (CT) is a novel technique that can provide valuable information about the 3D features of the soil such as connectivity, length density, and tortuosity, that largely controls water flow through the macropores. In this study, X-ray CT and image analysis were employed to quantify the soil macropore characteristics from four combinations of different land uses and soil tillage practices - native grassland (Nat), alfalfa (Alf), conventional till-corn (CT), and no-till corn (NT) system. A total of 15 undisturbed soil columns, 150 mm in diameter and 500 mm in length were collected from different sites. The macropore characteristics were distinctively different for different land use and tillage treatments, especially near the surface depth (top 100 mm). The soil macropores under CT were highly connected and concentrated mostly in the surface soil layer. In contrast, macropores under NT were larger and had well-developed pore networks. Under different land use practices, alfalfa had relatively larger and vertically oriented macropores as compared to the native soils. Relatively higher macroporosity and higher number of macropores were observed in the surface of native soils. Macropore characteristics were mostly similar between Alf and NT treatments. The results of this study provided quantitative evaluation of 3D soil macropore features with significant implications for non-equilibrium flow prediction and contaminant transport modeling in soils.

Keywords: Image analysis; Pore network; Preferential flow; Soil structure; Tillage

4.2 Introduction

Preferential flow via soil macropores (e.g., root channels, earthworm burrows, inter-aggregate voids) can cause rapid transport of water and contaminants through the unsaturated zone into deep soil and even to the ground water (Šimůnek et al., 2003; Jarvis, 2007). In certain soils, preferential flows can transport more than 90% of water and solutes (Shaffer et al., 1979). Therefore, it is essential to quantify macropore characteristics to better understand subsurface transport of various contaminants. Detailed understanding of different macropore characteristics, such as, macropore diameter, connectivity, number of macropores etc., can enhance our understanding of preferential flows and help develop reasonable mathematical models (Zhang et al., 2017). For example, with the addition of a macropore flow component, Borah and Kalita (1999) reported a remarkable improvement in the prediction capability of a solute leaching model (LEACHM).

Different factors such as, biological activities, land use, tillage, management practices and interaction among these factors can influence macropore characteristics (Cameira et al., 2003; Luo et al., 2010). For example, land use type will affect plant residue and roots characteristics, which can influence macropore properties. Although differences in soil type, soil texture, climate, and fauna can influence soil macroporosity to some extent, results of Shougrakpam et al. (2010) show that the most significant variable that provides the first-order control of the soil macroporosity is vegetation and its root network. Perennial vegetation, such as grasslands, increases soil porosity compared to row crops (Udawatta et al., 2008). Besides, crops like alfalfa have deep penetrating root systems creating vertical biopores that has strong influence on preferential transport processes (Pagenkemper et al., 2014). Macropore characteristics and formation can also vary as a function of tillage practices (Pires et al., 2019; Dal Ferro et al., 2014). In no-tilled soils, pores are mainly formed as a result of biological processes, such as, soil organisms and crop roots (Benjamin, 1993),

whereas pores are formed primarily by the tillage tools in a tilled soil. In agricultural soils, compaction due to wheel traffic causes changes in the pore structure, thereby destroying larger pores and restricting water movement (Fuentes et al., 2004). In the past researchers have evaluated effect of land use/tillage practice on soil macropore characteristics (e.g., Dal Ferro et al., 2014; Udawatta et al., 2008), however contradictory results have been reported in the literature. For example, Pires et al. (2019) and Zaraee and Afzalinia (2016) reported soil macroporosity under no-tillage (NT) is usually less compared to conventional tillage (CT), whereas Galdos et al. (2019) reported opposite results. Such contrary results could be due to climate at a particular location (Zhang et al., 2016), and duration of time that the soils have been managed under the particular management practice (Galdos et al., 2019) besides the land cover. Therefore, it is necessary to further investigate impact of land use type and tillage practices on soil pore characteristics under a wide range of climate conditions and soil management practices. The differences in soil pore characteristics will help to diagnose changes due to agricultural management practices and to design appropriate management guidelines.

There are a number of methods to quantify two-dimensional (2D) soil porosity, such as, dye tracers (Wahl et al., 2004), resin impregnation (Singh et al., 1991), and tension infiltrometer (Cameira et al., 2003). Although 2D analysis of macropore characteristics provide useful information of the pore space and related land use impacts, quantifying macropore characteristics in its true three dimensions (3D) form is essential to understand impact of macropores on soil hydraulic functions (Luo et al., 2010; Katuwal et al., 2015). Recently, X-ray computed tomography (CT) has proven to be a very powerful technique to quantify macropore geometry in 3D, without disturbing the sample (e.g., Pires et al., 2019; Luo et al., 2010). Three-dimensional image analysis is the only way to quantify the connectivity and tortuosity of macropores, which affects flow and contaminant

transport through soil substantially (Jassogne et al., 2007). However, though CT method itself might be non-destructive, soil sampling could induce some disturbances along the soil core edges, which should be addressed at the time of image analysis. Nonetheless, X-ray CT provides vital information to characterize the architecture of the soil macropores for better understanding of soil functions such as water flow, gas exchange, and solute transport (Katuwal et al., 2015; Soto-Gomez et al., 2018).

With the exception of few studies (e.g., Luo et al., 2010; Galdos et al., 2019; Pires et al., 2019; Dal Ferro et al., 2014), most of the work focused on characterizing effect of land use on soil macropore characteristics has been done in 2D analysis of soil macropores (e.g., Udawatta et al., 2008; Shougrakpam et al., 2010; Hu et al., 2018; Hu et al., 2015; Zhang et al., 2016). Moreover, previous studies investigating impact of land use and soil management practices on soil macropores quantified topsoil pore properties (<200 mm) (e.g., Munkholm et al., 2012; Pires et al., 2019; Soto-Gomez et al., 2018; Galdos et al., 2019; Carof et al., 2007; Hellner et al., 2018). The rooting characteristics of arable crops on a global scale can influence soil macropore characteristics to depths 200 mm below the soil surface (Canadell et al., 1996) affecting the water and nutrient distribution in deep soils. The properties of deep soils might be more important in influencing the response of the land use due to the effects of deep roots or tillage activities in agricultural lands (Li et al., 2019). Additionally, depending on the local climate, e.g., rain or snow-fed precipitation, soil aggregation and macropore formation processes may be different due to the differences in root profiles (Schenk and Jackson, 2005; Li et al., 2019), thus, necessitating the use of relatively longer soil cores to capture the heterogeneity evident in soils.

Numerous studies have been conducted towards understanding the influence of land use on soil macroporosity, most of these studies, however, focused on either humid subtropical (e.g., Galdos

et al., 2019), Oceanic (e.g., Abdollahi et al., 2014; Pires et al., 2019; Dal Ferro et al., 2014), or a Mediterranean climate regions (e.g., Soto-Gomez et al., 2018; Carof et al., 2007). We know from these studies that soil structure can vary substantially for the same land use types, which may be related to the agro-climatic zones besides the land use/cover and soil management practices. Insufficient information exists for continental climate regions, including the Wisconsin, USA landscapes, characterized by much longer and colder winters, and greater snow cover than the other temperate regions. Factors like moisture regimes, temperature, wetting-drying cycles, and freeze-thaw cycles can further influence the effects of land use on soil macropore characteristics (Bronick and Lal, 2005). Extreme soil freezing and frost in the continental climate regions may affect the macropore system by producing cracks and reducing the population of soil animals (Beven and Germann, 1982). To better understand the potential combined effects of land use and climate features on soil macroporosity, we need to expand our knowledge in these regions. The results of this study, in conjunction to the previous studies conducted on relatively low-latitude areas, can provide useful information on the effects of land use on soil macropore characteristics. Additionally, use of relatively deeper soil cores in this study would take into consideration the heterogeneity of the soil, therefore, providing more representative results on the land use and soil management effects on soil macropore characteristics. Hence, the objective of this study was to quantify the effect of different land use types (e.g., alfalfa, native grassland and corn) on 3D soil macropore characteristics. A further objective was to investigate the effect of different tillage systems (i.e., no-till vs. conventional tillage) on soil macropore characteristics.

4.3 Materials and methods

4.3.1 Study sites and soil sampling

Undisturbed soil samples were collected from four combinations of different land uses and soil tillage practices – no till corn field (NT), conventional till corn field (CT), Alfalfa (Alf), and Native (Nat) located at the Arlington Research Station (43˚ 18’ 9.47” N, 89˚20’ 43.32” W) in Wisconsin, USA. The soils consisted of Joy series (Fine-silty, mixed, superacitve, mesic Aquic Hapludolls) and Plano series (Fine-silty, mixed, superactive, mesic Typic Argiudolls) which have a silt loam texture with a slope of 3%, formed in loess. The area has a humid continental climate (Köppen climate classification Dfb) with a mean annual temperature of 8 °C, and the mean annual precipitation of 900 mm (1991-2020). Besides, the average annual snowfall is about 1080 mm, out of which a substantial portion falls during the winter (830 mm).

A total of 15 intact soil columns, 150 mm in diameter and 500 mm in length, were randomly sampled from each site to investigate the impacts of land use and tillage on soil macropore characteristics. Three replicates were collected from each of the native, CT, and alfalfa fields, whereas NT consisted of 6 soil samples. The cores collected in corn plots (NT and CT) had a 3-year history of alfalfa followed by 2 years of corn, whereas cores from alfalfa plots had a 3 years history of corn with no-till (NT) followed by 2 years of alfalfa. Both fields were in 5th year of rotation when cores were collected. CT consisted of fall and spring passes with a Case-IH True-tandem 330 Turbo tillage implement (CNH Industrial, Amsterdam, Netherlands). The NT plot was grown with cereal rye as a cover crop and had not received any tillage for at least 5 years at the time of sampling. The native plot (grassed areas) consisted of an Orchard grass that was established in fall of 2013 and was minimally trafficked. A drop hammer mounted on the back of a truck was used to push the PVC pipes into the soil. For extracting the undisturbed soil core samples, the soil

around the cores was dug out, and cores filled with soil were taken out. After sampling, the airspace on the top of the soil core was sealed with stiff insulation foam and secured firmly with plastic caps before transportation. All the samples were stored in the refrigerator until further analysis.

4.3.2 CT scanning and image processing

A Discovery CT750 HD medical CT scanner (GE Healthcare, Chicago, IL) was used to scan all the soil cores at an energy level of 140 kV and 140 mA. This provided 16-bit 512*512 images with a voxel size of 0.35*0.35*0.625 mm^3. Since the soil samples were collected at different times and from different locations, the initial moisture content in the soil columns would not be the same. Differences in soil water content can affect the shape of X-ray attenuation value histogram and also the value of threshold used for segmenting the soil pores and non-pores (Luo et al., 2010). Thus, to minimize the variability among the soil cores and to make the comparison between different land uses more consistent, each individual column was saturated with water and drained for about 3 days. The soil cores were assumed to be at approximately field capacity before CT scanning.

The images were analyzed using the public domain software ImageJ version 1.52t (Rueden et al., 2017) and associated plugins. It is a digital image processing software developed by the US National Institutes of Health (Bethesda, MD). Firstly, the images were cropped to reduce the diameter from 150 mm to 136 mm to avoid any possible voids near the core walls during sampling. This was done by using the Region of Interest (ROI) tool in ImageJ. A median filter, a commonly used image-processing method to reduce the noise, with a radius of 1 pixel, was used to reduce noise in the images (Jassogne et al., 2007). To improve the contrast, and to enhance the edges of the pores, the “Unsharp mask” command was used before any further analyses. The images were segmented using auto-local thresholding method of Phansalkar et al. (2011), which is a

modification of Sauvola's thresholding method to deal with low contrast images. In this method, image segmentation was conducted using a threshold value of each pixel calculated using a radius of 5 and default values for other parameters set in ImageJ software (i.e., k = 0.25 and r = 0.5). The images were also visually inspected to ensure the performance of the segmentation procedure in separating the pores and solids.

For the analyses of macropores, the binary images with pores > 8 voxels were considered, and isolated pores smaller than 9 voxels were removed to avoid misclassification of noise from the porous fraction of the images (Jefferies et al., 2014; Pires et al., 2019). After all the image processing and analyses, only the pores with macropore diameter twice the resolution i.e., 0.70 mm (2*0.35 mm) that could be reliably identified using the image processing technique (Katuwal et al., 2015) were quantified in this study.

4.3.3 Quantification of macropore networks

A commonly used Bone-J (Doube et al., 2010) plugin was used for the quantification of different macropore characteristics including macroporosity, surface area density, diameter, length density, network density, interconnectivity, vertical length, macropore branch length, and tortuosity. The macroporosity distribution along the soil depth was calculated using the macroporosity value for each individual slice of the binary image. A local thickness algorithm proposed by Dougherty and Kunzelmann (2007) was used to calculate the diameter of macropores. The diameter of macropores was calculated as:

$$MD = \frac{\sum_{i=1}^{n} D_i V_i}{\sum_{i=1}^{n} V_i} \quad \text{..... (1)}$$

where Di and Vi are the diameter and volume of each macropore, respectively. The 3-D macroporosity was defined as the percentage of the CT-derived macropore volume to the volume of ROI. The surface area density was calculated as the total macropore wall area divided by the volume of ROI. The node density, which is the number of nodes where at least two macropore branches connect per unit volume was used to quantify the interconnectivity of macropores (Luo et al., 2010). A high value of node density is linked with an extensive and well-connected macropore network (Munkholm et al., 2012). The length of the macropores was derived from the skeletons of the macropores, which is the centerline of each macropore network obtained using Skeletonize 3D and Analyze Skeleton modules in ImageJ. To compute length of the macropores, only the macropore branches with lengths larger than 4 voxels were considered. This was done to reduce the effect of noisy skeletons (Zhang et al., 2019). The vertical tortuosity of the macropores, i.e., average value of ratio of the actual length to shortest length between the end points of the macropores, and macropore network density, i.e., number of macropore networks per unit volume, were both achieved from the output of the Skeletonize 3D and Analyze skeletons modules in ImageJ. The vertical length of the macropores is important to vertical flow and contaminant transport along a soil column (Luo et al., 2010). Hence, vertical length of each individual macropore network was analyzed to investigate the vertical length distribution of different land uses.

Previous studies (e.g., Luo et al., 2010; Muller et al., 2018) have shown that flow and transport processes are associated with the size of the macropores. Hence, to analyze the effects of land uses on different sizes of macropores, all the pores were divided into five pore size intervals: <1 mm; 1-2 mm; 2-3 mm; 3-4 mm, and >4 mm. Hence, macroporosity contribution by each pore size class was compared as a function of land use and tillage practices. In addition, preliminary analyses of

the images showed that macropore characteristics varied with depth. Hence, the entire soil column was divided into 3 depth layers: a surface layer (0-100 mm), the transition layer (100-250 mm), and the subsurface layer (250-500 mm) for computation of macropore characteristics. The 3D soil macropore characteristics were calculated for the entire column section, and individually for the 3 depth layers.

4.3.4 Statistical analyses

All the statistical analysis was performed in SAS version 9.4 (SAS Institute, USA) using one-way analysis of variance (ANOVA) within the General Linear Model (Proc GLM). The assumption of normality and homogeneity of variance was made after diagnosis of the residuals. Different soil pore size classes and CT-measured macropore parameters that violated the assumptions of ANOVA were subjected to necessary transformations before making any statistical inference. Pearson's correlation coefficient was used to test the correlation between different 3D macropore characteristics. Pairwise comparisons between different treatments were done using Tukey's multiple comparison test at the 95% confidence level.

4.4 Results and discussion

4.4.1 Macroporosity and macropore number variation with depth

Macropore properties will be distinguished on the basis of land use type (Alf, Nat, and NT corn)) and tillage practices (CT and NT corn). Three-dimensional visualizations of representative macropore networks under different land uses and tillage combinations are shown in Figure 4.1. From a visual inspection of the 3D images, we observed that the spatial macropore characteristics were distinctly different for both treatments. Macropores which were highly continuous and round in shape were formed by biopores (e.g., roots and earthworm burrows), whereas smaller and isolated macropores were probably the inter-aggregate pores (Luo et al., 2010) (Figure 4.1).

Relatively larger and continuous macropores were observed in the alfalfa soil cores compared to the other land use types. Besides, macropores in the alfalfa cores were comparatively well distributed throughout the entire depth of the soil column. This result is consistent with Pagenkemper et al. (2014), who conducted a study on macropore networks of various precrop species and found alfalfa crops to be highly dominated by vertical oriented biopores, which they attributed to their deep penetrating root systems. This may indicate enhanced water and contaminant flow processes in alfalfa fields, as they have a continuous connections into the deeper soil layer. On the other hand, most of the macropores in the samples collected from native plots were concentrated in the surface soil layers (Figure 4.2 and Figure 4.3). The greater macroporosity and higher number of macropores in the surface of native soils are likely associated with less disturbance due to wheel traffic, compared to the other agricultural soil cores (alfalfa and no-till corn). Similarly, Hu et al. (2015) reported smaller, less continuously distributed, and highly concentrated macropores in the upper 200 mm soil layer of interspace grass patches in the Inner Mongolia grassland of northern China. The results of Hu et al. (2015) provided deeper insight into effects of macropore characteristics on transport processes, however, no efforts were made to quantify the macropore networks in 3D that could largely affect the macropore flows. The distribution of macropores for soils under NT was similar to that of alfalfa soils. Macropores were relatively larger and well distributed throughout the entire depth of the NT soil cores.

On comparing the effects of tillage practices on soil macropore characteristics, we found that CT treatment resulted in smaller and highly concentrated macropores near the soil surface (Figure 4.1). This was not the case for samples taken under NT where the macropores were larger, undisturbed, and more consistent with depth. Similar results were presented by Hellner et al. (2018) and Pires et al. (2017) who showed that CT resulted in higher values of macroporosities

closer to the soil surface. Higher porosity under CT is due to soil loosening and disturbance, which favors the formation of macropores (D. Jabro et al., 2009). However, results of this study are contradictory to Galdos et al. (2019), who reported higher macroporosity under NT (19.7%) compared to the CT (14.3%) for a clay textured soil at the surface layer (0-120 mm). Such higher values of macroporosity in NT could be due to long term adoption of NT (~30 years) that promoted undisturbed faunal and floral activity. This suggests that duration of time that the soils had been managed under NT is an important factor that should be considered while assessing the impact of tillage on soil macropore characteristics.

Figure 4.2 and Figure 4.3 illustrates the depth distribution of macroporosity and macropore number, respectively as a function of land use and tillage practice. The number of macropores and macroporosity variation with depth followed a similar distribution for all the land use and tillage treatments. Relatively less fluctuations in macroporosity values were observed for all the treatments at depths between 200 mm and 500 mm, whereas at depths between 0 to 100 mm, macroporosity declined sharply for the native and CT plots. On the other hand, the general patterns of macropore distribution observed in the alfalfa and NT plots were similar, i.e., macroporosity and macropore number declined only gently from 0 to 100 mm, and remained stable at depths below 100 mm. As reported by Udawatta et al. (2006, 2008), higher macroporosity and macropore number in the native plot was likely due to permanent vegetation that enhances development of macropores as compared to the agricultural crops. However, such change in soil macroporosity is observed only on the top 0-100 mm of the soil profile which can be attributed to the roots of the permanent vegetation and minimal mechanical disturbance of soil. These differences in soil porous system induced by land use and tillage practices can cause significant modifications in the soil hydraulic properties.

4.4.2 Macropore size distribution

The variations in the pore size distribution of soils can impact the soil aeration and water transport, which are crucial for maintaining the soil functions and processes (de Andrade Bonetti et al., 2017). No significant differences were observed in the overall mean macropore diameter among different land uses and tillage practices (Table 4.1). However, significant differences ($P<0.05$) were observed while comparing the macroporosity contribution by different pore size classes (i.e., <1 mm, 1-2 mm, 2-3 mm, 3-4 mm and >4 mm) (Figure 4.4) and different depth layers (Figure 4.5). The CT practice mainly influenced pores with smaller diameter (<1 mm). Significantly less macroporosity ($P<0.05$) due to <1 mm pores was observed in NT field as compared to the CT. This was likely because CT operations affect the soil porous system by operations such as harrowing, which increases porosity and loosen the surface soil (Mangalassery et al., 2014). Galdos et al. (2019) also reported an increase in number of smaller pores under CT compared to NT which they attributed to aggregate breakdown at the topsoil (0-100 mm) in a long-term experiment (~ 30 years) managed under no-till and conventional tillage systems. However, the increase in smaller pores was probably at the expense of large diameter pores under CT. Macroporosity due to large diameter pores (3-4 mm and >4 mm) was markedly less in the CT field compared to the NT field; however, the difference was not significant.

The trends in macropore size distribution among all land uses and tillage systems were similar. The primary contribution to the overall macroporosity (6%, 87%, and 75% in alfalfa, native, and NT, respectively) were by two size classes (1-2 mm and 2-3 mm) in all the land uses. Similarly, Hu et al. (2015), reported that more than 50% contribution of the detected macropores was by three size fractions (<1 mm, 1-2 mm, and 2-3 mm) in a shrub-encroached grassland. In another study Hu et al. (2018) reported the same macropore size classes accounted for more than 85% of the

overall detected macropores for 3 different fields (meadow, farmland, and sand). Pores <1 mm in diameter contributed the least to the overall porosity; 6.7 and 7.3%, respectively in alfalfa and NT. However, in the native treatment, larger pores contributed the least to the overall CT-measured macroporosity (i.e., 1.51% and 1.54% by 3-4 and >4 mm pore classes, respectively). On the other hand, the contribution of pores> 4 mm to the overall porosity was highest for alfalfa, 21.2%, compared to the other land use treatments (1.54%, and 9.34% in native, and NT, respectively). These results again correspond well with the macropore distribution visualized in the 3D image (Figure 4.1).

The above findings indicate that the effect of land use and tillage practice on soil macropores can be different for different pore size classes. We observed significant differences in the macroporosity only for the pore size classes <1 mm and >4 mm. This implies that the effect of different treatments likely impacts pores smaller than those resolved and quantified in this study. Galdos et al. (2019), who assessed the effects of zero-tillage on the macroporosity of Brazilian soils, observed a significant difference in macroporosity values between CT and NT for pores smaller than that quantified in our study (<0.70 mm). However, their results were based on relatively smaller soil samples (75 mm diameter and 120 mm depth) that facilitated scanning soil cores with relatively higher resolutions. The lack of significant difference in macroporosity between the other pore size classes (1-2 mm, 2-3 mm, and 3-4 mm) could also be due to similar macropore distribution among the treatments at deeper depths (Figure 4.5). This might have compensated the macroporosity differences observed near the surface layer. A high concentration of small, isolated pores were observed in the soils under CT and native fields, whereas relatively larger diameter pores were seen under NT and alfalfa fields.

4.4.3 Quantification of 3D network parameters

The water flow via soil macropores largely depends on their 3D structure and geometry (Li et al., 2016). Quantitative data on 3D soil macropore characteristics for different land uses and tillage practices are presented in Table 4.1. The average macroporosity was 2.22 (± 0.29) % in the native field as compared to 2.14 (± 0.29) % in the alfalfa and 1.70 (± 0.27) % in the NT corn. The macropores in the native field were of small diameter, 2.16 (± 0.31) mm, and mostly distributed in the top 100 mm of the soil column. On the other hand, relatively larger macropores 2.75 (± 0.35) mm, were observed in the alfalfa fields which were well distributed throughout the soil column. The 3D images in Figure 4.1 show that soils under native seemed to have a high proportion of small connected macropores relative to alfalfa and NT. Although the differences in macroporosities between different treatments were not statistically significant (Table 4.1), results suggest that land use had influenced the macropore distribution in the surface soil. For example, at the surface (0-100 mm), CT had significantly higher macroporosity compared to the NT. Nonetheless, we observed significantly high overall interconnectivity ($P<0.05$) and length density in native as compared to the soils under alfalfa and NT. The interconnectivity values of soils under native were about twice as large as that in the alfalfa and NT fields. Higher values of interconnectivity are likely because of inclusion of numerous small pores that form connecting bridges between different pore networks (Vogel et al., 2010). No significant differences were observed between alfalfa and NT soils for any macropore characteristics. This is probably because both of them have been under rotational cropping for the last 5 years. Although the current land use practice might have impacted the macropore characteristics of both the fields to some extent, the overall differences between alfalfa and no-till treatments were likely compensated by the influence of land use practice in the past.

Macroporosities calculated for the corn field under contrasting tillage practices were higher for CT compared to the NT systems. In the soils under CT, macroporosity was 1.3 times higher than the NT, whereas mean macropore diameter was 1.28 times lower compared to the NT. Besides, network density was significantly higher ($P<0.05$) in the CT field compared to the NT field. The large macroporosity with relatively large number of small diameter pores under CT is probably associated with the tillage operations, which contribute to the disaggregation of the soil structure at the topsoil (Bauer et al., 2015). At the surface layer (0-100 mm), CT had the lowest macropore diameter as compared to any other treatments; however, the difference was not significant (Figure 4.5). Besides, the macropore network density was significantly higher under CT as compared to the NT at the surface layer (0-100 mm). This finding agrees with the results of Galdos et al. (2019) who reported larger porosities due to smaller pores (<1 mm in diameter) under CT compared to the NT treatment. However, their soil samples were collected from a long-term experiment (~ 30 years) compared to that in our study (~ 5 years). On the other hand, we hypothesized that the higher macropore diameter in NT, 2.30 (± 0.22) mm, as compared to 1.80 (± 0.27) mm in CT was likely due to the undisturbed faunal and floral activity. No-tillage technique allow the soil to develop a complex and well-developed pore network because they do not disrupt earthworm activity and root channels in the soil profile (Cannell, 1985). The macropores under NT had significantly less surface area density compared to the CT. This was expected because of the type of pores present in the NT; the wall surface of macropores in the NT field were probably formed by earthworms, making the pores relatively smoother with reduced surface area (Pagenkemper et al., 2015). Greater pore-wall surface area are mostly associated with irregular pores that result in more resistance to flow (Li et al., 2016). Besides, NT had significantly large ($P<0.05$) macropore

branches (Figure 4.6) compared to the CT. This was likely due to earthworm activity and undisturbed decaying roots from the past crop in NT systems (Soto-Gomez et al., 2018).

The results obtained here for differences in macropore characteristics are extremely valuable due to their importance in water and contaminant transport. Previous studies have revealed connectivity and tortuosity to be more important in governing fluid flow and contaminant transport than macropore volume alone (Luo et al., 2010; Blackwell et al., 1990). However, in this study, we observed good positive correlation between macroporosity and connectivity parameters like network density ($r = 0.54$), length density ($r = 0.74$), and node density (interconnectivity; $r = 0.62$) (Table 4.2). This implies that macroporosity alone could serve as an index of the macropore network connectivity. Macroporosity, on the other hand, was only weakly correlated with tortuosity ($r = -0.09$). Tortuosity values varied within a narrow range of 1.28 to 1.30 for soils cores under different land uses and tillage practices. In a previous study, Katuwal et al. (2015), attributed such small variation in tortuosity values to the presence of significant proportion of vertical biopores (earthworm burrows or root channels). Macropores in silty soils are predominantly formed by biopores such as decaying roots and by earthworm burrows (Kordel et al., 2008).

The results of interconnectivity under different tillage practices were in line with that of the different land uses. Significantly high interconnectivity ($P<0.05$) was observed in soils under CT facilitated by presence of numerous small pores compared to the relatively larger diameter pores in NT. On comparing different land uses, significantly high interconnectivity ($P<0.05$) was reported for soils under native, which had relatively smaller diameter pores and higher network density (number of 3D macropores per unit volume) compared to the other land uses. A negative correlation was observed between interconnectivity and macropore diameter as shown in Table

4.2. Thus, interconnectivity result reported in our study could be due to bridging connections formed by smaller pores (Vogel et al., 2010).

The contribution of different vertical length of macropores to the total macropore vertical length was computed for different land uses and tillage practices (Fig. 7). The overall vertical length, in general, was higher for CT and native compared to NT and alfalfa treatments. Because of highly irregular pores at the surface of CT and native, the skeletons produced might be noisy, resulting in overestimation of the macropore vertical length (Luo et al., 2010). The primary contribution to the total vertical length; 86% and 80% in CT and native, respectively, were by pores <10 mm in vertical length. In alfalfa and NT, pores with vertical length<10 mm contributed relatively less; 67% and 69%, respectively, to the overall macropore vertical length. The contribution of relatively larger and continuous pores (>50 mm in vertical length) to the overall vertical length was higher in the alfalfa and NT fields; 6 and 5%, respectively. On contrary, pores with vertical length>50 mm contributed the least in CT and native fields; 3% and 4%, respectively. The results are in agreement with the average macropore branch length shown in Figure 4.6. The mean macropore branch length under NT; 5.12 mm, was significantly higher compared to that under CT; 3.87 mm. Also, under different land use treatments, significantly higher mean macropore branch length was observed in alfalfa; 5.05 mm, as compared to the native; 4.47 mm, land use type. Numerous small macropores creating dense macropore network on the surface of CT and native might assist lateral mixing of the flow with the soil matrix resulting in more homogenous flow through them (Katuwal et al., 2015). Hence, the effect of dense macropore network in CT and native can be contradictory to preferential flow. An important requirement for the functionality of the pores for transport processes is that the pores are continuous, especially vertical biopores (Pagenkemper et al., 2014). Although high interconnectivity and greater macroporosity are considered as important factors

controlling the hydraulic properties of the soil (Luo et al., 2008; Perret et al., 2000), increase in the proportion of vertical biopores, such as those in NT and alfalfa, would improve air and water permeability throughout the soil profile (Holland, 2004; Mossadeghi-Björklund et al., 2016). Biopores are relatively continuous and effective in transporting water and contaminants than non-biopores (Zhang et al., 2019). Besides, it is expected that the occurrence of ponding is more frequent in relatively compacted surface of NT and alfalfa soils compared to the CT and native fields. At locations where such ponding occurs, the presence of tension-free water near the surface soil make the macropores "hotspots" for water and contaminant leaching to the deeper layers (Vuaille et al., 2020). Katuwal et al. (2015) reported stronger preferential flow in the samples with lower macroporosity and less inter-connected macropores compared to those with higher macroporosity and interconnectivity where the flow was more homogeneous. Similarly, Vanderborght et al. (2002) observed higher preferential flow in the soil cores that had fewer large pores compared to the soil cores with denser macropore networks. Luo et al. (2010b), who related soil macropore characteristics to preferential flow and transport, reported a greater degree of preferential flow in cropland soils with relatively lower macroporosity compared to pasture soils. Overall, we expect soil cores with relatively high proportion of larger and vertical biopores; alfalfa and NT, to be more influential in preferential flow compared to those with higher macroporosities resulting from highly connected small diameter pores; CT and native. These macropore characteristics need to be linked to soil hydraulic properties for better understanding of the subsurface transport processes and to develop appropriate management practices.

4.5 Conclusion

Quantification of the 3D soil macropore characteristics has improved our understanding of soil porous structure under different land uses and tillage treatments. Both tillage practices and land

use types had noticeable influences on different macropore characteristics, especially at the surface soil layer (0-100 mm). The CT cores had significantly higher surface area density, length density, interconnectivity, and network density than the soils under NT. Although CT facilitated formation of dense macropore networks near the surface soil, it disrupted the larger and continuous vertical biopores that could directly affect the water movement. Significantly higher macropore diameter and macropore branch length were observed for NT soils as compared to the soils under CT. This likely resulted from undisturbed faunal and floral activity under NT. The higher proportion of continuous and vertically oriented macropores in alfalfa was closely associated with their deep penetrating root system. Nevertheless, significant differences in macroporosity among different land use and tillage treatments was reported only for the pores size classes <1 mm and >4 mm. We therefore recommend further studies on using higher resolution X-ray CT for the investigation of pores <0.70 mm to draw firmer conclusions on the effect of land use and tillage practices on macropore characteristics.

4.6 Acknowledgement

This work was supported by the USDA-NIFA AFRI award #2018-67019-27806 and USDA-NIFA Hatch Project (ALA014-1-19052). We thank staff at the Arlington Research station in Wisconsin, USA for assistance in this project.

4.7 References

Abdollahi, L., Munkholm, L.J., Garbout, A., 2014. Tillage System and Cover Crop Effects on Soil Quality: II. Pore Characteristics. Soil Sci. Soc. Am. J. 78, 271–279. https://doi.org/10.2136/sssaj2013.07.0302

Bauer, T., Strauss, P., Grims, M., Kamptner, E., Mansberger, R., Spiegel, H., 2015. Long-term agricultural management effects on surface roughness and consolidation of soils. Soil Tillage Res. 151, 28–38. https://doi.org/10.1016/j.still.2015.01.017

Benjamin, J.G., 1993. Tillage effects on near-surface soil hydraulic properties. Soil Tillage Res. 26, 277–288. https://doi.org/10.1016/0167-1987 (93)90001-6

Beven, K., Germann, P., 1982. Macropores and water flow in soils. Water Resour. Res. 18, 1311–1325. https://doi.org/10.1029/WR018i005p01311

Blackwell, P.S., Ringrose-Voase, A.J., Jayawardane, N.S., Olsson, K.A., Mckenzie, D.C., Mason, W.K., 1990. The use of air-filled porosity and intrinsic permeability to air to characterize structure of macropore space and saturated hydraulic conductivity of clay soils. J. Soil Sci. 41, 215–228. https://doi.org/10.1111/j.1365-2389.1990.tb00058.x

Borah, M. J., and Kalita P. K. 1999. Development and evaluation of a macropore flow component for LEACHM. Trans. ASABE 42, 65–78.

Bronick, C.J., Lal, R., 2005. Soil structure and management: A review. Geoderma 124, 3–22. https://doi.org/10.1016/j.geoderma.2004.03.005

Cameira, M.R., Fernando, R.M., Pereira, L.S., 2003. Soil macropore dynamics affected by tillage and irrigation for a silty loam alluvial soil in southern Portugal. Soil Tillage Res. 70, 131–140. https://doi.org/10.1016/S0167-1987 (02)00154-X

Canadell, A. J., Jackson, R. B., Ehleringer, J. R., Mooney, H. A., Sala, O. E., & Schulze, E., 2009. Maximum rooting depth of vegetation types at the global scale. Oecologia. 108, 583–595.

Cannell, R.Q., 1985. Reduced tillage in north-west Europe-A review. Soil Tillage Res. 5, 129–177. https://doi.org/10.1016/0167-1987 (85)90028-5

Carof, M., De Tourdonnet, S., Coquet, Y., Hallaire, V., Roger-Estrade, J., 2007. Hydraulic conductivity and porosity under conventional and no-tillage and the effect of three species of cover crop in northern France. Soil Use Manag. 23, 230–237. https://doi.org/10.1111/j.1475-2743.2007.00085.x

Dal Ferro, N., Sartori, L., Simonetti, G., Berti, A., Morari, F., 2014. Soil macro- and microstructure as affected by different tillage systems and their effects on maize root growth. Soil Tillage Res. 140, 55–65. https://doi.org/10.1016/j.still.2014.02.003

de Andrade Bonetti, J., Anghinoni, I., de Moraes, M.T., Fink, J.R., 2017. Resilience of soils with different texture, mineralogy and organic matter under long-term conservation systems. Soil Tillage Res. 174, 104–112. https://doi.org/10.1016/j.still.2017.06.008

Doube, M., Klosowski, M.M., Arganda-Carreras, I., Cordelières, F.P., Dougherty, R.P., Jackson, J.S., Schmid, B., Hutchinson, J.R., Shefelbine, S.J., 2010. BoneJ: Free and extensible bone image analysis in ImageJ. Bone 47, 1076–1079. https://doi.org/10.1016/j.bone.2010.08.023

Dougherty, R., Kunzelmann, K.-H., 2007. Computing Local Thickness of 3D Structures with ImageJ. Microsc. Microanal. 13, 1678–1679. https://doi.org/10.1017/s1431927607074430

Fuentes, J.P., Flury, M., Bezdicek, D.F., 2004. Hydraulic Properties in a Silt Loam Soil under Natural Prairie, Conventional Till, and No-Till. Soil Sci. Soc. Am. J. 68, 1679–1688. https://doi.org/10.2136/sssaj2004.1679

Galdos, M. V., Pires, L.F., Cooper, H. V., Calonego, J.C., Rosolem, C.A., Mooney, S.J., 2019. Assessing the long-term effects of zero-tillage on the macroporosity of Brazilian soils using X-ray Computed Tomography. Geoderma 337, 1126–1135. https://doi.org/10.1016/j.geoderma.2018.11.031

Hellner, Q., Koestel, J., Ulén, B., Larsbo, M., 2018. Effects of tillage and liming on macropore networks derived from X-ray tomography images of a silty clay soil. Soil Use Manag. 34, 197–205. https://doi.org/10.1111/sum.12418

Holland, J.M., 2004. The environmental consequences of adopting conservation tillage in Europe: Reviewing the evidence. Agric. Ecosyst. Environ. 103, 1–25. https://doi.org/10.1016/j.agee.2003.12.018

Hu, X., Li, Z., Li, X., Wang, P., Zhao, Y., Liu, L., Lu, Y., 2018. Soil Macropore Structure Characterized by X-Ray Computed Tomography Under Different Land Uses in the Qinghai Lake Watershed, Qinghai-Tibet Plateau. Pedosphere 28, 478–487. https://doi.org/10.1016/S1002-0160(17)60334-5

Hu, X., Li, Z.C., Li, X.Y., Liu, Y., 2015. Influence of shrub encroachment on CT-measured soil macropore characteristics in the Inner Mongolia grassland of northern China. Soil Tillage Res. 150, 1–9. https://doi.org/10.1016/j.still.2014.12.019

D. Jabro, J., B. Stevens, W., G. Evans, R., M. Iversen, W., 2009. Tillage Effects on Physical Properties in Two Soils of the Northern Great Plains. Appl. Eng. Agric. 25, 377–382. https://doi.org/https://doi.org/10.13031/2013.26889

Jarvis, N.J., 2007. A review of non-equilibrium water flow and solute transport in soil macropores: Principles, controlling factors and consequences for water quality. Eur. J. Soil Sci. 58, 523–546. https://doi.org/10.1111/j.1365-2389.2007.00915.x

Jassogne, L., McNeill, A., Chittleborough, D., 2007. 3D-visualization and analysis of macro- and meso-porosity of the upper horizons of a sodic, texture-contrast soil. Eur. J. Soil Sci. 58, 589–598. https://doi.org/10.1111/j.1365-2389.2006.00849.x

Jefferies, D.A., Heck, R.J., Thevathasan, N. V., Gordon, A.M., 2014. Characterizing soil surface structure in a temperate tree-based intercropping system using X-ray computed tomography. Agrofor. Syst. 88, 645–656. https://doi.org/10.1007/s10457-014-9699-0

Katuwal, S., Norgaard, T., Moldrup, P., Lamandé, M., Wildenschild, D., de Jonge, L.W., 2015. Linking air and water transport in intact soils to macropore characteristics inferred from X-ray computed tomography. Geoderma 237–238, 9–20. https://doi.org/10.1016/j.geoderma.2014.08.006

Kördel, W., Egli, H., Klein, M., 2008. Transport of pesticides via macropores (IUPAC Technical Report). Pure Appl. Chem. 80, 105–160. https://doi.org/10.1351/pac200880010105

Li, H., Liao, X., Zhu, H., Wei, X., Shao, M., 2019. Soil physical and hydraulic properties under different land uses in the black soil region of northeast China. Can. J. Soil Sci. 99, 406–419. https://doi.org/10.1139/cjss-2019-0039

Li, T.C., Shao, M.A., Jia, Y.H., 2016. Application of X-ray tomography to quantify macropore characteristics of loess soil under two perennial plants. Eur. J. Soil Sci. 67, 266–275. https://doi.org/10.1111/ejss.12330

Luo, L., Lin, H., Halleck, P., 2008. Quantifying Soil Structure and Preferential Flow in Intact Soil Using X-ray Computed Tomography. Soil Sci. Soc. Am. J. 72, 1058–1069. https://doi.org/10.2136/sssaj2007.0179

Luo, L., Lin, H., Li, S., 2010a. Quantification of 3-D soil macropore networks in different soil types and land uses using computed tomography. J. Hydrol. 393, 53–64. https://doi.org/10.1016/j.jhydrol.2010.03.031

Luo, L., Lin, H., Schmidt, J., 2010b. Quantitative Relationships between Soil Macropore Characteristics and Preferential Flow and Transport. Soil Sci. Soc. Am. J. 74, 1929–1937. https://doi.org/10.2136/sssaj2010.0062

Mangalassery, S., Sjögersten, S., Sparkes, D.L., Sturrock, C.J., Craigon, J., Mooney, S.J., 2014. To what extent can zero tillage lead to a reduction in greenhouse gas emissions from temperate soils? Sci. Rep. 4, 1–8. https://doi.org/10.1038/srep04586

Mossadeghi-Björklund, M., Arvidsson, J., Keller, T., Koestel, J., Lamandé, M., Larsbo, M., Jarvis, N., 2016. Effects of subsoil compaction on hydraulic properties and preferential flow in a Swedish clay soil. Soil Tillage Res. 156, 91–98. https://doi.org/10.1016/j.still.2015.09.013

Müller, K., Katuwal, S., Young, I., McLeod, M., Moldrup, P., de Jonge, L.W., Clothier, B., 2018. Characterising and linking X-ray CT derived macroporosity parameters to infiltration in soils with contrasting structures. Geoderma 313, 82–91. https://doi.org/10.1016/j.geoderma.2017.10.020

Munkholm, L.J., Heck, R.J., Deen, B., 2012. Soil pore characteristics assessed from X-ray micro-CT derived images and correlations to soil friability. Geoderma 181–182, 22–29. https://doi.org/10.1016/j.geoderma.2012.02.024

Pagenkemper, S.K., Athmann, M., Uteau, D., Kautz, T., Peth, S., Horn, R., 2015. The effect of earthworm activity on soil bioporosity - Investigated with X-ray computed tomography and endoscopy. Soil Tillage Res. 146, 79–88. https://doi.org/10.1016/j.still.2014.05.007

Pagenkemper, S.K., Puschmann, D.U., Peth, S., Horn, R., 2014. Investigation of Time Dependent Development of Soil Structure and Formation of Macropore Networks as Affected by Various Precrop Species. Int. Soil Water Conserv. Res. 2, 51–66. https://doi.org/10.1016/S2095-6339(15)30006-X

Perret, J., Prasher, S.O., Kantzas, A., Langford, C., 2000. A Two-Domain Approach Using CAT Scanning to Model Solute Transport in Soil. J. Environ. Qual. 29, 995–1010. https://doi.org/10.2134/jeq2000.00472425002900030039x

Phansalkar, N., More, S., Sabale, A., Joshi, M., 2011. Adaptive Local Thresholding for Detection of Nuclei in Diversity Stained Cytology Images. 2011 Int. Conf. Commun. Signal Process. 218–220.

Pires, L.F., Borges, J.A.R., Rosa, J.A., Cooper, M., Heck, R.J., Passoni, S., Roque, W.L., 2017. Soil structure changes induced by tillage systems. Soil Tillage Res. 165, 66–79. https://doi.org/10.1016/j.still.2016.07.010

Pires, L.F., Roque, W.L., Rosa, J.A., Mooney, S.J., 2019. 3D analysis of the soil porous architecture under long term contrasting management systems by X-ray computed tomography. Soil Tillage Res. 191, 197–206. https://doi.org/10.1016/j.still.2019.02.018

Rueden, C.T., Schindelin, J., Hiner, M.C., DeZonia, B.E., Walter, A.E., Arena, E.T., Eliceiri, K.W., 2017. ImageJ2: ImageJ for the next generation of scientific image data. BMC Bioinformatics 18, 1–26. https://doi.org/10.1186/s12859-017-1934-z

Schenk, H.J., Jackson, R.B., 2005. Mapping the global distribution of deep roots in relation to climate and soil characteristics. Geoderma 126, 129–140. https://doi.org/10.1016/j.geoderma.2004.11.018

Shaffer, K.A., Fritton, D.D., Baker, D.E., 1979. Drainage Water Sampling in a Wet, Dual-Pore Soil System. J. Environ. Qual. 8, 241–246. https://doi.org/10.2134/jeq1979.00472425000800020022x

Shougrakpam, S., Sarkar, R., Dutta, S., 2010. An experimental investigation to characterise soil macroporosity under different land use and land covers of northeast India. J. Earth Syst. Sci. 119, 655–674. https://doi.org/10.1007/s12040-010-0042-5

Šimůnek, J., Jarvis, N.J., Van Genuchten, M.T., Gärdenäs, A., 2003. Review and comparison of models for describing non-equilibrium and preferential flow and transport in the vadose zone. J. Hydrol. 272, 14–35. https://doi.org/10.1016/S0022-1694 (02)00252-4

Singh, P., Kanwar, R.S., Thompson, M.L., 1991. Macropore Characterization for Two Tillage Systems Using Resin-Impregnation Technique. Soil Sci. Soc. Am. J. 55, 1674–1679. https://doi.org/10.2136/sssaj1991.03615995005500060029x

Soto-Gómez, D., Pérez-Rodríguez, P., Vázquez-Juiz, L., López-Periago, J.E., Paradelo, M., 2018. Linking pore network characteristics extracted from CT images to the transport of solute and colloid tracers in soils under different tillage managements. Soil Tillage Res. 177, 145–154. https://doi.org/10.1016/j.still.2017.12.007

Udawatta, R.P., Anderson, S.H., Gantzer, C.J., Garrett, H.E., 2008. Influence of Prairie Restoration on CT-Measured Soil Pore Characteristics. J. Environ. Qual. 37, 219–228. https://doi.org/10.2134/jeq2007.0227

Udawatta, R.P., Anderson, S.H., Gantzer, C.J., Garrett, H.E., 2006. Agroforestry and Grass Buffer Influence on Macropore Characteristics. Soil Sci. Soc. Am. J. 70, 1763–1773. https://doi.org/10.2136/sssaj2006.0307

Vanderborght, J., Gähwiller, P., Flühler, H., 2002. Identification of Transport Processes in Soil Cores Using Fluorescent Tracers. Soil Sci. Soc. Am. J. 66, 774–787. https://doi.org/10.2136/sssaj2002.7740

Vogel, H.J., Weller, U., Schlüter, S., 2010. Quantification of soil structure based on Minkowski functions. Comput. Geosci. 36, 1236–1245. https://doi.org/10.1016/j.cageo.2010.03.007

Vuaille, J., Daraghmeh, O., Abrahamsen, P., Jensen, S.M., Nielsen, S.K., Munkholm, L.J., Green, O., Petersen, C.T., 2020. Wheel track loosening can reduce the risk of pesticide leaching to surface waters. Soil Use Manag. 1–15. https://doi.org/10.1111/sum.12641

Wahl, N.A., Bens, O., Buczko, U., Hangen, E., Hüttl, R.F., 2004. Effects of conventional and conservation tillage on soil hydraulic properties of a silty-loamy soil. Phys. Chem. Earth 29, 821–829. https://doi.org/10.1016/j.pce.2004.05.009

Zaraee, M., Afzalinia, S., 2016. Effect of Conservation Tillage on the Physical and Mechanical Properties of Silty-Clay Loam Soil. Int. J. Plant Soil Sci. 12, 1–7. https://doi.org/10.9734/ijpss/2016/26327

Zhang, J., Xu, Z., Li, F., Hou, R., Ren, Z., 2017. Quantification of 3D macropore networks in forest soils in Touzhai valley (Yunnan, China) using X-ray computed tomography and image analysis. J. Mt. Sci. 14, 474–491. https://doi.org/10.1007/s11629-016-4150-9

Zhang, Z., Lin, L., Wang, Y., Peng, X., 2016. Temporal change in soil macropores measured using tension infiltrometer under different land uses and slope positions in subtropical China. J. Soils Sediments 16, 854–863. https://doi.org/10.1007/s11368-015-1295-z

Zhang, Z., Liu, K., Zhou, H., Lin, H., Li, D., Peng, X., 2019. Linking saturated hydraulic conductivity and air permeability to the characteristics of biopores derived from X-ray computed tomography. J. Hydrol. 571, 1–10. https://doi.org/10.1016/j.jhydrol.2019.01.041

Figures:

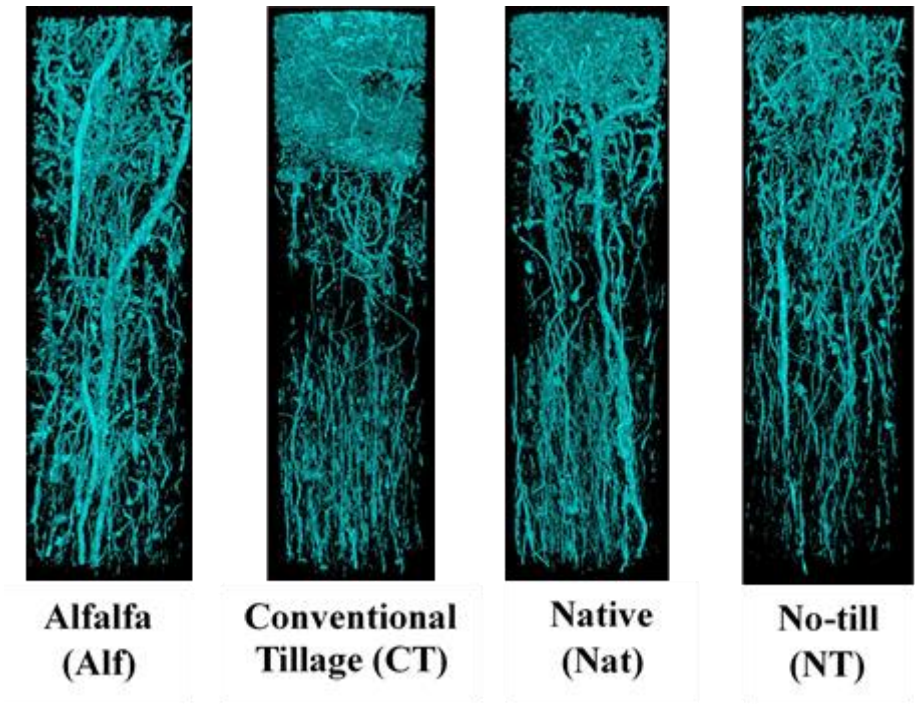

Figure 4.1 3D macropore network visualizations of selected soil cores for the four treatments: corn conventional tillage (CT), corn no-tillage (NT), Native grassland (Nat) and Alfalfa (Alf). Macropores are shown in cyan and non-pore in black color in 3D images.

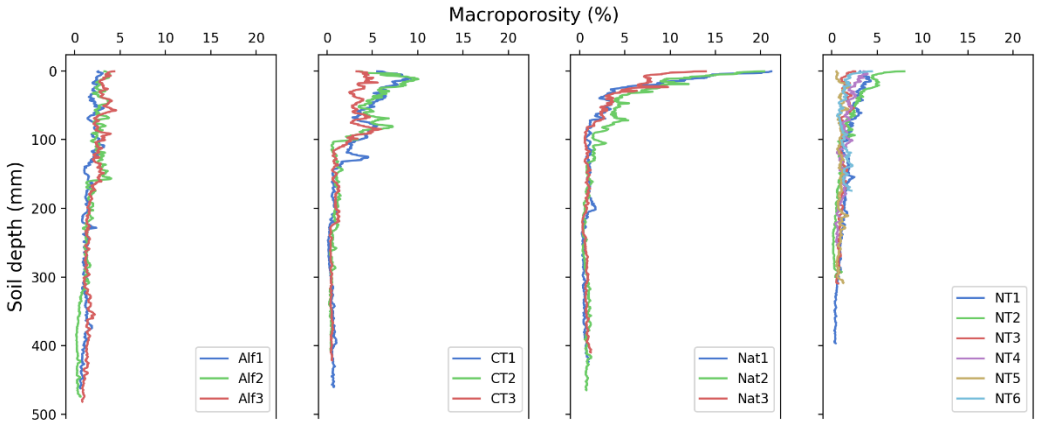

Figure 4.2 Depth distribution of soil macroporosity (%) for all soil cores of corn conventional tillage (CT), corn no-tillage (NT), Native grassland (Nat) and Alfalfa (Alf).

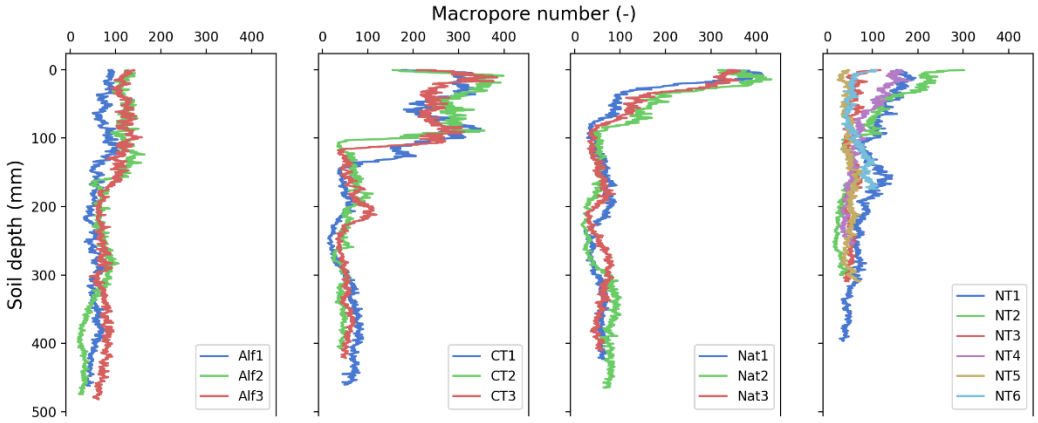

Figure 4.3 Depth distribution of soil macropore number (-) for all soil cores of corn conventional tillage (CT), corn no-tillage (NT), Native grassland (Nat) and Alfalfa (Alf).

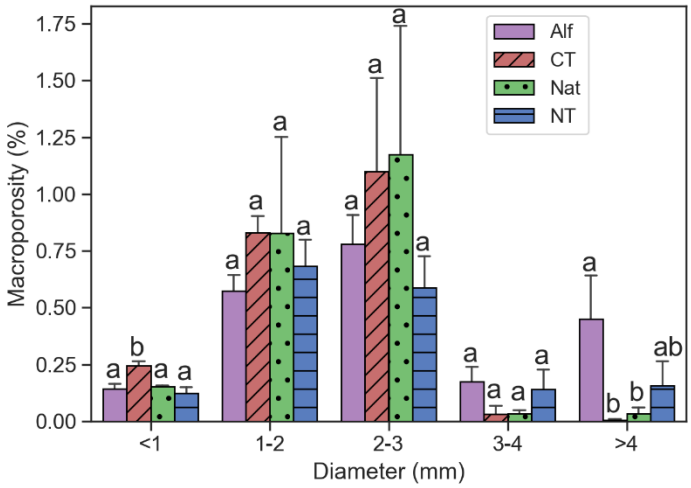

Figure 4.4 Contribution of different macropore size classes on overall macroporosity (%) in soil cores sampled under corn conventional tillage (CT, 3 replicates), corn no-tillage (NT, 6 replicates), Native grassland (NT, 3 replicates) and Alfalfa (Alf, 3 replicates) fields. Within each diameter class, different letters indicate a significant difference in macroporosity (%) between different treatments ($P<0.05$). Error bars indicate standard deviation.

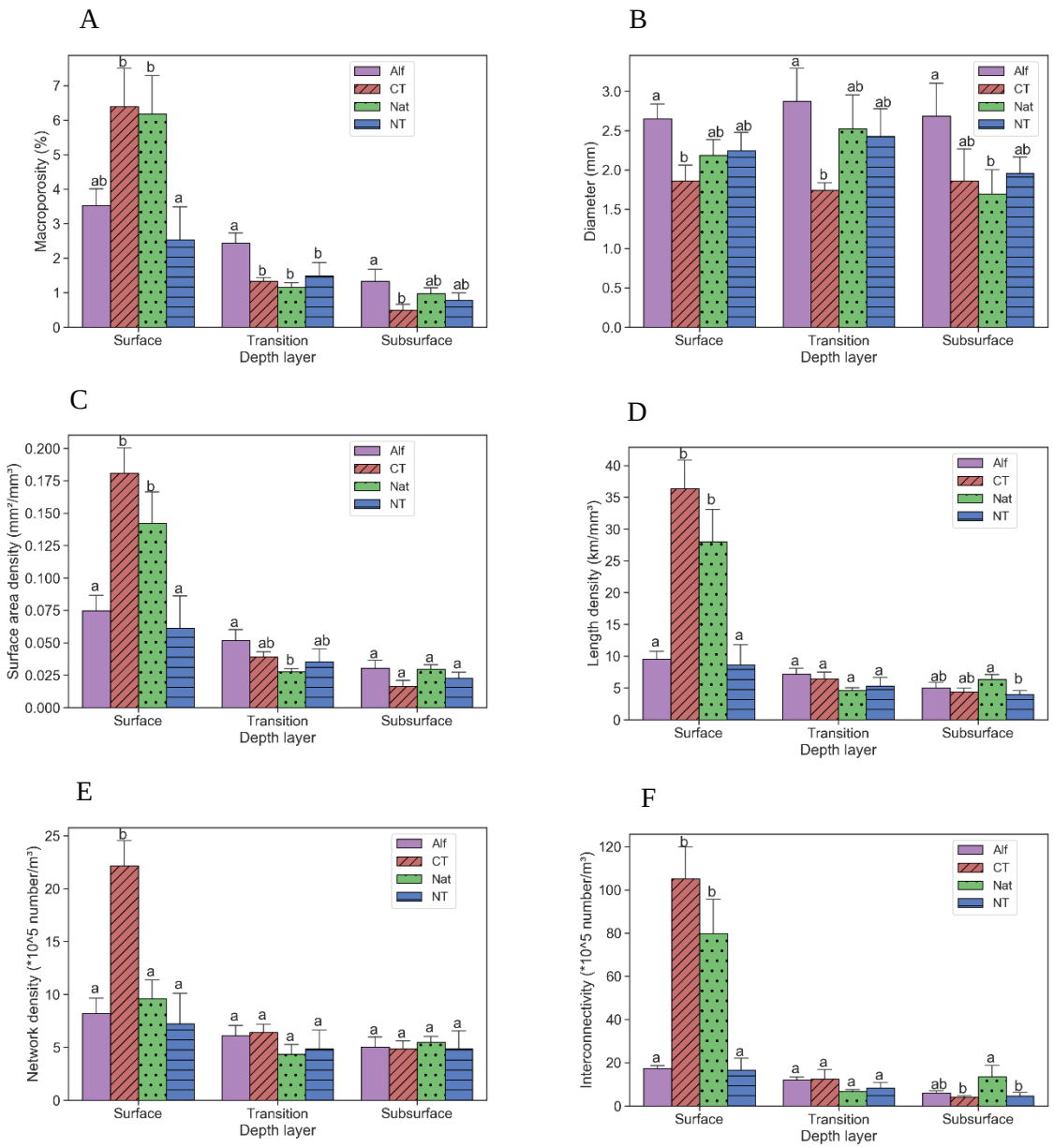

Figure 4.5 3D macropore characteristics of soil columns under different land use treatments (Alf: Alfalfa; Nat: Native grassland; NT: corn no-tillage) and tillage treatments (CT: corn conventional tillage; NT: corn no-tillage) at different depth layers: surface (0-100 mm), transition (100-250 mm), and subsurface (250-500 mm). Error bars indicate standard deviation. For each graph, within each depth layer, different letters indicate a significant difference in macropore characteristics between different treatments ($P<0.05$). A) Macroporosity, B) Diameter, C) Surface area density, D) Length density, E) Network density, and F) Interconnectivity.

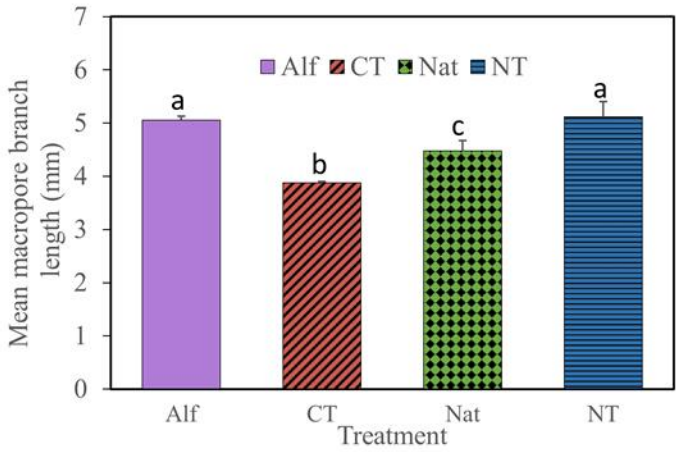

Figure 4.6 Mean macropore branch length for soil cores of corn conventional tillage (CT, 3 replicates), corn no-tillage (NT, 6 replicates), Native grassland (Nat, 3 replicates) and Alfalfa (Alf, 3 replicates). Different letters indicate a significant difference in mean macropore branch length between different treatments ($P<0.05$). Error bars indicate the standard deviation.

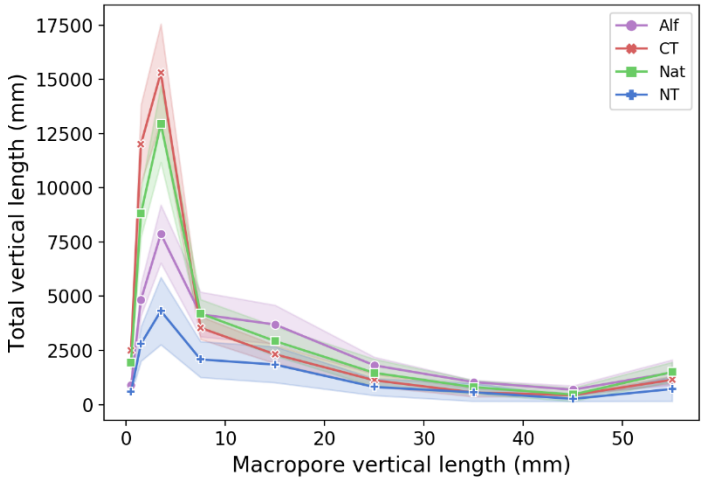

Figure 4.7 Vertical length distribution of macropores for soil cores of corn conventional tillage (CT), corn no-tillage (NT), Native grassland (NT) and Alfalfa (Alf). The shaded region represents the standard deviation.

Tables:

Table 4.1 Mean (Std. Dev.) macropore characteristics of all soil columns under different land uses and tillage practices.

Soil column	Macroporosity (%)	Surface area density (mm^2 m^{-3})	Macropore diameter (mm)	Length density (km m^{-3})	Interconnectivity of macropores(* 10^5) (number m^{-3})	Network density (*10^5) (number m^{-3})	Tortuosity
Alf	2.14 (0.29) a	0.050 (0.01) ac	2.75 (0.35) a	6.6 (0.9) a	10.22 (0.88) a	5.93 (1.09) a	1.29 (0.01) a
CT	2.22 (0.34) a	0.070 (0.010) b	1.80 (0.21) b	12.0 (1.0) b	30.43 (4.64) b	9.31 (0.92) b	1.30 (0.00) a
Nat	2.22 (0.29) a	0.060 (0.000) ab	2.16 (0.31) ab	10.6 (1.1) b	24.94 (1.49) b	5.98 (0.36) a	1.29 (0.00) a
NT	1.70 (0.27) a	0.040 (0.010) c	2.30 (0.22) ab	6.1 (1.0) a	10.45 (1.76) a	5.30 (1.27) a	1.29 (0.01) a

Mean values of different properties followed by the same letters after parenthesis are not significantly different among the different treatments at the 0.05 probability level.

Table 4.2 Pearson's correlation matrix of CT-derived 3D macropore characteristics for all the soil samples.

Properties	A1	A2	A3	A4	A5	A6	A7
Macroporosity (A1)	1.00	0.84 (<0.00**)	-0.05 (0.86)	0.74 (0.00**)	0.62 (0.01*)	0.54 (0.03*)	-0.09 (0.73)
Surface area density (A2)		1.00	-0.55 (0.03*)	0.94 (<0.00**)	0.87 (<0.00**)	0.85 (<0.00**)	0.05 (0.83)
Diameter (A3)			1.00	-0.59 (0.02*)	-0.61 (0.01*)	-0.63 (0.01*)	-0.06 (0.83)
Length density (A4)				1.00	0.96 (<0.00**)	0.74 (0.00**)	0.14 (0.61)
Interconnectivity (A5)					1.00	0.67 (0.00**)	0.28 (0.30)
Network density (A6)						1.00	0.12 (0.66)
Tortuosity (A7)							1.00

Significance levels: *0.05, **0.01.

Chapter 5

Conclusions

The effect of topographical location on 2D and 3D soil macropore characteristics were investigated. Macroporosity, macropore number, interconnectivity, surface area density, and length density were lowest at the downslope surface soil (0-100 mm) as compared to the soils at the upslope and midslope locations. This can be attributed to higher degree of compaction along with higher soil moisture content at the downslope location compared to the upper slope locations. In addition, we also observed significant change in soil macropore characteristics with season, especially at the soil surface (0-100 mm). Among different pore size classes, pores smaller than 2 mm in diameter were found to be highly sensitive to topographical differences. Similarly, macroporosity due to smaller diameter pores (0.7-1 mm), in Season 2, was twice the macroporosity value observed in Season 1, at the surface (0-100 mm) soil layer. This suggests further studies focused on using higher resolution X-ray CT to investigate pores <0.70 mm in diameter to draw firmer conclusions on the topographical and temporal variation in soil macropore characteristics.

Additionally, the effect of different land uses and tillage practices were also studied. The CT practice facilitated formation of dense macropore networks near the surface soil, however, disrupting larger and continuous vertical biopores that could directly affect the water movement. Larger and higher proportion of vertically oriented macropores were observed in alfalfa and NT which was mostly associated with the deep penetrating root system of alfalfa and undisturbed biological activities (e.g., earthworm movement) in the NT treatment. However, significant differences in macroporosity between different treatments were observed only for pore size classes <1 mm and >4 mm.

In conclusion, it was found that topographical location and land use greatly affects the soil macropores. The results obtained for differences in macropore characteristics are extremely valuable due to their importance in water and contaminant transport. Future studies should be conducted to link macropore information with different hydraulic parameters to develop relationship between the macropore characteristics and contaminant transport processes in soil subsurface.

Appendix A

Photos

Figure A.1 Images showing collection of soil samples.

Figure A.2 Transportation and storage of the soil samples.

Figure A.3 Saturation of soil columns before CT Scanning.

Figure A.4 Images showing earthworm exiting soil core during saturation (Left) and artificial macropores of known diameter created using Plexiglas rods (Right).

Figure A.5 Performing X-ray CT scan on the soil samples.